Impact sand extraction Maasvlakte 2

Mud transport, nutrients and primary production

Port of Rotterdam

9 August 2006
Final Report
9P7008.O9

SVASEK HYDRAULICS
COASTAL, HARBOUR AND RIVER CONSULTANTS

WL | delft hydraulics

ROYAL HASKONING
thinking in
all dimensions

A COMPANY OF

ROYAL HASKONING

HASKONING NEDERLAND B.V.
COASTAL & RIVERS

Barbarossastraat 35
P.O. Box 151
Nijmegen 6500 AD
The Netherlands
+31 (0)24 328 42 84 Telephone
+31 24 3605483 Fax
info@nijmegen.royalhaskoning.com E-mail
www.royalhaskoning.com Internet
Arnhem 09122561 CoC

Document title	Impact sand extraction Maasvlakte 2
Document short title	Impact sand extraction Maasvlakte 2
Status	Final Report
Date	9 August 2006
Project name	Maasvlakte 2
Project number	9P7008.O9
Client	Port of Rotterdam Wil Borst, Sander Boer
Reference	9P7008.O9/R002/MVLED/Nijm

Drafted by	Bram van Prooijen, Thijs van Kessel, Arno Nolte, Hans Los, Johan Boon, Wiebe de Jong, Mathijs van Ledden
Checked by	Mathijs van Ledden
Date/initials check	9 August 2006 .....
Approved by	Mark van Zanten
Date/initials approval	9 August 2006 .....

CONTENTS

			Page
1	INTRODUCTION		1
	1.1	Background	1
	1.2	Objective	2
	1.3	Approach and Outline	2
	1.4	Assumptions	3
2	SEASONAL WATER-BED EXCHANGE		5
	2.1	Introduction	5
	2.2	Large scale transport of fine sediment in the North Sea	5
	2.3	Mechanisms for water-bed exchange	8
	2.4	Model formulations	10
	2.4.1	Situation	10
	2.4.2	Erosion formulations	12
	2.4.3	Deposition formulations	13
	2.4.4	Overview of parameters	13
	2.5	Calibration and validation	14
	2.5.1	Approach	14
	2.5.2	Results	15
	2.5.3	Conclusions	18
3	MODEL SET-UP AND CALIBRATION WITH FINEL2D		19
	3.1	General	19
	3.2	Hydrodynamics	19
	3.3	Set-up and calibration of the silt model	24
	3.3.1	Introduction	24
	3.3.2	Model set up	24
	3.3.3	Calibration of the NW10 data	25
	3.3.4	Qualitative validation with silt atlas of RIKZ	27
	3.4	Concluding remarks	27
4	MODEL SET-UP AND CALIBRATION WITH DELFT3D		29
	4.1	Introduction	29
	4.2	Grid and bathymetry	29
	4.3	Hydrodynamics	31
	4.4	Waves	32
	4.5	Mud transport	36
	4.6	Nutrients and primary production	40
	4.7	Concluding remarks	42
5	RESULTS OF SCENARIO COMPUTATIONS		43
	5.1	Introduction	43
	5.2	Effects of silt transport with FINEL2D	43
	5.2.1	Introduction	43
	5.2.2	Definition scenarios and sensitivity simulations	43
	5.2.3	Presentation of the results	45
	5.2.4	Interpretation	46
	5.2.5	Summary and conclusions	49

5.3	Effects on mud transport with Delft3D	49
5.3.1	Parameter settings	49
5.3.2	Sensitivity simulations	50
5.3.3	Scenario results	51
5.4	Comparison of 2D and 3D approach	62
5.4.1	Introduction	62
5.4.2	The effect of a three-dimensional water motion	62
5.4.3	Parameter settings	67
5.5	Effects on nutrients and primary production	68
5.5.1	General	68
5.5.2	Impact results	68
5.5.3	Concept of limiting factors	70
5.5.4	Impacts of sand extraction	72
5.5.5	Uncertainties	75

6 DISCUSSION AND CONCLUSIONS 79

7 CONCLUSIONS 83

REFERENCES 85

1 INTRODUCTION

1.1 Background

The land reclamation near the harbour of Rotterdam, Maasvlakte 2, requires a huge amount of sand for construction of the sea wall and the inner harbor area. This sand volume will mainly be extracted from the North Sea nearby the Rotterdam harbour (search radius of 30 km) and partly from the new harbours basins (socalled internal borrow areas) The search area for the sand extraction activities at the North Sea is presented in Figure 1.1. The locations of the sand borrow areas take into consideration the local contraints, but are primairaly to allow the development of a basic design alternative for the EIA. The final choice will be part of the “design and construct” tender process in which the contractor plays an important role. The locations are indicated with P2, P4, P5 and P6. The sea bed at these locations consists predominantly of medium sand with a small percentage of mud (particles < 0.063 mm).

Figure 1.1: Search area for sand extraction Maasvlakte 2. The blue rectangles (P2, P4, P5 and P6) indicate the locations of the sand borrow areas.

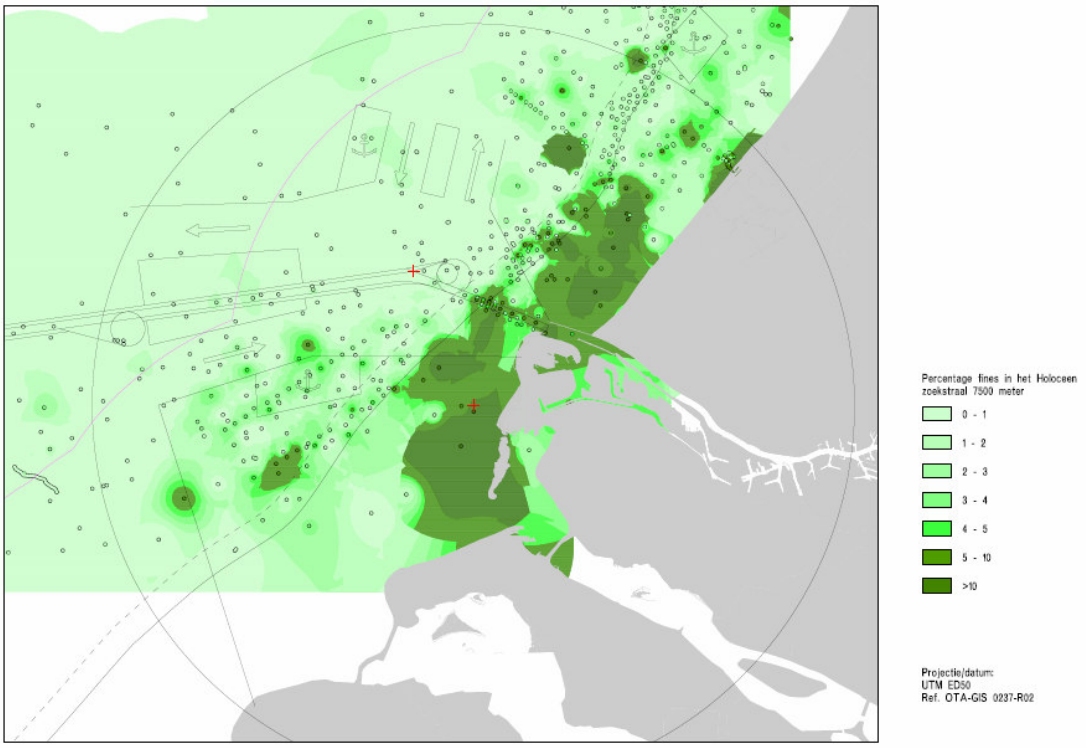

The total volume of sediment that is needed for the land reclamation is 400 Mm^3. About 300 Mm^3 of this volume will be extracted from the sand extraction pits at the North Sea (see Figure 1.1). These volumes include the loss of fines (mud and fine sand) during dredging (+/- 15%) and also the loss of sediment during construction (+/- 9%). The loss during dredging partly consists of fine sand and partly consists of mud. The sand fraction will deposit rather quickly in the neighbourhood of the sand extraction pits due to the relatively high settling velocity (+/- 5 – 10 mm/s). However, the mud fraction has a relatively low settling velocity (+/- 0.25 mm/s) and can be transported over large(r) distances.

In general two plumes are distinguished: a dynamic plume (going straight to the seabed as a density current) and a passive plume (which may travel to the far field)

It is necessary to predict the effects on mud transport as accurate as possible. A change in mud concentration affects the transparency in the water column. On its turn, this influences the period of phytoplankton bloom and the visibility of preys. These parameters may affect the higher-order species in the food chain such as birds and fishes. These effects are of crucial importance because of the Voordelta in relative close proximity to the borrow areas. The Voordelta is a so-called Special Area of Conservation (SAC) in the framework of the Birds and Habitat Directives of the European Communion. The previous Environmental Impact Assessment (PKB Mainport Rotterdam) has stated that no significant effects may occur in this area as a result of the sand extraction activities.

This report describes the effects of sand extraction i.e. the transport of fines being released during the dredging activities by trailing suction hopper dredgers as suspended sediments in the overflow, and as a consequence the impact on nutrients and primary production in the North Sea. This study was initiated after discussion about the initial mud transport computations with DELFT3D in the framework of the Environmental Impact Assessment of the construction and the presence of Maasvlakte 2. Based on time constraints, it was decided at the start of the study (early 2005) to neglect the sediment buffering in and release from the sediment bed at a seasonal scale. This process is qualitatively known, but well-validated model formulations did not exist up till now.

Mid November 2005 it was decided that a more comprehensive approach was needed to quantify the impact of sand mining during the construction of Maasvlakte 2. This approach should take into account the seasonal effects as a result of availability of fines and the relation with the meteorological conditions, in particular wave action during storms.

1.2 Objective

The objective of this study is:

"to quantify and explain the effects of sand extraction including the band width on mud transport, nutrients and primary production in the North Sea coastal zone in the framework of Maasvlakte 2 with explicitly taking into account the role of seasonal water-bed exchange in the sediment bed"

1.3 Approach and Outline

The following approach is adopted in this study:

- In Chapter 2, we discuss the process of water-bed exchange at the sediment bed at a seasonal scale in detail. In addition, model formulations are proposed that are included into process-based models. These parameters in this formulation are calibrated against field data.
- Chapter 3 describes the set-up of a ***two-dimensional*** model for the Southern North Sea using the software package FINEL (Finite Element model). Attention is paid to

the grid and bathymetry, and the calibration of the hydrodynamics and the mud transport for the Dutch coastal zone. The implementation and calibration of the water-bed exchange from Chapter 2 are discussed as well.

- Chapter 4 starts with a brief description of the existing ***three-dimensional*** model of the Southern North Sea based on the software package DELFT3D. This model consists of several modules for hydrodynamics (currents and waves), mud transport and nutrients and primary production. The implementation and calibration of the water-bed exchange from Chapter 2 are disucssed as well.
- Next, the results of the scenario computations are discussed in chapter 5. The results of the two-dimensional model FINEL and the three-dimensional model DELFT3D are discussed separately.
- An integral discussion of the results including the confidence level is given in Chapter 6.

The appendixes are not included in this hardcopy, but can be found on the CD which is applied with this document.

1.4 Assumptions

Several assumptions are made in this study:

1. The time span of the construction phase is 7 years resulting in a sand extraction volume of 50 Mm^3/year at the North Sea. The loss of sediment (going through the TSHD overflow) at the borrow areas is estimated at 15% (fine sand and mud). In the reference scenario, sand extraction is carried out simultaneously from four borrow areas (P2, P4, P5 and P6).
2. We assume that the fine sand fraction behaves as a dynamic plume (density driven) and deposits directly in the neighbourhood of the sand extraction pits. This is a local effect and this sediment fraction is therefore not considered in this study. Only the mud fraction (defined in this study as fines < 63 µm) that can be dispersed over larger distances is taken into account.
3. We assume that the (average-) mud content of the North Sea bed at the sand extraction locations is 2.5%. In combination with the sand extraction volume this results in a mud release (particles < 63 µm) of 2 Mton/year due to sand extraction.
4. The mud release at the sand extraction locations is assumed to be constant in time and equivalent in each sand pit, i.e. 0.5 Mton/year (for 4 borrow areas). We take into account only one mud fraction and do not make a distinction between silt and clay (all fines < 63 µm).
5. The plume of the fines coming from the sand extraction activities is assumed to be 100% “passive”. No fines < 63 µm are directly transported in a dynamic plume towards the sediment bed. From field observations, it is known that a dynamic plume with sediments towards the sediment bed occurs as well. However, this process is only partly understood at present (2005). Hence, we assume a 100% passive plume. This approach can be considered as an “upper limit” for the effects on nutrients and primary production.

These assumptions will be re-addressed during the discussion of the results and the corresponding effects on the Voordelta in Chapter 6.

2 SEASONAL WATER-BED EXCHANGE

2.1 Introduction

The seasonal exchange of mud between the water column and the sediment bed plays a central role in this study. This exchange is determined by the buffering of mud in the sandy sediment bed of the North Sea. Qualitatively, this phenomenon is known for a long period, but validated formulations were not available to account for this effect up till now. Therefore, the classical concept for water-bed exchange has been applied in several studies for Maasvlakte 2 (Figure 2.1, left panel). This concept accounts for exchange of mud at the bed surface, but neglects the buffering in the sediment bed. In this study we apply a new concept (Figure 2.1, right panel). Temporal buffering and sediment exchange between the sand bed with a small amount of mud and the water column is taken into account as well.

Figure 2.1: Classical concept with sediment exchange between the water column and the bed surface (left) and the concept applied in this study (right) with sediment exchange between the water column and the bed surface and between the water column and the sand layer including a small percentage of mud.

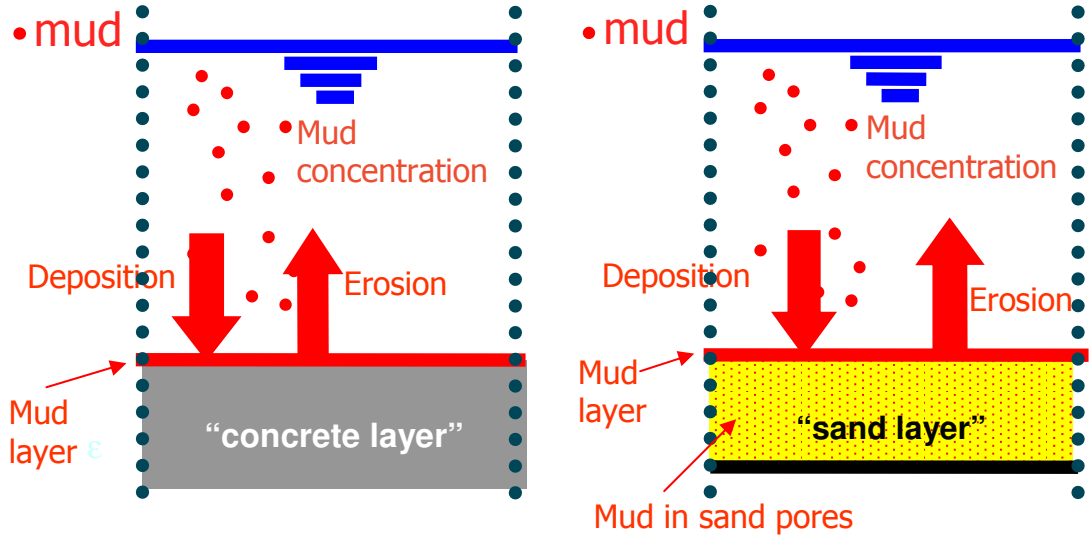

This chapter describes the way in which the phenomenon of water-bed exchange is treated in this model study. First, a summary is given on the water-bed exchange processes of fines in the North Sea and their influence on the large scale transport processes in Section 2.2. Next, mechanisms are discussed in Section 2.3 that could be responsible for this seasonal exchange. Section 2.4 contains a description of a possible algorithm to describe the water-bed exchange processes in numerical models. Finally, the calibration and validation of the parameters are discussed in Section 2.5.

2.2 Large scale transport of fine sediment in the North Sea

The flux of fine-grained cohesive sediment in the Dutch coastal zone is currently estimated at about 25 Mton/year, though this flux may appear to be larger (Salden, 1998, MARE, 2001). At present, it is believed that the majority of these sediments stem

from erosion of the French cliff coast along the Dover Strait. The residual flux of water through Dover Strait is estimated at 100 to 150 x 10^3 m^3/s. Hence, the annual mean suspended sediment concentration in Dover Strait has to be at least 8 mg/l, if it is assumed that all these sediments are transported towards the Dutch coastal zone.

Other sources that are relevant for mud transport in the Southern North Sea are:
1. Flemish Banks (a few MT/y).
2. English coast (Holderness, Suffolk, Norfolk, total 5 - 10 MT/y, note that these sediments are not directly available for the Dutch coast because of the prevailing residual currents).
3. Rivers, of which the Seine, Humber, Western Scheldt and the New Waterway are the most important regarding sediment load. Total load 2.5 MT/y.

The location of the cliff coasts along the Dover Strait is about 200 to 300 km south of the Dutch coastal zone. Hence the direct travel time of fine sediments from Dover Strait to the Dutch coastal zone is estimated at one to two months at least. However, the actual travel time may deviate considerably - see below. Suijlen and Duin (2001) analysed the 1975 -1983 WAKWON near-surface SPM-data, as archived in the DONAR database.
The major conclusions, relevant for the present study, read:
- SPM-concentrations (Suspend particle matter) in the Dutch coastal zone show a significant seasonal variation: winter values (20 - 60 mg/l) are about three times larger than summer values (10 - 30 mg/l), see also Figure 2.2 as an example.
- The major part of the SPM-flux (near the water surface!) occurs in a narrow band of 6 km along the coast, whereas the fresh water content in the Rhine River plume decreases more or less linearly over a band of 40 to 50 km, e.g. Figure 2.3.
- Larger SPM-concentrations are correlated with wave activity (swell with wave periods of 10 to 30 s). Increases in SPM occur more or less simultaneously over the entire study area.

Figure 2.2: Summer mean total SPM (left panel) and winter mean total SPM (right panel) after Suijlen and Duin (2001). The Suspended particle Matter (SPM) is equal to Total Suspended Matter (TSM).

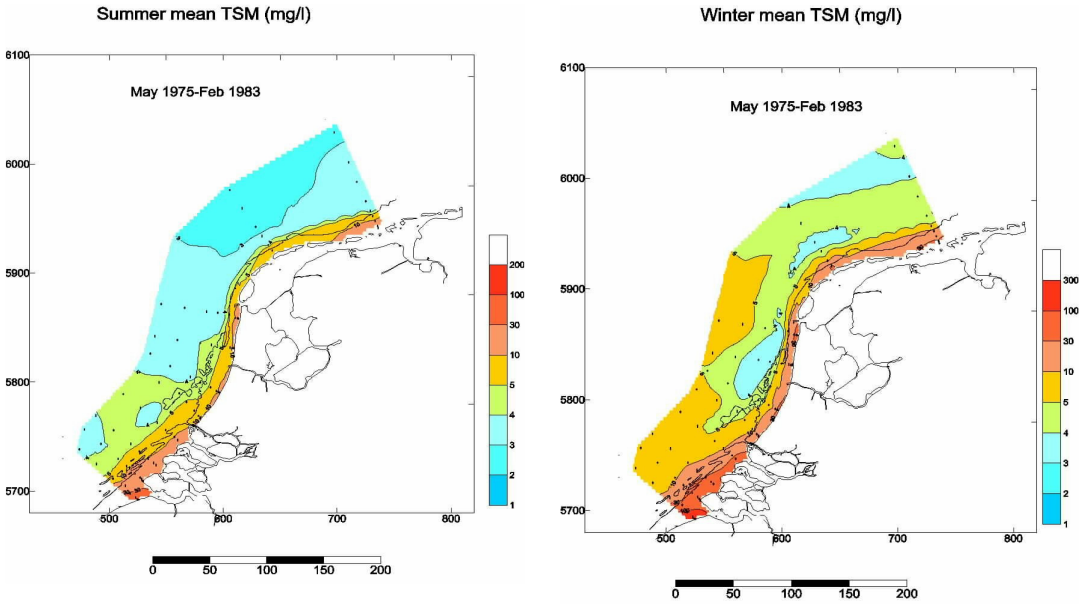

Figure 2.3: Example of cross-shore salinity and SPM (=TSM) distribution after Suijlen and Duin (2001)

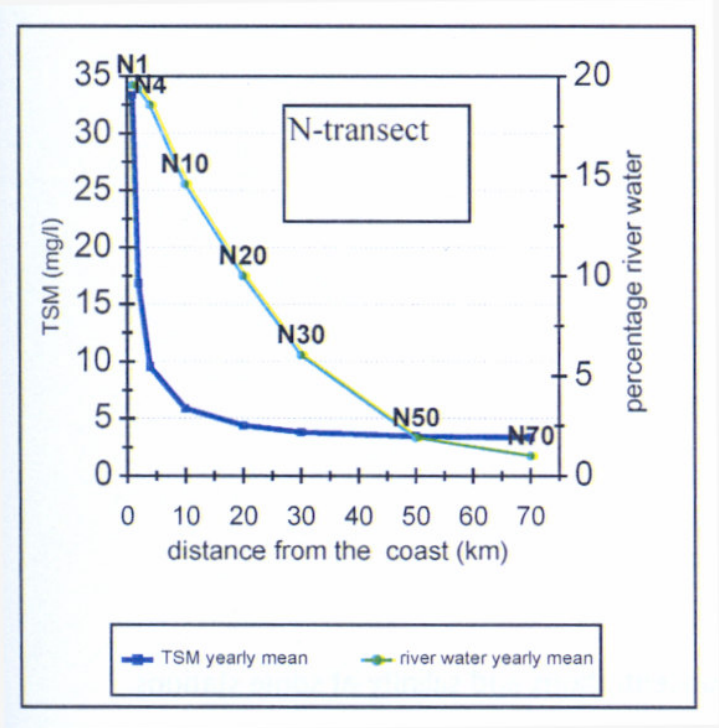

Torenga (2002) reported a preliminary study on the transport of fine sediment by wave-induced effects in the breaker zone, a zone of 400 – 600 m wide along the uninterrupted Dutch coast. From this study two more important conclusions can be drawn:
During storm conditions, the residual, wave-induced (northern) flow velocities are an order of magnitude larger than the tide-induced residual flow velocity (e.g. MARE, 2001 and Torenga, 2002). It is estimated that the weighted yearly sediment transport in this breaker zone is about two to three times larger than the tide-induced transport,
The large wave-induced residual flow velocities also imply a travel time in the breaker zone along the uninterrupted Dutch coast during storm conditions of about one week only (if not weighted for occurrence and frequency of the storms).

The observations from field data imply that fine sediments must be buffered in the seabed during calm weather conditions, to be mobilised during storm conditions: transport times are too large to explain a simultaneous increase throughout the coastal system, with the possible exception of the breaker zone. These observations lead to the following conceptual picture:

- Fine-grained cohesive sediments are eroded from the French cliff coasts. The erosion rate can be expected to correlate with storm conditions. Hence, the supply of fine-grained cohesive sediments will have seasonal effects. However, no detailed information is available on the seasonal variation in sediment supply form the cliff coasts.
- These sediments are transported in suspension by tide- and wind-induced currents in northern direction towards the Dutch coastal zone. Part of this transport is intermittent, as sediments are (temporarily) trapped in the sea arms of the Zeeuwse Delta and the ebb tidal deltas. During storm conditions, the fine sediments

deposited in and behind the ebb tidal deltas are remobilised to be transported further north. As a result the net travel time in the southern part of the Dutch coastal zone will be considerably larger than the one to two months mentioned above.
- Sediments are also temporarily trapped in the turbid area around the Port of Zeebrugge, where a circulation cell is formed by tidal stresses. Wind stresses and/or waves release sediments from this cell, to be transported further north (and into the Western Scheldt). Note that this process is not yet fully understood, but the current view is that the Flemish Banks themselves, located in this turbid zone, do not form a net sediment source through erosion of the clay deposits in these banks.
- During calm weather conditions, part of the sediments is also buffered in the seabed, to be remobilised during storm conditions.

The conceptual picture is substantiated by an analysis of the siltation data in Rotterdam Port. Bhattacharya (2002) found that the same wave conditions during summertime resulted in larger siltation rates than during wintertime. This observation suggests that during summertime more sediment is stored in the seabed than during wintertime. From a few observations (e.g. FLYLAND-report on the impact of sand extraction) the concentration of fines in the upper part of the seabed is estimated at a few percent (1 – 5%). The buffer capacity in a coastal area of 10×200 km^2 and a (minimal) buffer thickness of 10 centimeters would amount (at least) to about 3 - 16 Mton. Note that the estimated amount of mud that is released during the construction phase of Maasvlakte 2 has the same order of magnitude (+/- 12 Mton). This already indicates that seasonal buffering could have an important effect on the dispersion of mud during the construction phase of Maasvlakte 2.

2.3 Mechanisms for water-bed exchange

A number of mechanisms can be identified that entrain sediment into the seabed. These are discussed below:

Waves (wind waves, swell and tidal waves)
Waves generate pressure fluctuations in the seabed, as a result of which pore water flow is induced and water over- and underpressures occur. As a result of these underpressures, fine-grained sediment is entrained into the seabed. This entrainment process is fairly complicated because of the oscillating nature of the forcing agents, and needs further research, as it is currently poorly understood. However, probably only longer waves are effective.

Note that the permeability of 200 µm sand, typical for the North Sea seabed amounts to about 10^{-6} m/s. This permeability drops rapidly by at least an order of magnitude when the clay content (%< 2 µm) increases up to 5 %, e.g. Figure 2.4. This implies that the entrainment rate of fine material into the seabed will decrease rapidly with increasing clay content. Hence, it may be expected that the amount of fine-grained sediment in the seabed is limited to a few percent. This conclusion is in agreement with the sparse observations.

Figure 2.4: Permeability as a function of clay content for various sand/silt/clay mixtures.

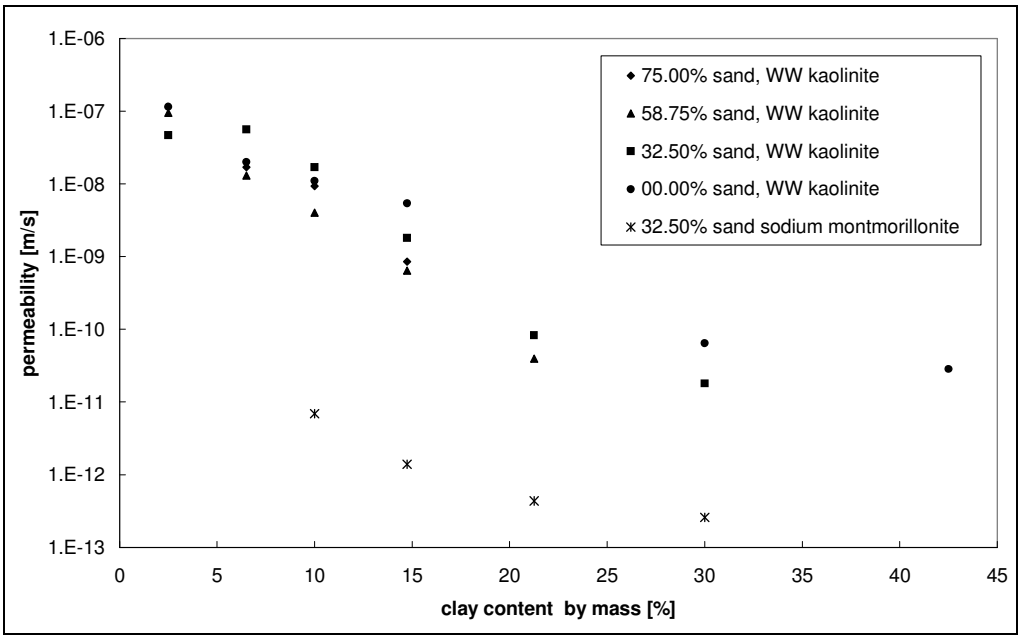

Pressure differences

The flow around/over bed irregularities, such as ripples and dunes, generates underpressures at the upstream sides of these irregularities and overpressures at their lee side. The literature describes empirical evidence that these pressures can generate groundwater flow within the bed irregularities, and can cause an influx of nutrients, ambient water and even algae into the bed (e.g. Thibodeaux and Doyle, 1987, and various papers by Huettel (e.g. Boudreau and Jorgensen, 2001). As an example, the flow patterns measured by Thibodeaux are presented in Figure 2.5.

Basically, these underpressures would also entrain fine sediments into the seabed, though at present no empirical evidence has (yet) been found in the literature. Moreover, the entrainment rate will slow down significantly when the permeability decreases with increasing silt content, as discussed before.

Figure 2.5: Flow lines in bed ripples as measured by Thibodeaux and Doyle (1987).

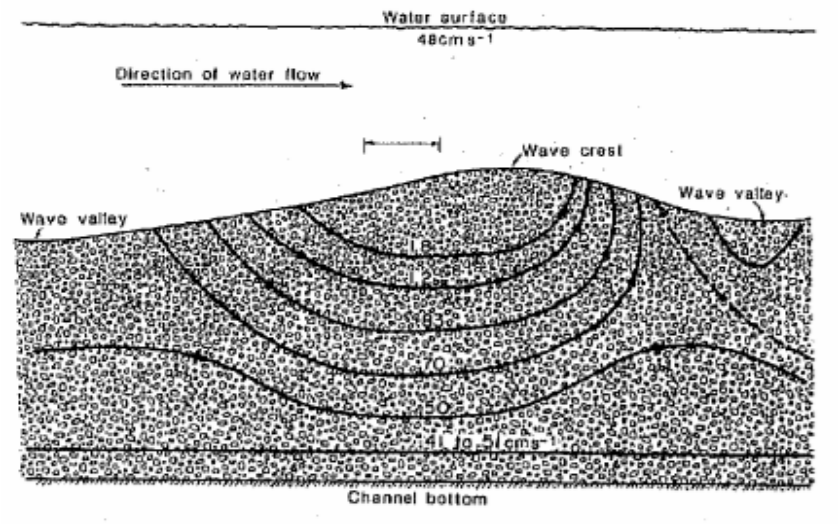

Burial en resuspension due to migration of sand bed irregularities
During calm flow conditions, fine sediments can settle and accumulate in the troughs of ripples and other bed irregularities. When the bed irregularities migrate, these fine sediments are buried. On the other hand, bed irregularities can also cause resuspension of fines.

Bioturbation
Fine sediment can be reworked and mixed over the upper part of the seabed by a number of organisms, a process known as bioturbation (Dankers, 2005). Typical mixing depths range from a few cm to about 1 dm. Bioturbation may result in fines contents larger than those resulting from the physical effects described above. The effects of bioturbation are expected to be larger during the summer than during the winter season, as biological activity increases with increasing water temperature.

Probably, a combination of these effects plays a role. With respect to the physical processes, it is likely that a combination of pressure-induced infiltration, trough accumulation and ripple/dune migration is an efficient agent entraining fines into the seabed. This process could be accelerated by biological effects.

Unfortunately, accurate descriptions of the mechanisms above are not available. Hence, we will follow a semi-empirical approach in the next section to derive relationships for the seasonal water-bed exchange.

2.4 Model formulations

2.4.1 Situation

We consider the following schematic situation with a water column with depth h, a layer at the bed surface with depth δ_1 and a bed layer with thickness δ_2 in a domain with surface area A (Figure 2.6). Fine sediment depositing in the near-bed layer can be remobilized by tidal currents, fine sediment entrained into the bed can be released during storm conditions only. The amount of fines in the near-bed layer is not limited, but shall not be large in general. No fines accumulate in the near-bed layer throughout a

spring-neap cycle. The amount of fines that can be entrained into the bed is limited by the permeability of the bed, and limited to p_{cr}. Within the 1DV domain, fines are released at a rate of S [kg/s], because of sand extraction and fines are transported into the domain from the outside world, which is characterized by a concentration c_0 and a diffusion coefficient k [m^2/s]. All concentrations are by mass [kg/m^3]. Of course, c nor p can become smaller than zero.

Figure 2.6: Sketch of model set-up

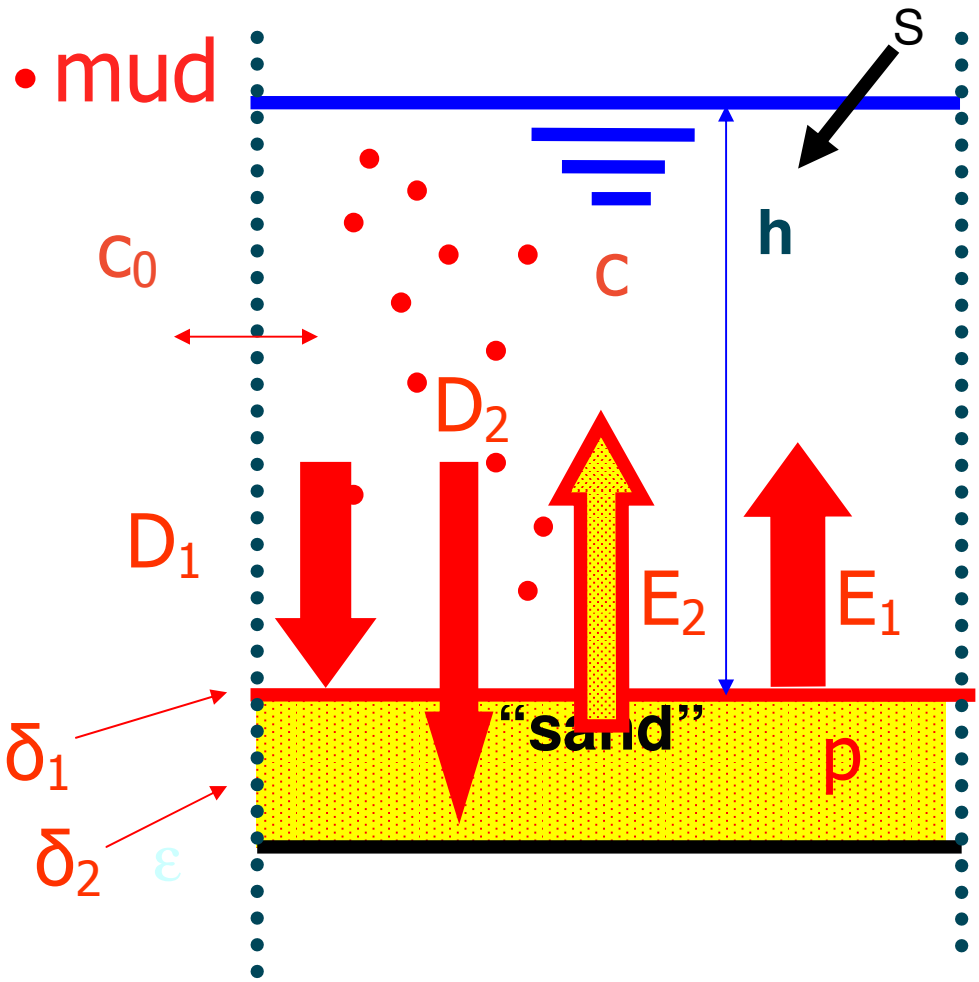

Then we have the following balance equations for the three layers (water column, bed surface indicated with "1", and sediment bed indicated with "2"):

$$h\frac{\partial c}{\partial t} = E_1 - D_1 + E_2 - D_2 + k(c_0 - c) + S \tag{2.1}$$

$$\rho_{dry}\delta_1\frac{\partial p_1}{\partial t} = D_1 - E_1 \tag{2.2}$$

$$\rho_{dry}\delta_2\frac{\partial p_2}{\partial t} = D_2 - E_2 \tag{2.3}$$

with concentration c, depth h, erosion E, deposition D, density of silt ρ_{dry}, silt volume percentage in a layer p and layer depth δ. The subscripts 1 and 2 refer to layer 1 (bed surface) and 2 (sediment bed). The model formulations of the vertical exchange processes (D_1, E_1, D_2, E_2) are described in section 2.4.2 and 2.4.3.

2.4.2 Erosion formulations

For the erosion of the first layer, the near bed layer, the formulation of Partheniades is used (see e.g. Van Rijn, 1993). This concept is disputable as it is formulated for a 100% silt layer, instead of the sand layer with ca. 2,5% silt (see assumption paragraph 1.4) we are dealing with. However, a better alternative is not available at this moment:

$$E_1 = p_1 M_1 \left(\frac{\tau_b}{\tau_{e,1}} - 1 \right) H\left(\frac{\tau_b}{\tau_{e,1}} - 1 \right) \tag{2.4}$$

with the erosion flux E, the erosion rate M, the bed shear stress τ_b and the critical erosion shear stress τ_b. The Heaviside function, H, equals 1 when the argument is larger than 0, and equals 0 when the argument is less or equal than 0.

The erosion of the surface layer is scaled with the silt percentage in that layer so that only that percentage of surface layer can erode. This turned out to be necessary to simulate the so-called leakage time scale (see also Chapter 3). Furthermore this change made the formulations linearly scalable.

> A linearly scalable model has the advantageous property that for relatively small percentages of silt (< 15%) the transport of silt due to dredging can be simulated separately from the transport of background silt, and that the results scale with the disposal rate. No new simulations are therefore required for a change in production rate.

For the wave-induced erosion from the sediment bed during storm we use Van Rijn's empirical pick-up function yielding for particles in the range of 130 to 1500 µm as a first guess:

$$E_2 = p_2 M_2 \left(\frac{\tau_b}{\tau_{e,2}} - 1 \right)^{1.5} H\left(\frac{\tau_b}{\tau_{e,2}} - 1 \right) \tag{2.5}$$

with

$$M_2 = 3.3 \cdot 10^{-4} \rho_s \left((s-1) g d_{50} \right)^{0.5} D_*^{0.3}$$

with the specific density $s = \rho_s/\rho_w$ and the dimensionless diameter $D_* = d_{50}[(s\text{-}1)g/\nu^2]^{1/3}$, the sediment density ρ_s, the sand diameter d_{50}. During calibration it appears that the value of 3.3×10^{-4} in eq. (2.5) has to be adapted drastically to obtain a good correlation with the measured data. Hence, the link with the original Van Rijn formulation is not valid anymore. The exponent of 1.5 in eq. (2.5) is not changed, although comparable results

could possibly have been obtained with other values in combination with other erosion rates M_2.

Note that the erosion formulation of layer 1 eq. (2.4) is linearly scalable with the silt percentage of layer 1. The same holds for layer 2, see eq. (2.5).

A final remark is made about the physical evidence of the presented formulations. The erosion formulations for the surface layer and the bed layer have a high empirical character. There is for example no sound physical basis for the used exponents. There is however no more evidence for a better physical foundation. Fortunately, these empirical formulations turned out to represent the important features of the CEFAS measurements at Noordwijk 10.(-10 m depth) concentration data surprisingly well. Nonetheless, additional observations are required to obtain a better physical foundation.

2.4.3 Deposition formulations

The deposition of mud on the bed surface is given by:

$$D_1 = (1-\alpha) w_s c \tag{2.6}$$

The entrainment of fines into the sediment bed is given by:

$$D_2 = \alpha w_s c \tag{2.7}$$

with the deposition rate D, the settling velocity w_s and the coefficient α. The combination of eq. 2.6 and eq. 2.7 results in a total deposition flux ($D_1 + D_2 = D_{tot} = w\ c$). Note that this flux does not include a critical shear stress for deposition as it is the case in the classical deposition formulation of Krone (see e.g. Van Rijn, 1993).

The coefficient α in eq. (2.6) and (2.7) describes the distribution of deposited sediment between the surface layer and the sediment bed. We assume that the entrainment into the sandy North Sea seabed according to eq. (2.7) only occurs if the mud percentage of the seabed is below a certain threshold value (p_{crit}). Above this value, we assume that no mud can be entrained in the seabed. Hence, we apply $\alpha = 0$ for $p > p_{crit}$.

2.4.4 Overview of parameters

The two-layer model in Section 2.4 includes several parameters that have to be calibrated against field data. These parameters are listed below:

- erosion shear stress surface layer ($\tau_{e,1}$);
- erosion rate surface layer (M_1);
- erosion shear stress sediment bed ($\tau_{e,2}$);
- thickness of sediment bed layer (δ_2);
- entrainment coefficient (α);
- settling velocity (w_s).

These coefficients are calibrated against data. This is described in the next section.

2.5 Calibration and validation

2.5.1 Approach

The two-layer model from Section 2.4 has been calibrated with the CEFAS Smartbuoy data for Noordwijk 10 km. These data consist of surface SPM concentration measurements with a high temporal resolution (every hour) over a period of more than one year (2000 – 2001). This enables a calibration of settings for vertical sediment exchange on both short and long timescales. In addition to the CEFAS data, also some observations by Laane *et al.* (1999) were used on the mud percentage of the seabed.

In this section, only the main aspects of the calibration are considered. The calibration was carried out using a 3D box model with DELFT3D. The box consists of 20×1 grid cells in horizontal direction and 10 vertical layers. The distribution of the vertical layer is: 4.0, 5.9, 8.7, 12.7, 18.7, 18.7, 12.7, 8.7, 5.9 and 4.0%. So the upper layer has a thickness of 4% of the total thickness of the box. For example, at a water depth of 15 m, the thickness of both the surface and the near-bed layer is 0.6 m (0.04*15).

The horizontal grid size is 2.5 km, so the box length is 20×2.5 = 50 km. The box width of 1 km is arbitrary. The water depth is 15 m. In the box model, the bed shear stress by waves was calculated from the measured wave height and wave period at Meetpost Noordwijk for the calibration period (2001). The Swart formulation was used with wave roughness height 0.05 m and water depth 18 m. This formulation is equivalent with the formulations proposed by Jonsson (see Van Rijn, 1990). The current-induced bed shear stress was calculated from the depth-averaged velocity from the ZUNO-coarse model at Noordwijk 10, assuming a logarithmic velocity profile. The current-induced roughness height was set at 0.1 m, which is equivalent with C = 60 $m^{1/2}$/s at a depth of 18 m.

The schematized model is applied in two ‘modes’:
1. with open boundaries at which a time-averaged concentration is prescribed;
2. with closed boundaries and with a prescribed sediment mass (in kg/m^2) as initial condition in the systems.

For mode 1, the sediment influx equals the product of the concentration boundary condition and the tidal velocity at Noordwijk 10, the sediment out-flux equals the product of the computed concentration at the out flowing boundary and the tidal velocity at Noordwijk 10. For mode 2, the sediment in- and out-flux is zero, due to the closed boundaries.

Sedimentation and resuspension within the box is governed by the bed shear stress as a function of time. For mode 1, transport within the box occurs by advection (tidal velocity at Noordwijk 10) and diffusion, for mode 2 by diffusion only. The horizontal diffusion is set at 1 m^2/s.

The time-averaged value of the CEFAS concentration data for Noordwijk 10, year 2001 is 4.3 mg/l. For mode 1 a constant boundary concentration of 7.5 mg/l was used, however. The reason for this is that the depth-averaged sediment flux into the box model is substantially underestimated if the suspended sediment concentration near the surface is used as a proxy for the depth-averaged concentration. The CEFAS Smartbuoy data have been collected at a depth of 1 m below the water surface. The application of a depth-averaged boundary concentration of 7.5 mg/l results in a

computed time-averaged concentration of 4.1 mg/l at a depth of 1 m below the water surface, which is close to the measured average of 4.3 mg/l.

2.5.2 Results

Various model settings have been applied to the schematized box model and tested against the CEFAS measurements. The proper order-of-magnitude parameter values were determined with analytical expressions for the behaviour of the two bed layers for idealized bed shear stress conditions, targeting for a realistic reproduction of the average SPM concentration and its fluctuation because of the tide and storms. This is not discussed hereinafter. Fine-tuning of the settings was carried out with the actual time series on bed shear stress. The maximum mud fraction in layer 2 was set at 15% but this value has never been reached during the calibration. The final calibration results are shown in Figure 2.7. The applied settings are shown in Table 2.1:

Table 2.1: Final setting after calibration with the schematized box model.

Parameter	Value	Units
$\tau_{e,2}$	1.5	Pa
M_2	$3.5\ 10^{-7}$	$kg/m^2/s$
$\tau_{e,1}$	0.3	Pa
M_1	$5.6\ 10^{-7}$	1/s
w_s	0.25	mm/s
d_2	0.15	m
α	0.1	-
p_{max}	0.15	-

Figure 2.7: Calibration result for CEFAS data Noordwijk 10, year = 2001 ('measured') and the DONAR data. Note that data between 6/8 and 21/8 are probably erroneous. Boundary concentration = 7.5 mg/l (depth-averaged, mode 1). Bed thickness = 0.15 m.

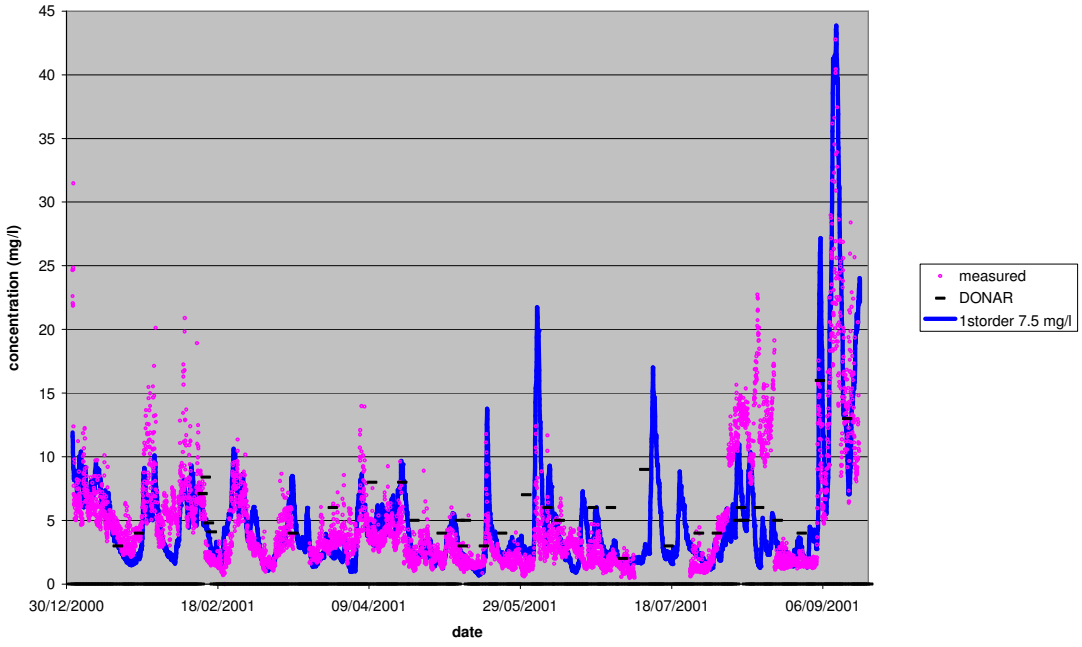

Figure 2.8: Mud fraction in seabed. Bed thickness = 0.15 m. Range approx. 0.6%. See Figure 2.7 for simultaneous SPM concentration.

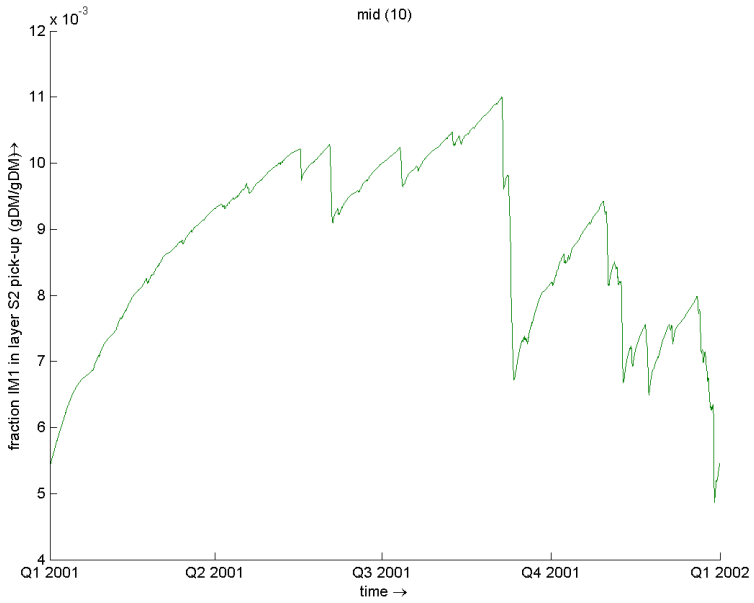

The final calibration results show that with the model formulations applied, the measured suspended sediment concentration is reproduced quite well. The mud fraction in the bed ranges between 0.5 and 1.1 % over the year, which is assumed to be realistic. The amount of mass available in the system at equilibrium is about 3.5 kg/m^2, of which typically only 0.1 kg/m^2 is in suspension.

An important observation is that from the CEFAS data, the typical amount of resuspendable mass cannot be determined. If the thickness of the (2nd) bed layer is doubled, the concentration response in the water column does not change (see Figure 2.9), whereas the available mass nearly doubles. The thickness of the bed layer and its equilibrium mud percentage can be calibrated with observations on the mud fraction in the sea bed as a function of time and depth. Unfortunately, this data is not available. By Laane et al. (1999), an active depth of 0.4 m and a typical mud percentage of the North Sea bed of 1–2% are mentioned. This implies a sediment pool of 6 to 12 kg/m^2. Laane et al. (1999) mention a typical residence time of mud in the seabed of about 2 years. The exchange between the sediment surface and the sediment buffer layer is therefore of the order of 3 to 6 kg/m^2/yr. Note that this estimate depends on an assumed flux of suspended matter of 10–25 MT/yr along the Dutch coast.

It should be noticed that the DONAR concentration data is significantly higher than the CEFAS concentration data (both measurements) for the summer period, see Figure. 2.7.

Figure 2.10 shows the concentration response for a closed system with a sediment mass of 7 kg/m^2 ('mode 2') The similarity between the blue lines in Figure 2.10 and Fig. 2.7 demonstrates that the suspended sediment concentration response in the water column is dominated by local vertical exchange. Notwithstanding, the available sediment mass at a certain location is on the long-term determined by both sediment supply and the local bed shear stress 'climate'.

Figure 2.9: Concentration as a function of time; blue: bed thickness 30 cm; red: bed thickness 15 cm (hardly visible because of strong overlap with blue curve).

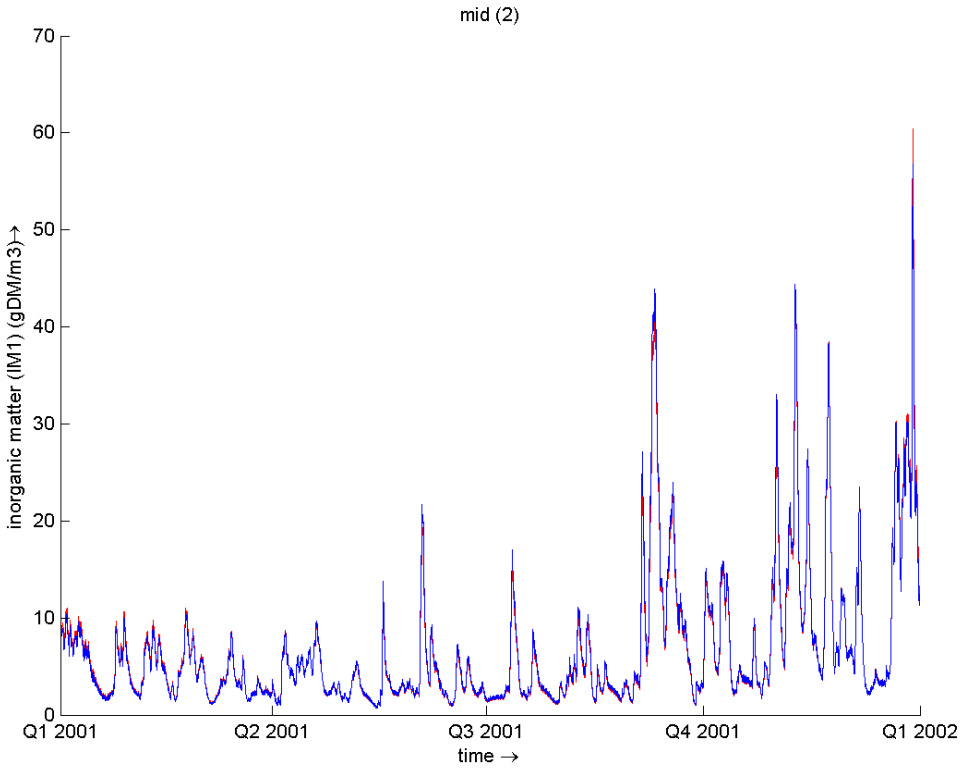

Figure 2.10: Calibration result for CEFAS data Noordwijk 10, year = 2001. Note that data between 6/8 and 21/8 are probably erroneous. Closed system, mass = 7 kg/m^2 (mode 2). Bed thickness = 0.30 m.

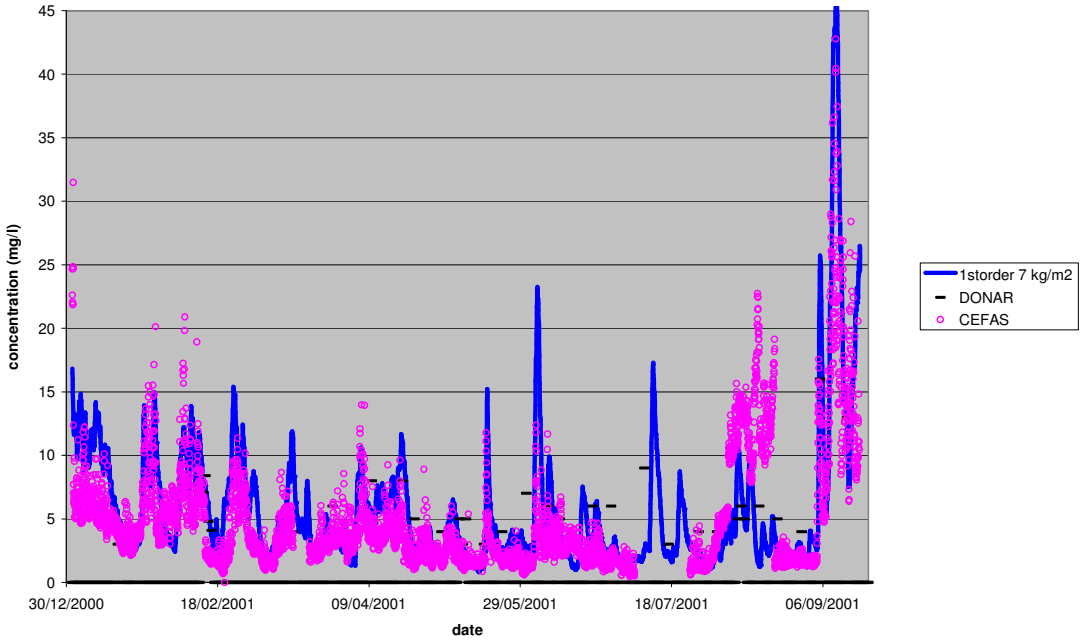

Figure 2.11: Mud fraction in seabed. Bed thickness = 0.30 m. Range approx. 0.4%. Maximum buffer capacity = 7 kg/m^2. See Figure 2.10 for simultaneous SPM concentration.

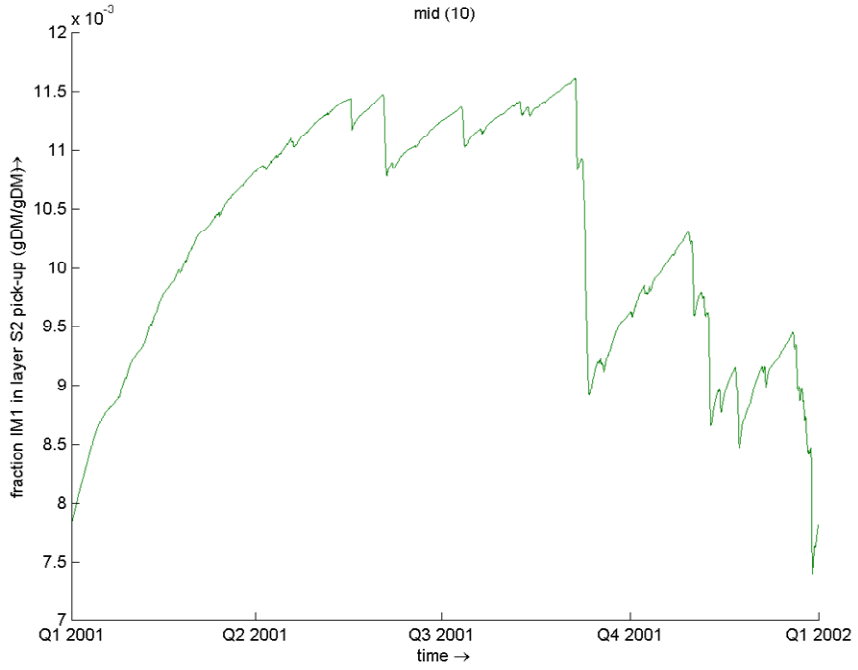

In this chapter the concept was used in the framework of a 1DV model. The calibration is carried out with a two-dimensional model in Chapter 3. Explicit attention is paid to the performance of the proposed water bed exchange concept on different timescales (tidal, neap and spring tide cycle, storm events and the seasonal timescale). Furthermore the spatial behaviour is validated with the silt atlas (Suijlen and Duijn 2001). A validation with the three-dimensional model is carried out with the DONAR measurements (www.donarweb.nl).

2.5.3 Conclusions

Based on the calibration of the two-layer model on the CEFAS-data, it is concluded that:

1. The two-layer model reproduces the measured SPM concentration data well. Hence, this two-layer model is applied in the effect scenarios in Chapter 5. It should be noted that the parameters settings are derived for a schematized situation. After application for a more complex situation, it appeared that these parameter settings have to be adapted slightly (see Chapter 3 and 4).
2. The CEFAS-data alone are insufficient to result in a unique set of parameter settings. Setting with a completely different total mass per unit area may show the same SPM concentration response. Additional data on the evolution of the mud percentage in the seabed is required as well, which is scarce. In the present calibration, a layer thickness of 30 cm and an equilibrium mud percentage of 1% has been assumed, which yields a sediment mass of approximately 5 kg/m^2. To account for this uncertainty, settings with 2.5 and 10 kg/m^2 have also been applied for the impact calculations discussed in Chapter 5.

3 MODEL SET-UP AND CALIBRATION WITH FINEL2D

3.1 General

As described in Chapter 1, two different ways are followed to determine the effect of sand extraction on the concentration of silt in the water. In this chapter the two-dimensional approach with high spatial resolution is followed, in contrast to the three-dimensional model with low resolution as described in Chapter 4. A three-dimensional approach with high spatial resolution would have lead to unacceptably long simulation times.

The validity of a numerical model in the context of civil and environmental engineering is highly determined by the level of calibration and validation, as not all processes are yet understood nor could be captured by a workable numerical model. A significant part of the study is therefore spent on this calibration and validation. Firstly, the hydrodynamic part is validated; secondly, the transport model for silt is tuned.

This chapter is built up as follows. First, the hydrodynamic calibration and validation is discussed in Section 3.2. A more thorough description is given in Appendix C. Secondly, the set-up, calibration and validation of the silt model is described in Section 3.3. Finally conclusions are drawn in Section 3.4.

3.2 Hydrodynamics

The hydrodynamic part of the FINEL2D model is based on the depth- and wave-averaged shallow water equations, consisting of a mass and two momentum conservation equations. Such a model is suitable to simulate the flow in rivers, estuaries and coastal seas. External forcings like wind, waves and air pressure can be imposed, whereas water levels, current velocities or discharges can be imposed as boundary conditions. In the presently applied explicit version of the model, horizontal mixing is not taken into account.

The governing equations are solved numerically by means of the finite elements method (FEM). A typical difference with the finite difference method (FDM) is the fact that FEM utilizes triangular elements, whereas FDM uses rectangular elements. The physical variables (water levels and current velocities) are represented by discrete values in the centre of each element. Sediment transport and bed change modules can be coupled to the hydrodynamic module, enabling the assessment of morphological changes due to the transport of sand and/or silt.

A more detailed description of the FINEL2D modelling software and the underlying physics can be found in Appendix C.

Based on partly contradicting considerations as computational time, availability of boundary conditions, desired resolution and size of the model domain, a computational grid is constructed, see Figure 3.1. The domain of this grid corresponds with the domain of the ZUNO model. Boundary conditions for this model are derived from nesting in a continental shelf model (CSM). The element size varies over the grid. Along the Dutch coast, the surface of the triangles is relatively small, viz. 0.6-0.7 km^2, corresponding to a characteristic length of 1.1 km. This is demonstrated in Figure 3.1b, depicting a detail of

the model domain. In the northern part of the North Sea and the western part of the British Channel, the surface of the triangles is relatively large, viz. 50 km^2, corresponding to a characteristic element length of 10 km. Altogether, the computational grid consists of approximately 51,000 elements spanned by 26,000 nodes.

The underlying bathymetry is constructed using the 1999 bathymetries of a number of WAQUA models of Rijkswaterstaat, viz. Zeedelta, Kustzuid, Kuststrook and ZUNO. The FINEL2D bathymetry is gradually build up using these bathymetries in decreasing order of resolution, starting by Zeedelta and ending with the bathymetry of the ZUNO model. The resulting bathymetry, together with the water level stations used for the hydrodynamic calibration, is shown in Figure 3.2.

Figure 3.1: The computational grid of the FINEL2D model of the southern North Sea

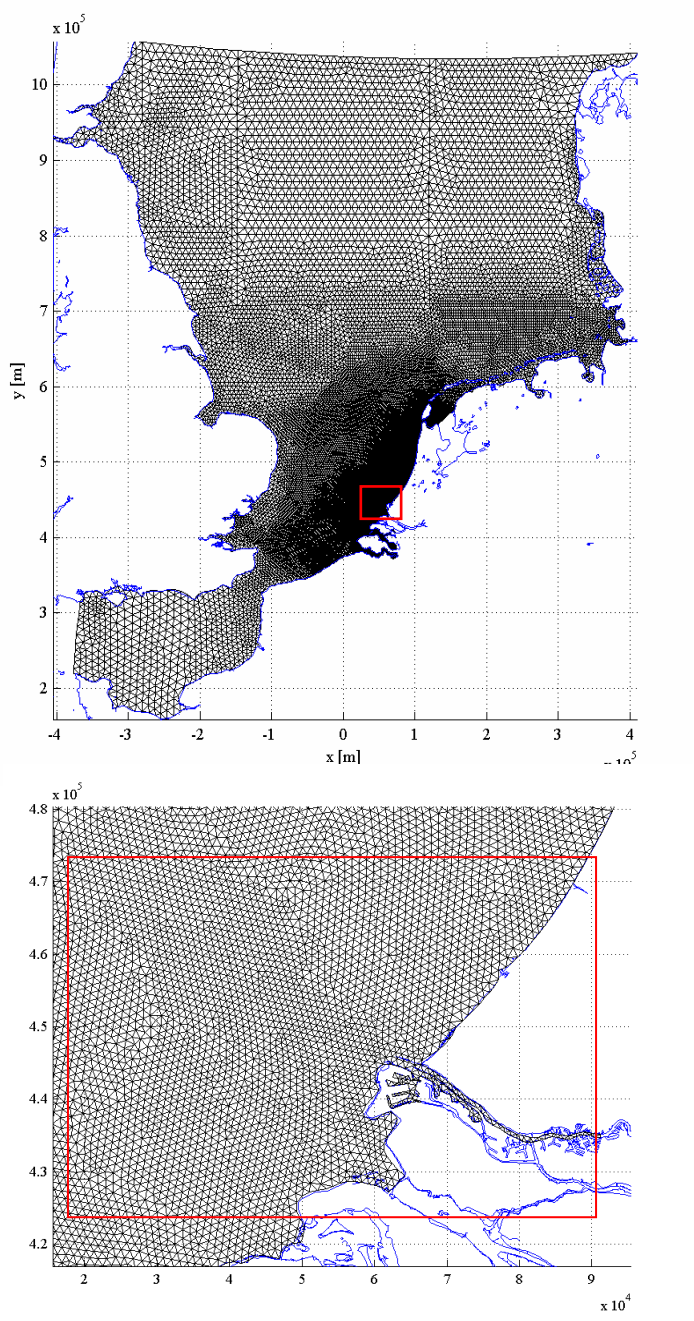

Figure 3.2: Bathymetry of the FINEL2D model, together with the location of the water level stations that have been used for the calibration. Depth is given in m. 1: Aukfield, 2: K13A, 3: Euro platform, 4: Lichteiland Goeree, 5: Scheveningen, 6: Meetpost Noordwijk, 7: Texel Noordzee, 8: Terschelling Noordzee and 9: Dover.

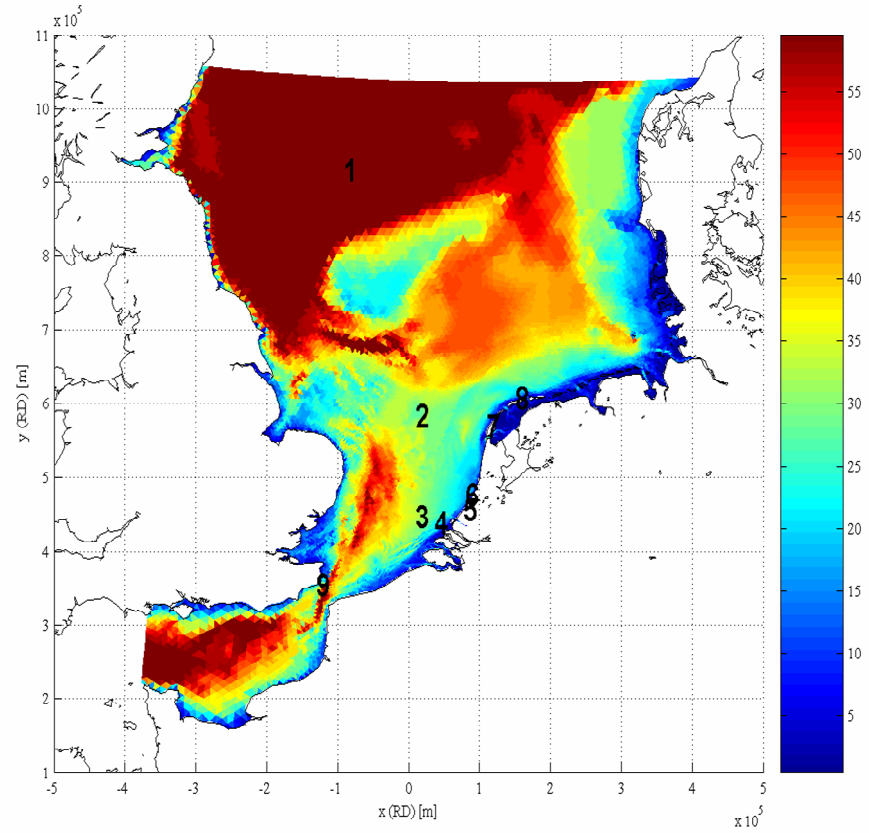

The hydrodynamic calibration is an iterative process, using both measured and computed data. Residual discharges have been used as a check, rather than a quantity for calibration.

Water levels:	Astronomical water levels in various stations 'measured' and computed between June 22 and August 22, 1992.
Current velocities:	Measured current velocity profiles and computed depth-averaged current velocities in Noordwijk 12 between June 22 and August 22, 1992.
Residual discharges:	Long term measured residual discharges are taken from literature. Computed residual discharges are based on the period January-October 2002.

This calibration process has resulted in a number of choices and adjustments in order to minimize the difference between measured and computed water levels and current velocities. These differences are caused by, among others, errors in the boundary conditions, uncertain bottom levels and uncertain values of physical parameters like the bed friction coefficient.

The first iteration loops yielded a choice for the Manning roughness formulation together with a roughness coefficient of 0.025. Furthermore, two minor adjustments of the boundary conditions yielded significantly better results. The first is an adjustment of the phase of the M2 component on the northern model boundary of 12 minutes. This adjustment is justified by the fact that a small error in the location of the M2 amphidromic system is predicted with the CSM model, resulting in a significant error in the phase of the M2 component imposed on the northern boundary. The second adjustment is an overall adjustment of the phase, which is in fact a shift of the reference time rather than an adjustment of the boundary condition.

Figure 3.3: Differences between measured and computed amplitudes and phases of the M2 tidal component.

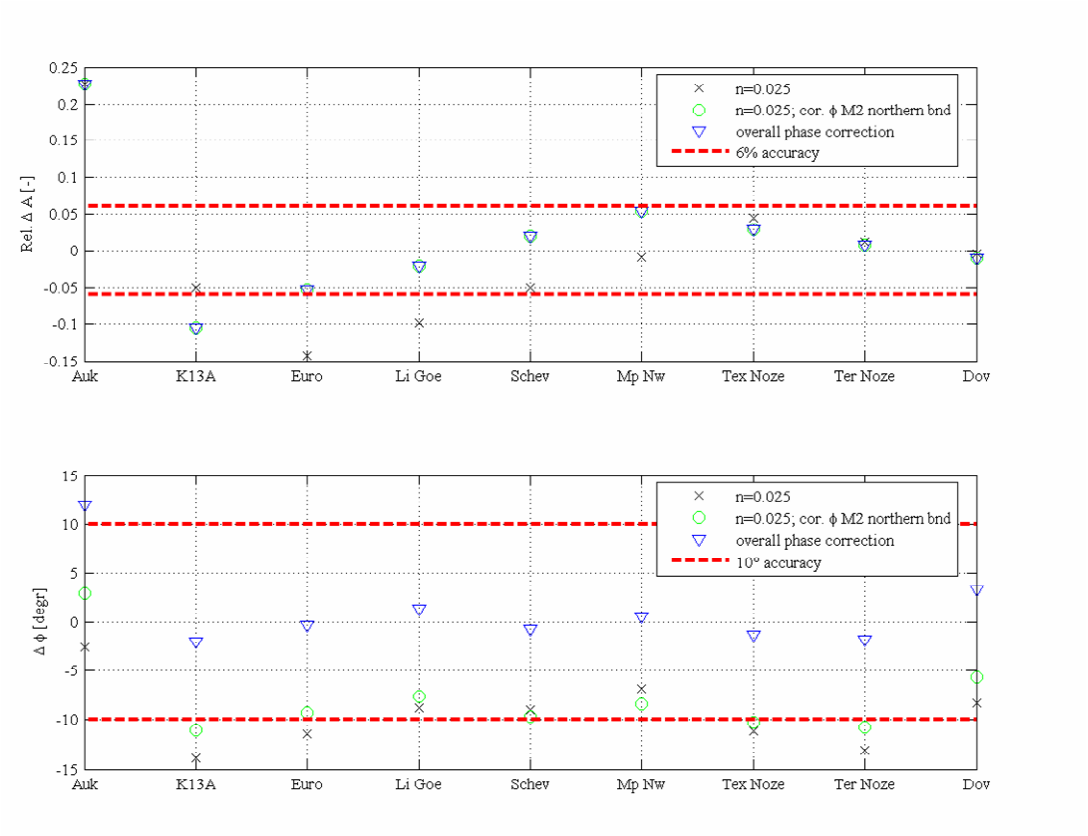

Figure 3.3 illustrates the effects of these adjustments on the difference between the computed and measured amplitudes and phases of the M2 tidal component in various stations. The range between the two dashed red lines in Figure 3.3 represents the achievements of a previous model study which are taken as a target, see De Goede and Van Maren (2005). If the difference between the computed and measured amplitudes and phases falls within this range, the model behaves sufficiently well. Figure 3.3 demonstrates that for the majority of the stations, viz. the stations that are in or close to the area of interest, the model behaves well regarding the M2 tidal component, since the amplitudes are generally predicted with an error less than 6% and the phases with an error less than 10°.

Similar analyses have been done for the M4 water level component and the M2 current velocity component (depth-averaged; the measured current velocity at a distance 0.4h

above the bed is assumed to be representative of the measured depth-averaged current velocity). The velocities have been considered in both north-south/east-west (NS/EW) and in longshore/cross-shore (LS/CS) direction, obtained by assuming an angle of 28° between the coast and true north. Note that the results of the worst achieving stations have been included in this table. Besides, the residual discharges through the Dover Strait and the Marsdiep (between Den Helder and Texel) have been considered as well.

Table 3.1: Hydraulic model performance

Parameter				Target		Performance	
Water levels along	Amplitude M2			<6%		<6%	
Dutch coast	Phase M2			<10°		<3°	
	Amplitude M4			<25%		<16%	
	Phase M4			<25°		<18°	
Velocities in Noordwijk 12 in 1992	Amplitude M2	NS	EW	<10%	<10%	<2%	<3%
		LS	CS	<20%	<20%	<12%	<75%
	Phase M2	NS	EW	<10°	<10°	<10°	<7°
		LS	CS	<20°	<20°	<5°	<20°
Net tide-driven discharge through Marsdiep source: Ridderinkhof et al. (2000)				O(2000) m^3/s		O(1200) m^3/s	
Net tide-driven discharge through Dover Strait source: Prandle et al. (1996)				O(40,000) m^3/s		O(26,000) m^3/s	
Net total discharge through Dover Strait source: Prandle et al. (1996)				O(100,000) m^3/s		O(100,000) m^3/s	

Regarding the results summarized in Table 3.1, the following remarks can be made:

- Even the poorest achieving stations yield M2 and M4 water level amplitudes and phases meeting the desired target quite well.
- The amplitudes and phases of all but one M2 velocity components are also well in the range of desired accuracy.
- Only the M2 amplitude of the cross-shore current velocity behaves poorly, but this can easily be explained by the fact that cross-shore velocities have large gradients in vertical direction, caused by processes that are not incorporated in the depth-averaged FINEL2D model. Furthermore, since the cross-shore velocities are very small, a small error already yields a large relative error.
- The net tide-driven discharge (i.e. the discharge without meteorological effects) can not be measured directly. These values have to be deduced indirectly and are therefore subject to significant uncertainties. These figures, therefore, have to be used indicatively. Taking this consideration into account, the model achieves rather well regarding the residual discharges: both the direction and the order of magnitude of the residual discharges are predicted fairly well.
- The net total discharge (i.e. including meteorological effects) through the Dover Strait is predicted very well by the model. It has to be remarked that at least 300 tides have to be taken into account in order to obtain a reliable prediction of the total residual discharge.

Considering these results, it can be concluded that the FINEL2D model of the southern North Sea is sufficiently well calibrated in order to give reliable predictions of the spreading of silt, as far as the hydrodynamics are concerned.

3.3 Set-up and calibration of the silt model

3.3.1 Introduction

The set up and calibration of the silt model has been an iterative process of translating physical concepts into numerical formulations and testing these against available data. First the set up of the silt model is described in Section 3.3.2. Next, the calibration is discussed. The data used for this testing were the time series of silt concentrations near the surface at NW10 for 2001, located 10 km seawards of the city Noordwijk (Section 3.3.3). Finally the results were validated in Section 3.3.4 against the measurements as given in the silt atlas of the Southern North Sea (Suijlen & Duin 2002).

3.3.2 Model set up

For the simulation of the transport of silt in the water column, an advection diffusion equation has to be resolved. To do so the silt module of FINEL2D is applied. For this study, the formulations as discussed in Chapter 2 have been implemented in FINEL2D. At each time interval the following steps are taken:

1. The concentration for the new time step is computed with an implicit numerical scheme for the advection diffusion equation, using the flow fields as input.
2. The shear stresses are computed, based on flow and wave fields, determining the erosion and deposition.
3. The concentration and the bed composition of both layers are updated explicitly with the erosion and deposition fluxes.

Essential for the interaction between the sea bed and the water column is the bottom shear stress, which is determined by flow and waves:

1. The flow is modelled for the year 2001 with the calibrated flow model as described in Section 3.2 and Appendix C. The result is a set of hourly flow fields containing the velocity and water level. These are translated to flow-induced bottom shear stress fields.
2. Wave fields are constructed from the wave measurements of Meetpost Noordwijk. At intervals of 4 hours a uniform wave field is imposed. These wave fields contain the wave height and the wave period. In shallow areas, the wave heights are adjusted by applying the breaker criterion of $H_s<0.7D$. The wave-induced bottom shear stress is determined by means of the linear wave theory.

The total bed shear stress is the sum of the flow-induced and wave-induced bed shear stress. A scheme of the silt model is given in Figure 3.4.

Figure 3.4: Scheme of the silt model

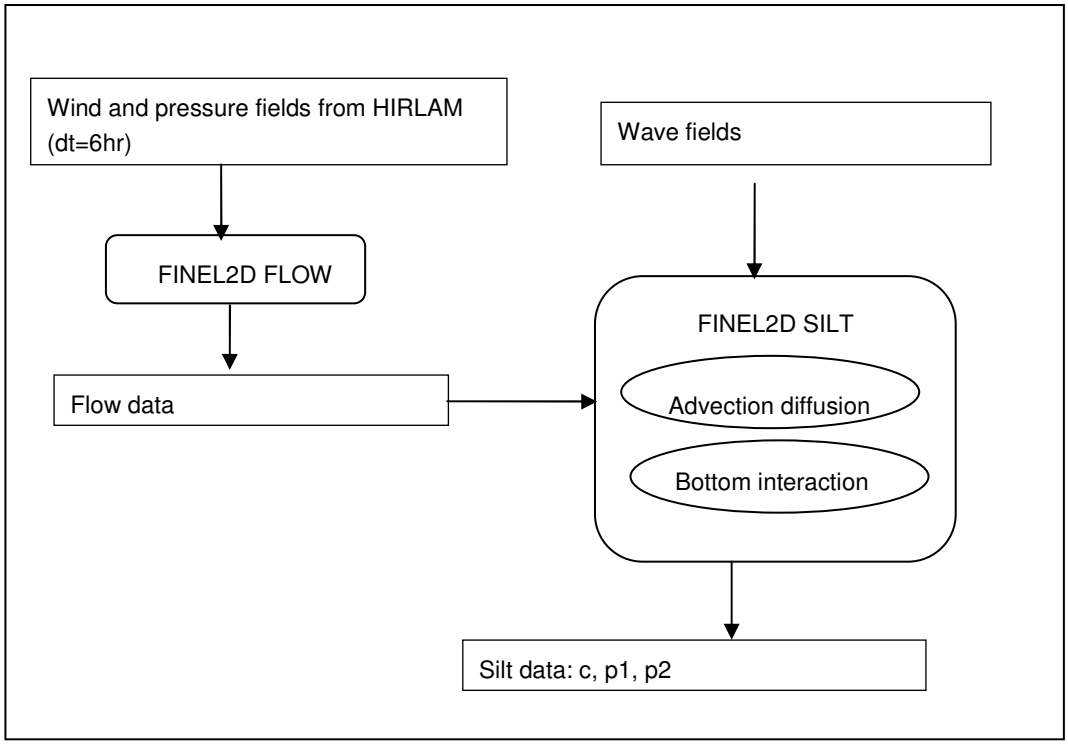

3.3.3 Calibration of the NW10 data

For the calibration of the model, the measured and computed concentrations near the surface of the water column are compared. The figures of this section are presented in Appendix D. The simulated depth-averaged concentrations are therefore translated to a concentration near the surface, using the instantaneous Rouse profile. The measured concentration and the computed total shear stress, containing the flow and wave contributions, are given in Figure D.1-D.2. There is some coherency between these time series. The fluctuations can be separated in different time scales:

- Tidal fluctuations (Figure D.3). These fluctuations are stronger during spring tide than during neap tide. The strongest tidal fluctuations are found during storm conditions.
- Spring-neap tide fluctuations (see Figure D.4). During spring tide the concentrations are higher than during neap tide. The time scale of these fluctuation is 14 days.
- Seasonal time scale (see Figure D.5). The timescale is of the order of magnitude of months and is only present in the concentration time series. At the beginning of the year (winter) the concentrations are higher than during the spring/summer season. A better separation would be the mild period and the stormy period.
- Storm events. These events are present in both the shear stress and the concentration time series. The concentration increases rapidly and decreases after the storm in a few days.

Although no thorough analysis of measurement errors has taken place, it is assumed that the concentration between day 210- day 232 is unreliable (see figure D.1). There is no indication for this high concentration in the shear stress signal (see figure D.2). This high concentration can also be caused by other causes, like algae, dumping of dredged material, offshore wind or trawl nets used for fishing. Furthermore, the concentration

drops instantaneously at day 232 from 18 mg/l to 2 mg/l, which is considered unrealistic. Therefore, this period is left out of the comparison.

In Chapter 2, the concept of the water bed exchange is explained. A parameter set was determined with a simplified box-schematisation using DELFT3D. The parameters as derived in chapter 2 were used as starting point for the calibration of FINEL2D. The setting of these parameters did not appear to be optimal for the shear stresses applied in this part of the study. The discrepancies are mainly caused by a larger shear stress simulated by DELFT3D compared to the shear stress simulated with FINEL2D. A new set of parameters is therefore derived. This parameter set (see Table 3.2) is optimized in such a way that the above mentioned time scales of the concentration signal are captured:

- **Tidal fluctuations.** The tidal fluctuations are visualised in Figure D.3a for the whole period. A short period is depicted in Figure D.3b. There is some resemblance on this time scale. A similar order of magnitude (1-3 mg/l) is found. Fluctuations on two time scales are present. The tidal scale (ca 12.5 hours) is a result of the cross shore tidal velocity and the concentration gradient (higher concentrations near the coast, lower concentrations at sea). The half tidal scale (ca 6.25 hours) is caused by the variation in the vertical profile. During slack tide lower concentrations are found at the surface, the Rouse profile is less uniform over the depth. The influence of the vertical profile is made clear by also plotting the depth-averaged concentration.
- **Neap-spring tide fluctuations.** There is a clear neap-spring tide cycle in the shear stress and in the concentration signal. At spring tide, higher concentrations are found due to the higher shear stress. This cycle is best visualised by the running mean over 1 day, as shown in Figure D.4.
- **The storm events**. Storms result in higher waves, higher shear stresses and subsequently higher concentrations (up to 40 mg/l at NW10). After a storm, the concentration diminishes in a few days. The concentrations during and after storms are reproduced fairly well.
- **Seasonal timescale**. At the beginning of the year, the response of the concentration to the spring-neap tide cycle is stronger than after for example 150 days. There is however no evidence for this behaviour in the shear stress. This relatively long time scale, in the order of months, is visualised by a running mean over 14 days, Figure D.5. As the measured data is not continuous, some periods have no value. It is noted that this time scale can only be simulated with a multi-layer and scalable model. The process can be interpreted as a leakage of silt from the upper layer to the lower layer. This is shown in the time series of the silt percentages of the first and second layer in Figure D.6-D.7.

The silt percentage of layer 2 is in the range of 2-2.5%. The associated mass per area is then: 0.025*0.3m*2650kg/m^3*0,6 = 12 kg/m^2, assuming that the silt is present in the pores of the sand.

Another combination of the initial silt percentage and for example the layer thickness (for example δ=0.6m and p=0.01) will therefore result in the same results. A layer thickness of δ=0.3m is set. The silt percentage in the layer 2 is chosen similar to the value used for the determination of the production rate: 2.5%. The sensitivity of the results due to these settings are discussed later on in this report.

Concluding, the simulated time series of the concentration are in good agreement with the measured ones. This is surprising regarding the relatively weak physical knowledge/concept of exchange of sediment between the water column and the seabed,

the imposed uniform wave field and the assumption of an initial uniform silt percentage in both layers.

Table 3.2: Input parameters

Description	Parameter	Unit	Setting
Mass density of water	ρ_w	[kg/m^3]	1020
Mass density of silt	ρ_s	[kg/m^3]	2600
Settling velocity	w_s	[m/s]	0.0004
Shear stress	τ	[m]	0.01
Erosion rate layer 1	M_1	[kg/m^2/s]	$6.0*10^{-5}$
Critical shear stress layer 1	$\tau_{c,1}$	[Pa]	0.15
Thickness of layer 1	δ_1	[m]	0.03
Erosion rate layer 2	M_2	[kg/m^2/s]	$1.1*10^{-4}$
Critical shear stress layer 2	$\tau_{c,2}$	[Pa]	1.1
Thickness of layer 2	δ_2	[m]	0.3
Entrainment coefficient	α	[-]	0.14

3.3.4 Qualitative validation with silt atlas of RIKZ

A qualitative validation is made with the measured concentration fields as given in the silt atlas of RIKZ (Suijlen&Duin 2002). Two comparisons are made: the yearly mean concentration and a concentration after a storm (day 252). The last comparison is a bit arbitrary when a different year, and therefore a different storm, is simulated. Also the period after the storm is of importance. The measured and simulated fields are given in Figure D.8 - D.9. There is a fair agreement: The patterns of low concentrations at sea and high concentrations near the coast are reasonably well simulated. The associated values for the yearly mean concentration and the concentrations after a storm period are also in fair agreement. It is noted that the model results at the Wadden Sea and the Voordelta are questionable as in reality waves penetrating into these areas are hindered by the Wadden Isles and the Hinderplaat respectively. The uniformly imposed wave field in the model does not incorporate this process.

3.4 Concluding remarks

A numerical model has been built to simulate the transport of silt and the interaction between the water column and the seabed. The input of the model resulted from simulated flow fields and wave fields based on measurements. An empirical expression for the water/bed interaction was applied as the knowledge on this subject is limited. More observations are required for a better physical foundation. Despite all possible sources of errors in input and modelling concepts, good results are obtained in the reproduction of the fluctuations on different time scales of the concentration time series at NW10. Furthermore the simulated concentration fields are in fair agreement with the observed silt pattern at the Southern North Sea (Suijlen & Van Duin, 2002).

4 MODEL SET-UP AND CALIBRATION WITH DELFT3D

4.1 Introduction

This chapter describes the set up and calibration of the three-dimensional model with Delft3D. The hydrodynamics (FLOW), waves (WAVES) sediment (SED) and algae modelling (ECO) was carried out using various modules of this modelling suite in this project. The following topics are discussed in this chapter:

- grid and bathymetry, see Section 4.2;
- hydrodynamics with Delft3D-FLOW, see Section 4.3;
- waves with Delft3D-WAVES, see Section 4.4;
- silt transport with Delft3D-SED, see Section 4.5;
- nutrients and primary production with Delft3D_ECO, see Section 4.6.

Simulations for the period 1996 to 2003 with Delft3D-FLOW have been performed using actual hydrological/meteorological forcings. The results of Delft3D-FLOW have been subsequently applied in the Delft3D-SED model to simulate the 3D fine sediments behaviour in the North Sea including the formulations of the water/bed exchange. Finally, the results of both the hydrodynamics and the fine sediments are input for the nutrients and primary production computations with Delft3D-ECO.

4.2 Grid and bathymetry

In this project the ZUNOGROF grid from the Southern North Sea has been used. (Figure 4.1). This grid consists of 8,710 computational elements and was developed in an earlier study of the effects of the proposed reclamation of an airport island (“Flyland” project in the North Sea).

Figure 4.1: ZUNOGROF computational grid

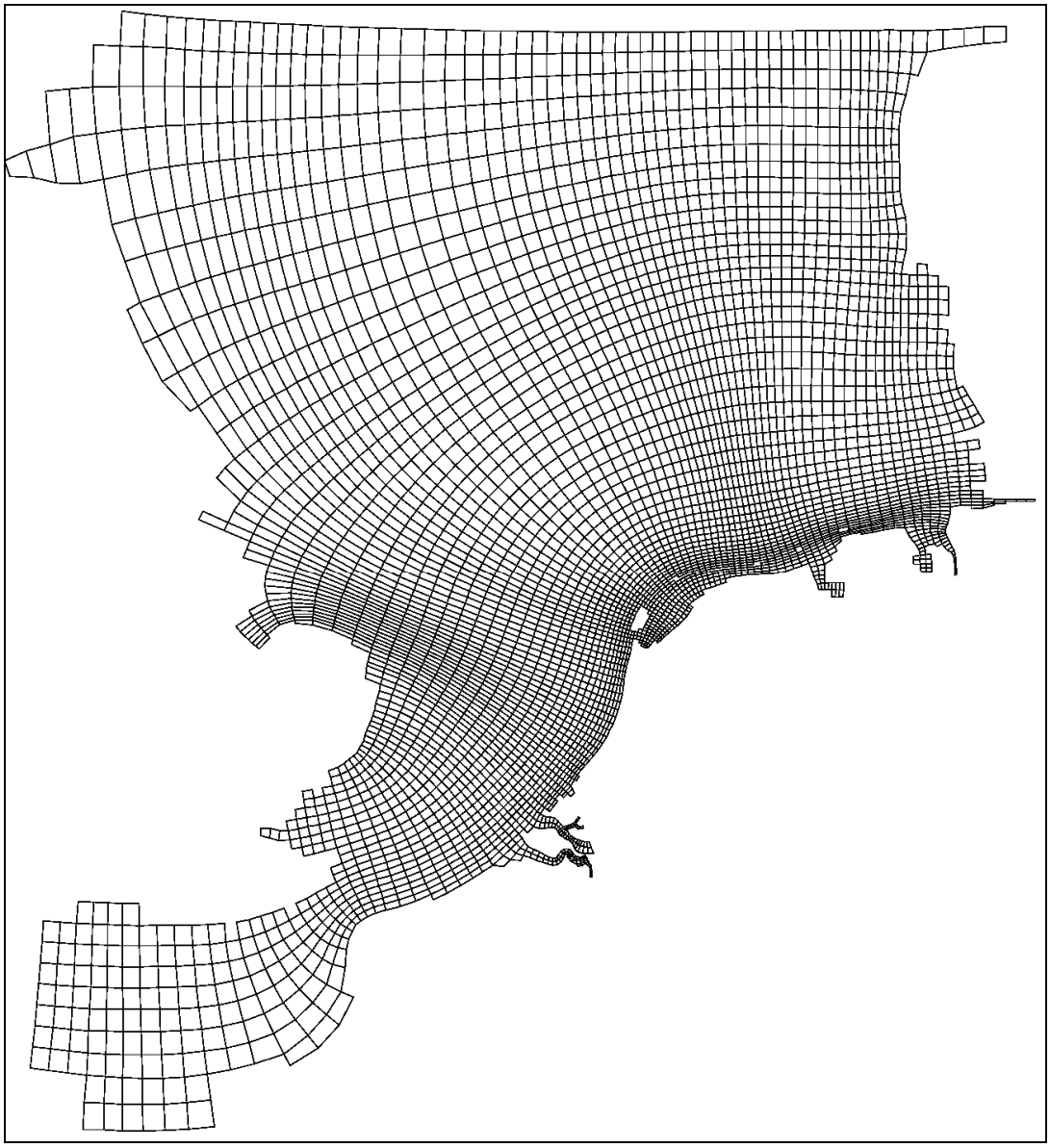

A detailed description of the ZUNOGROF model (including its calibration and validation) is beyond the scope of the present report, but can be found in Roelvink et al. (2001). Specific parameters of this model, as applied in the present study, are summarized in Table 4.1. The run time of the hydrodynamic model for a year long simulation on a 3.2 GHz Intel processor required approximately 15 hours. This relatively short run time made ZUNOGROF particularly suitable to perform a series of year-runs (simulating a total of 9 different years) that differ in their forcing of wind, air pressure and river discharges.

For the vertical dimension, the water column was subdivided into 10 layers, using a sigma-coordinated approach to ensure sufficient vertical resolution in the near-coastal zone (Stelling & Van Kester, 1994). From top to bottom, these layers respectively represent 4.0%, 5.9%, 8.7%, 12.7%, 18.7%, 18.7%, 12.7%, 8.7%, 5.9% and 4.0% of the water depth.

Table 4.1: Input parameters of the ZUNO GROF hydrodynamic model

Parameters	*Values*
Number of points (M,N,K)	64, 134, 10
Layer distribution (% of the depth)	4.0, 5.9, 8.7, 12.7, 18.7, 18.7, 12.7, 8.7, 5.9, 4.0
Integration time step	5.0 minutes
Resolution along the Dutch coast	Approximately 2.5 km perpendicular to the coast and 5.5 km along the coast
Hydrodynamic Boundary condition	Astronomical Tide (49 tidal components)
Heat exchange with atmosphere	Ocean Model as described by Gill (1982) & Lane (1989)
Turbulence model	K-epsilon model
Bed-stress coefficient	0.026 (Manning)
Horizontal Eddy viscosity en diffusivity	10.0 m^2/s en 10.0 m^2/s
Vertical Eddy Viscosity en diffusivity	$1 * 10^{-6}$ m^2/s en $1 * 10^{-6}$ m^2/s
Wind	see detailed description further in this report
River Discharges	see detailed description further in this report
Sigma-correction	No

The bathymetry was derived from a large number of datasets. Coastal data were taken from a number of recent morphological studies (Steijn et al (1998), Roelvink et al (1998a), Roelvink et al. (1998b), Boutmy (1998), Jeuken et al. (2000)). Additional data from recent Dutch Continental Shelf Data (TNO-NITG) and raw data from the Dutch Hydrographic Service were also included to derive the model bathymetry.

4.3 Hydrodynamics

In Delft3D-FLOW the flow equations are solved on a staggered, curvilinear finite-difference grid. This makes it possible to align the grids with curving boundaries and channels and to concentrate the resolution in areas of interest, while maintaining an accuracy and computational speed comparable to using rectangular grids. Hydrodynamic transport is computed using detailed bathymetry and open boundary forcing based on tidal constituents, with variable wind forcing and variable river discharges. The calibrated tidal flow used in this study is coming from previous studies (see e.g. Roelvink et al. 2001). The variable wind forcing and the variable river discharges are discussed below.

Wind forcing

The hydrodynamic model was forced with spatially and temporally varying meteorological data. With the exception of 1988/89, for which data were derived from an earlier NOMADS project (NOMADS2, 2001), all these data were obtained from the Royal Dutch Meteorological Service (KNMI) and are the output from the so-called HIRLAM numerical meteorological model. The HIRLAM data are comprised of two horizontal wind velocity components (at 10 m above mean sea level) and air pressure, archived every 6 hours. All data ordered for the purpose of this project (i.e. from the years 1996, 1997, 1998, 1999, 2000, 2001, 2002 and 2003) were enclosed between 14° W, 15° E and 46° W, 61.5° E degrees and 65 degrees North (ensuring complete coverage of the ZUNOGROF grid).

The orientation and projection of the HIRLAM data were adjusted so as to obtain the same orientation and projection as the ZUNOGROF grid. Missing values (few, mainly in

1997) were interpolated linearly in time between the previous and next available data fields. The meteo data were interpolated bi-linearly in space from the meteo grid and linearly in time within Delft3D-Flow to obtain the same time step and grid resolution as the hydrodynamic model. HIRLAM data quality was checked against measured hourly wind data as available on the website http://www.knmi.nl/samenw/hydra/index.html for the locations of the stations Vlissingen, Hoek van Holland, IJmuiden and Den Hoorn (Terschelling). Modelled (HIRLAM) and measured wind data showed good agreement.

River discharges
In total eighteen fresh water discharges are defined in the model. For 7 of these points, i.e. the Westerschelde, Oosterschelde, Haringvliet, Nieuwe Waterweg, IJmuiden, Den Oever and Kornwerderzand, time-varying discharges have been applied, using discharge rates for every 10-minutes (Haringvliet, Nieuwe Waterweg) or daily averages (other points) downloaded from the Waterbase web-site of the Dutch Ministry of Transport (http://www.waterbase.nl/). For the remaining 11 discharge points a constant discharge rate is prescribed, based on long-term averages for these river discharges (see De Goede & Van Maren (2005) for details). For all discharges, the temperature and the salinity concentration are assumed to be constant, respectively 10 °C and 0 ppt.

4.4 Waves

The bed shear stress induced by waves results in sediment resuspension during storms. Wave action is therefore an essential model component. For the period 1996 – 2003 wave parameters were computed on the ZUNO grid using SWAN. Because of the long distance (500 km) between the model boundary and the region of interest, *i.e.* the Dutch coastal zone, the model is steered completely by internally generated waves. At the northern boundary, a constant 'dummy' wave condition of H_s = 0.5 m, T_p = 15 s and direction 350° was applied (Jonswap spectrum).

The applied wind conditions are based on 6-hourly wind data. For each wind condition a wave computation was made, which implies 1460 computations per year and 11,680 computations for the period 1996 – 2003. Two major assumptions are made:
1. the wind is constant over the model domain;
2. the wave field is at equilibrium with the wind condition.

These assumptions were made for practical reasons such as software capabilities and computational time. A wind climate point was selected from the HIRLAM data, see Figure 4.2.

Figure 4.3 shows a comparison of the wave computation results with measured data for the first half year of 1996. Table 4.2 shows the main wave statistics for the year 2000, when the CEFAS SmartBuoy was operational. It is concluded that although the wave model fails in reproducing specific peaks in wave height, the statistics on wave height, wave period and bed shear stress reasonably agree. Swell is somewhat underestimated and for strong winds the wave height is often overestimated. Especially swell waves coming from the North Atlantic might have some influence for wind coming from the northwest.

Figure 4.2: HIRLAM wind climate point used for SWAN computations. Note: shown grid is HIRLAM grid, not SWAN grid.

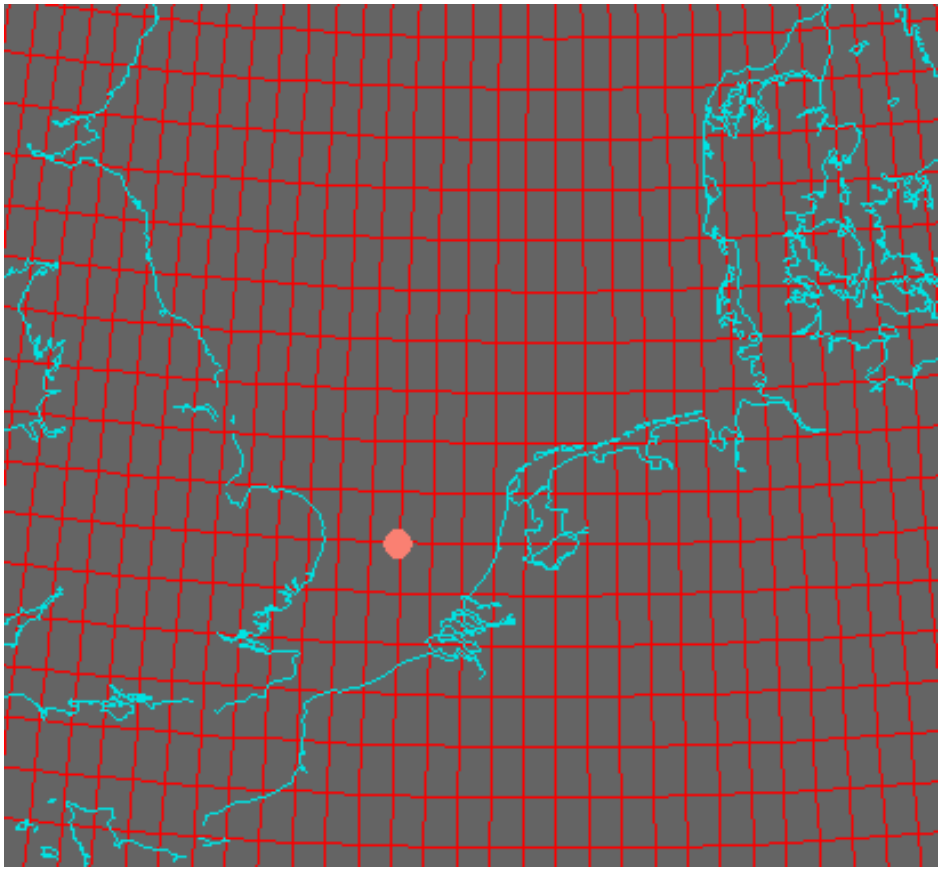

Figure 4.3. Measured and computed significant wave height at Meetpost Noordwijk (depth = 15 m).

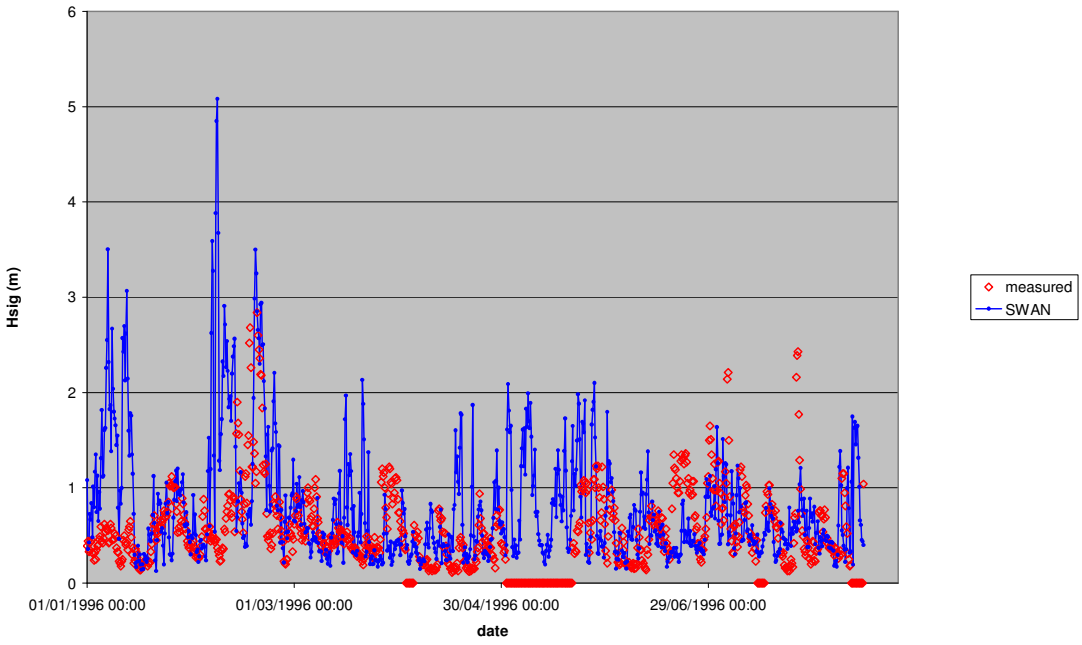

Table 4.2: Wave statistic for Meetpost Noordwijk for the year 2000. Measured and computed with SWAN.

Wave parameter	measured	computed
H_s, mean (m)	0.80	0.90
H_s, max (m)	3.3	3.8
T_p, mean (s)	5.8	4.1
T_p, max (s)	9.8	9.0
Perc. τ_{bed} > 2 Pa	3%	3%

The bed shear stress due to waves was computed from the significant wave height H_s, period T_p and near-bed orbital velocity $\hat{u}_{bot}$ according to:

$$L_0 = \frac{gT_p^2}{2\pi}$$ (wave length at deep water)

$$L = L_0\sqrt{\tanh\left(\frac{2\pi h}{L_0}\right)}$$ (wave length)

$$a = \frac{H_s}{2\sinh\left(\frac{2\pi h}{L}\right)}$$ (horizontal near-bed particle displacement)

$$f_w = \min\left(0.32, 0.00251\exp\left(5.21\left(\frac{a}{r_w}\right)^{-0.19}\right)\right)$$ (Swart formulations with r_w = wave roughness height = 0.05 m)

$$\tau_{bed,\max} = \tfrac{1}{2}\rho_w f_w \hat{u}_{bot}^2$$

Figure 4.4 shows the total bed shear stress (currents + waves) at Noordwijk 10 km for 2001. In the first quarter, the SWAN results will overestimate resuspension by waves (green peak > red peaks). However, in the last Quarter the SWAN results will underestimate resuspension by waves (red peak > green peaks). Notwithstanding, the typical height and frequency of the storm peaks in bed shear stress are similar. It is also remarked that the current-induced bed shear stress from the 3D ZUNO computation is smaller than the bed shear stress based on the depth-averaged velocity and assuming a logarithmic velocity profile. This can be explained by stratification effects and a slightly lower roughness: Manning = 0.026 is equivalent with C = 62.3 $m^{1/2}/s$ instead of 60 $m^{1/2}/s$ at h = 18 m, which results in an 8% lower bed shear stress.

It is concluded that for the present purpose, *i.e.* to provide a mechanism for sediment resuspension during periods with strong wind, the SWAN model results are suitable. However, for an accurate prediction of actual wave heights the application of space-varying wind and the modelling of dynamic wave growth are required. This is beyond the present study.

Figure 4.4: Total bed shear stress at Noordwijk 10. Red: based on measured wave height and period (r_w = 0.05 m) and depth-averaged velocity (r_c = 0.10 m equivalent with C = 60 m$^{1/2}$/s at h = 18 m) from ZUNO. Green: based on SWAN computations (r_w = 0.05 m) and direct bed shear stress output from ZUNO (Manning = 0.026). Left: all 2001. Right: detail of approximately 1 month (March).

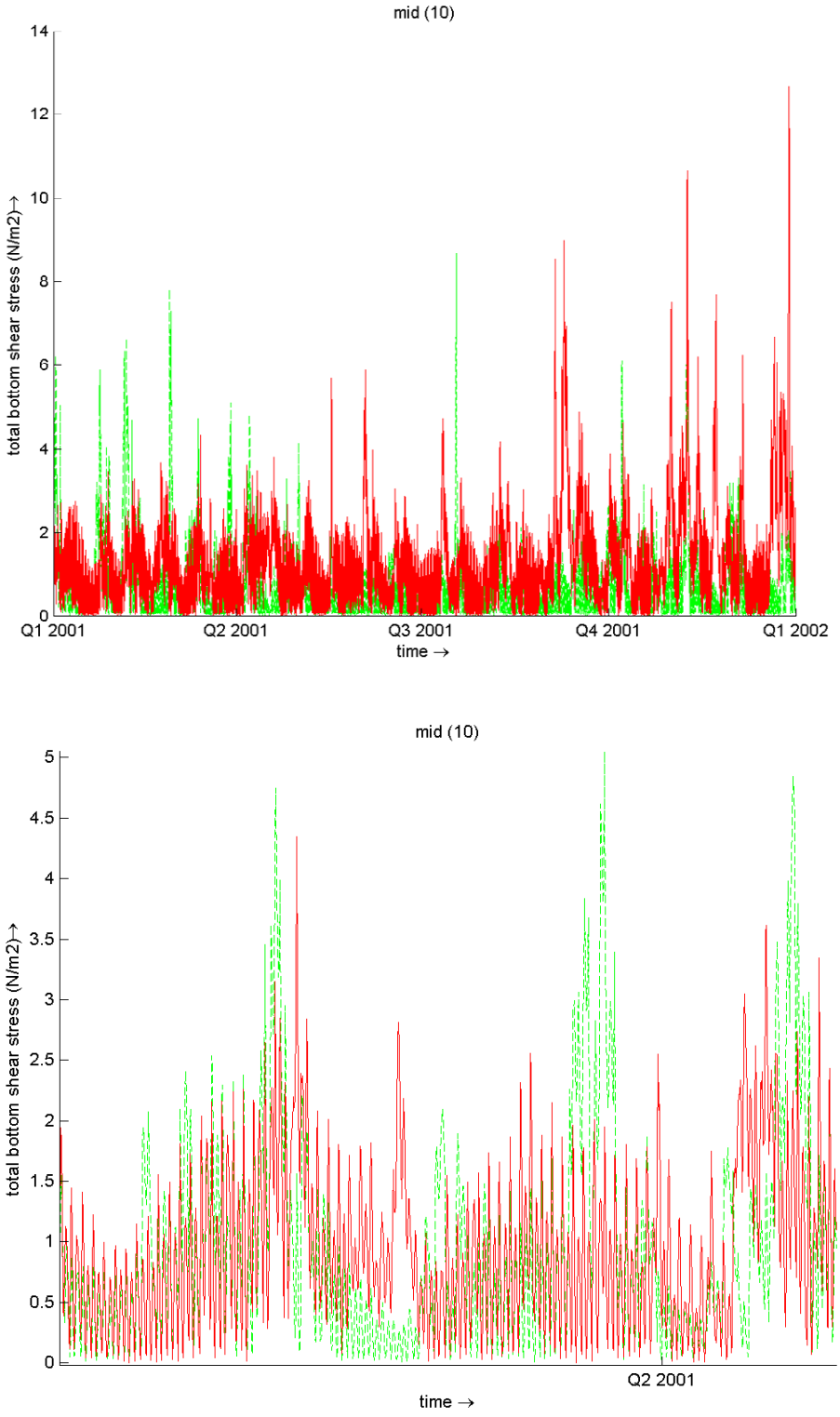

4.5 Mud transport

The two-layer model formulations to account for seasonal sediment buffering (see Chapter 2) have been implemented into DELFT3D. Although the present project does not include a calibration of the background concentration in the ZUNO model, a few calculations with a background concentration were made in order to check whether the single point calibration for Noordwijk 10 yields satisfactory results for the 3D model.

The background concentration was imposed via a concentration boundary condition of 7 mg/l (depth-averaged) in the Channel and 2 mg/l at the northern boundary. For an average residual flux of 94,000 m^3/s through the Channel (see Table 4.3), the sediment load via the Channel boundary is 21 MT/yr. Also, an erosion flux of 2 MT/y was assumed to occur near the Flemish banks. Finally, the suspended sediment concentration from the Rhine river discharge was assumed constant at 13.9 mg/l. This results in a river flux of approximately 0.7 MT/y. No other loads were imposed.

Table 4.3: Residual discharge through Dover Strait computed with ZUNO hydrodynamic model. Right column: resulting yearly sediment flux assuming a constant SPM concentration of 7 mg/l.

Year	Residual discharge Dover Strait (m^3/s)	Yearly sediment load Dover Strait (MT/y)
1996	57,616	12.7
1997	85,635	18.9
1998	118,009	26.1
1999	106,826	23.6
2000	127,994	28.3
2001	67,581	14.9
2002	114,898	25.4
2003	71,199	15.7
Average	93.720	20,70
Standard deviation	26.577	5,90

The sediment model was allowed to spin-up for 8 year (1996 – 2003), which was sufficient to reach a dynamic equilibrium. During this period, the actual wind, wave and tidal forced were applied. The initial sediment concentration was set at 100 mg/l, which is equivalent with 5 kg/m^2 at a depth of 50 m. Most of the initial sediment is quickly transported towards the buffer layer. With a domain area of approximately 6×10^4 km^2 between Dover Strait and the Dutch coastal zone and an anticipated active sediment mass of about 5 kg/m^2 (*i.e.* 1% mud in a 0.3 m thick layer), the total mass in this part of the system is 3×10^{11} kg or 300 MT. This would imply that approximately 12 years are required to replenish the total sediment pool in this part of the Southern North Sea. Note that these numbers are just order-of-magnitude estimates. The spin-up is likely to be both influenced by internal redistribution of the initial sediment mass and by the sediment flux through Dover Strait.

After the 8-year spin-up, another 8-year period (also 1996 – 2003) was simulated. For 2001, the computed surface concentration is shown at Noordwijk 2 and 10 km (green dotted line in Figure 4.5). It is observed that the computed concentration is too low compared to the DONAR measurements.

This may be caused by the following aspects:

1. An incorrect sediment supply and/or initial conditions.
2. A different wave- and current-induced bed shear stress in the ZUNO model compared with the box model.
3. The occurrence of cross-shore advection (which is absent in the box model).
4. Consolidation of the seabed is a phenomenon which is not taken into account by the model. After the summer period, it will take a couple of storms before the resuspension process fully takes place again.
5. Gradients in the grain size of the sandy sea bed.

In order to improve the model performance regarding the background concentration, two changes were made. Firstly, α was reduced from 0.1 to 0.05. In a closed model with a fixed amount of sediment, a twofold decrease of α results in a twofold increase of the concentration. In an open model with a prescribed time-averaged suspended sediment concentration, a decrease of α results in a decrease of the equilibrium mud percentage in the bed. As an alternative to the decrease of α, the initial and boundary loads could also have been doubled.

Secondly, the critical shear stress for erosion from the first bed layer was decreased from 0.3 to 0.1 Pa. This prevents excessive sedimentation in sheltered areas, which may significantly reduce the sediment flux through the model domain.

With these changes, a satisfactory agreement is obtained between computational results and DONAR data (see Figure 4.5 for Noordwijk 2 and 10 km). A good fit of the CEFAS data is maintained with the box model (Fig. 4.6). A drawback is that the equilibrium percentage mud in the seabed becomes rather low (approximately 0.5%, see Fig. 4.7). However, if required a higher buffer capacity is easily accomplished by increasing the thickness of the second layer. As such, more work on the 3D calibration of the background concentration of suspended matter is recommended. For example, the computed SPM-levels in the Voordelta are too low. The loads and initial conditions should be further optimized.

If the background concentration can be well reproduced with the present parameter settings (with a more detailed application of the sediment loads), the present computed impact of sand extraction will not be affected. However, if it might be necessary to change the sediment parameter settings to achieve an accurate reproduction of the background concentration, this will also affect the computed concentration level increase caused by sand extraction. This uncertainty should be put into perspective with other sources of uncertainty such as the buffer capacity of the seabed and the behaviour and light absorption capacity of the fines released by sand extraction compared with the natural background material.

Figure 4.5: Background concentration at Noordwijk 10 km (upper panel) and Noordwijk 2 km (lower panel) for original settings (τ_{crit1} = 0.3 Pa, α = 0.1, green dotted line) and improved settings (τ_{crit1} = 0.1 Pa, α = 0.05, blue line). All other settings are equal. Red crosses represent DONAR surface concentration data.

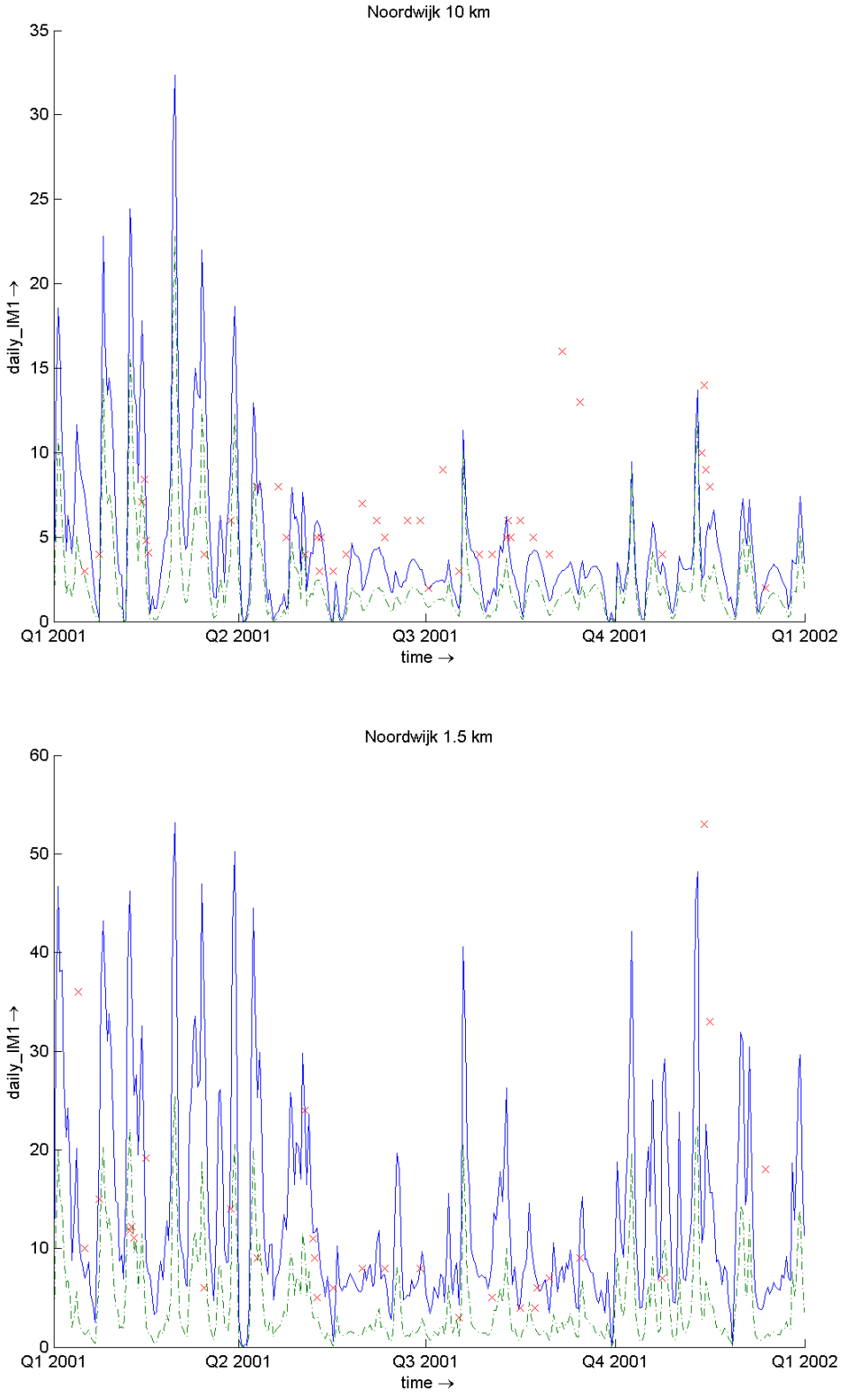

Figure 4.6: Calibration result for CEFAS data Noordwijk 10, year = 2001. Note that data between 6/8 and 21/8 are probably erroneous. Boundary concentration = 7.5 mg/l (depth-averaged). Difference with Figure 2.10: $\alpha = 0.05$ instead of 0.1, $\tau_{crit1} = 0.1$ Pa instead of 0.3 Pa, and current-induced bed shear stress exported from ZUNO (Manning = 0.026) instead of calculated from depth-averaged velocity, assuming a logarithmic profile ($C = 60\ \sqrt{m/s}$). Bed thickness = 0.30 m.

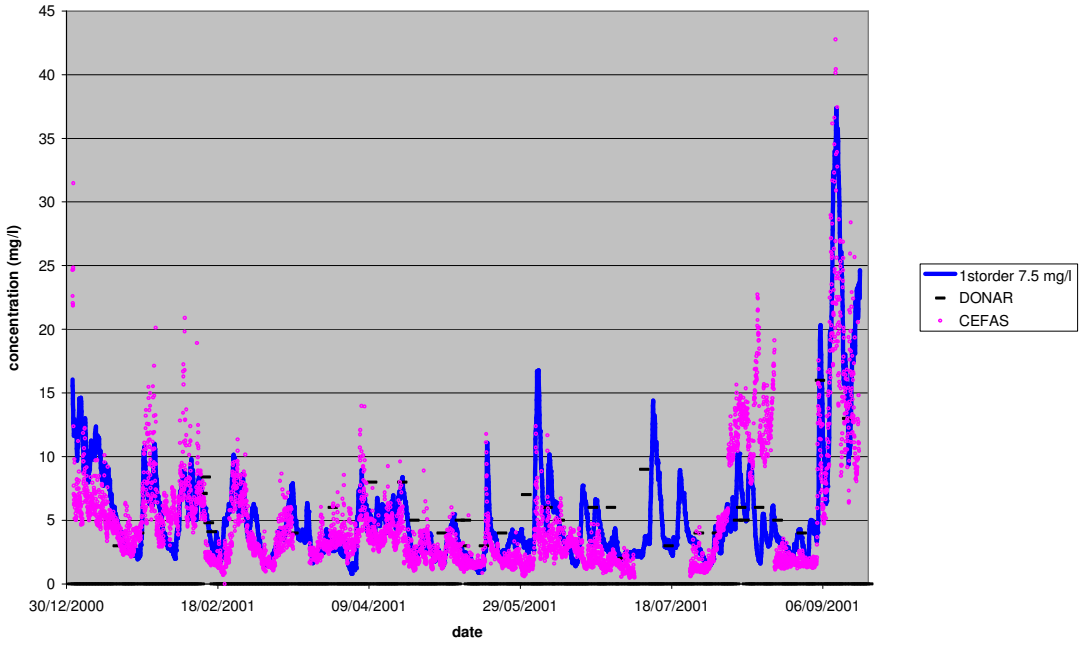

Figure 4.7: Mud percentage in bed for $\alpha = 0.05$. Note nearly twofold reduction compared with $\alpha = 0.10$ (see Fig. 4.5).

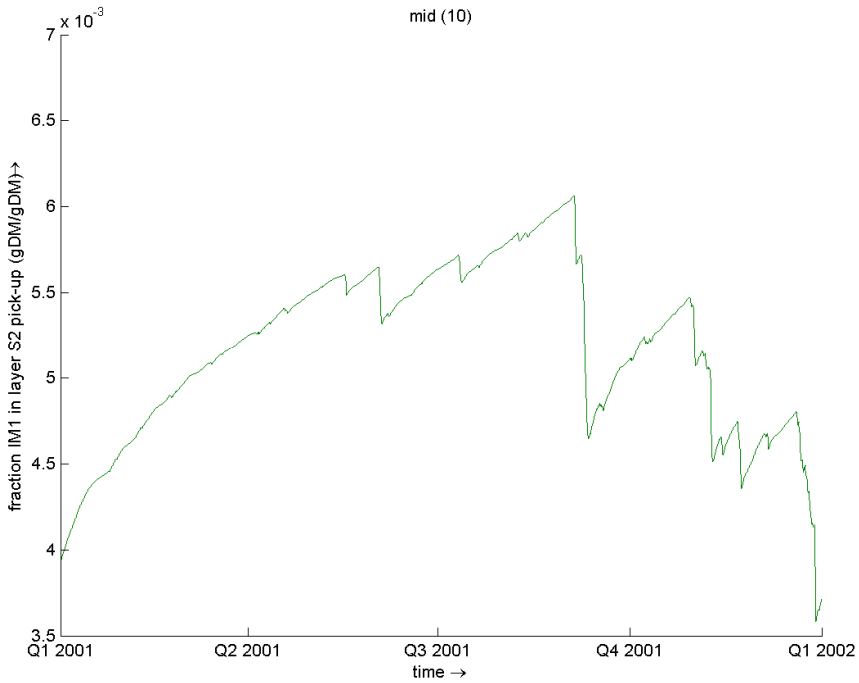

4.6 Nutrients and primary production

The impact of the sand extraction activities on the nutrients and primary production in the North Sea are simulated using the Delft3D-ECO (GEM) modelling framework. For a much more detailed description of the model and for all model settings (model grid, vertical aggregation, boundaries, parameter settings), we refer to previous reports (MARE, 2001; Delft Hydraulics, 2005). In this paragraph the validity of the model and the application for the present project are briefly summarized.

The modelling approach for nutrients and primary production in the Dutch coastal zone is based on the research carried out for a new Airport Island in the North Sea ('Onderzoek Nationale Luchthaven' also known as 'Flyland', e.g. MARE, 2001; MARE, 2002). The Flyland-GEM model is the culmination of many years of experience in modelling the southern North Sea and knows many predecessors dating back to the late 1980's. As such, it has been calibrated against independent datasets, including DONAR, 'Nerc', and 'Euzout' data. No other model describing nutrients and primary production in the southern North Sea has been scrutinised against this many measurements. The GEM model of the southern North Sea came first in a model comparison supported by the Environmental Assessment and Monitoring Committee (ASMO) of the Oslo and Paris Commission (OSPARCOM).

In this study, historic values were applied for river discharges, nutrient loads, wind, and solar irradiance for the period 1995 to 2003. Table 4.4 gives an overview of the yearly averages of irradiance, wind and river discharge.

Table 4.4: Yearly averages and 8-year average for irradiance, wind, and nutrient loads and discharges of the Nieuwe Waterweg and Haringvliet combined.

Year	Irradiance (W/m^2)	Wind (m/s)	River discharge (m^3/s)	Total P load (g/s)	Nitrate load (g/s)	Silicate load (g/s)
1996	116.9	5.5	1889.5	491.27	3571.16	6575.46
1997	121.5	5.4	1969.1	472.58	4076.04	6655.56
1998	108.6	6.1	1990.9	418.09	3265.08	6171.79
1999	124.8	5.8	2732.2	491.80	4070.98	7786.77
2000	114.2	5.8	2521.3	453.83	3529.82	6681.45
2001	124.3	5.4	2875.9	460.14	3192.25	7362.30
2002	119.9	5.6	2966.3	504.27	2402.70	7593.73
2003	134.6	5.2	1850.7	296.11	814.31	4571.23
8-year avg.	120.6	5.6	2349.5	446.41	3195.32	6766.56
st. dev	7,8	0,3	473,2	67,3	1.072,2	1.017,1
St. dev / average (%)	6%	5%	20%	15%	34%	15%

The following is observed:

- The annual river discharges vary significantly. The standard deviation is 20% of the average discharge. Discharges are low in 1996 through 1998 and 2003, high in the other years.

- Nutrients loadings vary less through the years. With the exception of 2003 and 2002 for nitrate only, the annual variation is less than 25%.
- The year 2003 is exceptional in every aspect: higher irradiance, less wind, smaller discharges and by far the lowest average loads.

Two different scenarios for the background SPM have been applied for nutrients and primary production computations:

- The ZUNO-DD background SPM with a super-imposed cosine function as used in the Maasvlakte-2 appropriate assessment (Delft Hydraulics, 2005). This cosine function is subject to randomization based on the historic wind for all eight years.
- The ZUNO-grof background SPM, which was derived from the Delft3D-SED model for the calibration of the sand extraction plume in this study (see also Section 4.5).

The reason for this is that the spatial and temporal variation of the background concentration is crucial for accurate results in the computations with nutrients and primary production.

In Appendix E salinity, suspended matter, chlorophyll and nutrients are plotted for the two background SPM forcings and the measurements (DONAR), for the entire eight year period. These graphs give a good impression of the annual variability. In general, the GEM model gives an acceptable representation of the measurements.

Wherever significant differences in SPM forcing are imposed on GEM, the simulation results for chlorophyll and nutrients are different as well. At location Noordwijk 2 the SPM simulation of ZUNO-grof agrees better with the measurements than the ZUNO-DD result. Consequently the simulated result for chlorophyll is also better using the ZUNO-grof SPM result. For the other northern locations, the ZUNO-DD and ZUNO-grof results of SPM are more similar and consequently the GEM results are similar as well.

At the southern locations (e.g. NZR1AP001, NZR2WC002 and NZR3SW010), the ZUNO-DD based SPM are much higher than those based on ZUNO-grof. According to the available measurements for SPM, results of ZUNO-DD are more realistic. In this case the most accurate SPM forcing does not result in the best result for chlorophyll. With ZUNO-grof SPM for instance the onset of the spring chlorophyll is earlier and somewhat better in agreement with the measurements at location Walcheren 2 km (NZR2WC002). This result is not obvious and the reader is referred to the textbox (’SPM concentration of ZUNO-grof and ZUNO-DD’) on the next page for an explanation.

SPM concentration of ZUNO-grof and ZUNO-DD

In the Voordelta and in the near-shore coastal zone, the background SPM concentration predicted by ZUNO-DD is considerable higher than predicted by ZUNO-grof. There are two main reasons, both related to model set-up and model behaviour.

- First, the ZUNO-DD grid has a higher grid resolution and therefore represents the cross-shore transport more accurately than the ZUNO-grof grid.
- Second, the ZUNO-DD simulation is based on a repeated 14-day spring-neap cycle while the ZUNO-grof simulation is a full-year simulation with actual hydrodynamic and meteorological forcing. It has been shown during the Maasvlakte study (Delft Hydraulics, 2005) that repeating the typical flow patterns in the 14-day hydrodynamic database results in an increase SPM concentrations in the Voordelta.

In the Voordelta SPM results of ZUNO-DD agree much better with the measurements than those computed by ZUNO-grof. In contrast simulated chlorophyll levels based on the ZUNO-grof background SPM give a better comparison with the measured data. To explain this result, another factor should be taken into account: the amount of dissolved organic matter (or yellow substance). From Appendix G it is clear that the simulated salinity is often lower than the measurements, particularly in spring. In the model this results in a considerable overestimation of the contribution of fresh water to the extinction coefficient. In the case of ZUNO-grof the error in SPM is compensated by the error in salinity and as a result the non-algal part of the extinction coefficient is more or less correct (compensating errors).

The compensating effects of salinity and SPM on the extinction coefficient explains why the reference simulation results at for instance Walcheren 2km using ZUNO-grof SPM agree better the measurements than those based on ZUNO-DD. The combination of more realistic SPM levels with too low salinities in the ZUNO-DD

4.7 Concluding remarks

The background SPM concentration in northern direction based on ZUNO-grof agrees well with the measurements and performs comparable with the previous results of ZUNO-DD. ZUNO-grof underestimates the background SPM concentration in the Voordelta compared with the measurements, but results in a better prediction of chlorophyll-a in this area than ZUNO-DD (see textbox 'SPM concentration of ZUNO-grof and ZUNO-DD' on next page). It is uncertain how this error affects the impact computations for nutrients and primary production. The Voordelta is a Special Area of Conservation (SAC) in the framework of the Birds and Habitat Directives of the European Communion. Therefore, computations have been carried out with the SPM background of ZUNO-DD and ZUNO-grof to investigate the effect of this uncertainty. The discussion of these differences can be found in Section 6.3.

5 RESULTS OF SCENARIO COMPUTATIONS

5.1 Introduction

This chapter describes the results of the scenario computations for mud transport and nutrients/primary production. As the model is linearly scalable, the sand extraction study can be carried out without taking into account the background concentration. The extra concentration due to sand extraction can be superposed on the background concentration of mud. Section 5.2 describes the results of the 2D silt computations with FINEL. Next, the results of the 3D computations with Delft3D are discussed in Section 5.3. Section 5.4 gives an overview of the scenarios with nutrients and primary production. An overall discussion of all results is given in Chapter 6.

5.2 Effects of silt transport with FINEL2D

5.2.1 Introduction

After calibration of the silt model (see Section 3.3)., the model is applied to the case with disposal of silt due to sand extraction Three scenarios are simulated, differing in the way the dredging (i.e. the sand extraction) is carried out.. In addition three sensitivity studies are carried out to obtain an impression of the upper limits due to more extreme hydrodynamic forcings and parameter settings. In this section, the different scenarios and sensitivity studies are defined. (Section 5.2.2). Secondly, the way the results are presented is described in Section 5.2.3. Thirdly, the results are interpreted in Section 5.2.4. Finally, conclusions are drawn in Section 5.2.5.

5.2.2 Definition scenarios and sensitivity simulations

Scenario 1, reference simulation

In the reference scenario, sand extraction is carried out from four sand pits (see Figure 5.1). A sand extraction rate of 50Mm^3/year is required. With a silt percentage of 2.5% and a porosity of 40%, 2 Mton silt per year will be disposed. This yearly amount of silt (expressed as weight) is spread uniformly over the four sandpits (P2, P4, P5 and P6) for a period of 6 years. This production rate is equal to the rate given in Chapter 2. As the effect of the sand extraction will last for a longer period than the mining period only, due to the buffering and consequent release of silt under storm conditions, another 4 years are simulated. The total simulation time is therefore 10 years.

Figure 5.1: Schematisation of the sandpits in the computational grid.

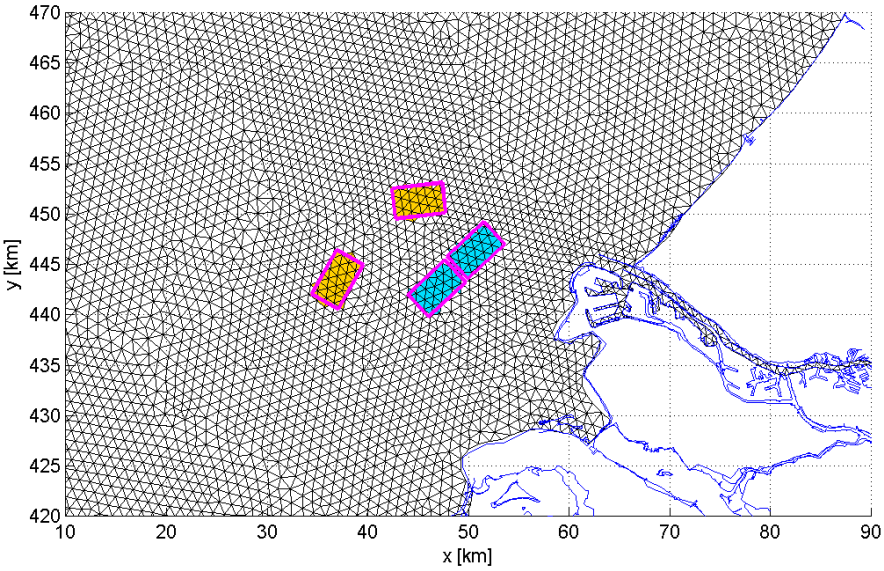

The hydrodynamic and meteorological conditions of 2001 are assumed to be representative for the averaged conditions. The wave and flow fields of 2001 are used each subsequent year. As a two-dimensional model is applied, three dimensional effects can only be taken into account by means of parameterisation. A secondary flow is present in front of the Dutch coast, due to density effects. At the bottom, this flow has a magnitude of approximately 2.5 cm/s towards the coast. At the surface the flow is also directed towards the coast, see Roelvink et al. (2001). A Rouse profile is used to determine the concentration distribution over the depth. Multiplying the velocity profile with the Rouse profile and integrating over the depth leads to an extra depth-averaged advection term towards the coast. A moderate value of this depth-averaged advection is then 1 mm/s, which is applied as standard. Note that a value of 5 mm/s (associated with a velocity at the surface and the bottom of ca 12.5 cm/s) is imposed in sensitivity study 2.

Scenario 2, two sandpits

In scenario 2, sand extraction is carried out in only two pits, viz.P2 & P4, the two closest to the coast (see Figure 5.1). The total production is spread evenly over these two pits, implying a double disposal rate per pit. This scenario is chosen since the distance from the sandpit to Maasvlakte 2 is smaller, leading to a more economic scenario. It is, however, expected that this scenario would have more impact on the Voordelta.

Scenario 3, double production rate

A double production rate is applied in scenario 3; hence the sand extraction period is halved. As the model is scalable, the first three years of scenario 1 are doubled, followed by 4 years of extension. This scenario was initiated by the idea to shorten the construction period. A shorter time span is expected to have a stronger effect during the construction period as the production rate increases.

Sensitivity study 1, higher waves

The waves are an important input for the water/bed interaction. To explore the sensitivity of this input, the shear stress by waves has been increased with 30%. This can be interpreted as a period of extreme stormy years.

Sensitivity study 2, advection by 3D effects

A two-dimensional depth-averaged model is applied. Three-dimensional effects by secondary circulations are therefore not captured, see the hydrodynamic calibration. These effects can be parameterized by means of an extra advection term towards the coast as described above. The effect is exaggerated in sensitivity study 2 by applying an amplitude of 12.5 cm/s for the cross shore residual flow, resulting in a depth-averaged advection of 5 mm/s towards the coast. It is expected that the extra advection towards the coast will result in a higher impact at the coast.

Sensitivity study 3, smaller thickness layer 2

The thickness of layer 2 does not play a major role in the calibration against the NW10 data. A thinner or thicker layer could therefore be applied as well, although a layer thickness of the active layer of 30 cm resulted from the expert discussions. A thin layer will capture the sediment for a shorter period (the erosion during storms will be stronger). A thin layer therefore has a smaller time scale and diminishes the effect of the water/bed exchange. The thickness of layer 2 is changed from 30 cm to 10 cm. Higher concentrations during storms are expected, resulting in a more severe impact of the sand extraction.

5.2.3 Presentation of the results

The results of scenario 1 will be discussed in greater detail, by means of contour maps (Figure F.1 to F.6, see Appendix F) and time series of the concentration in the water column and of the silt percentages in layer 1 and 2 (Figure F.7 to F.12, see Appendix F). The locations of the time series are given in Figure 5.2. These plots are meant to visualise the simulated physical process. Furthermore a relative error is estimated, based on the simulations of the background concentration. Note that a direct comparison with the measurements of the silt atlas was not possible, as these data were not available in digital format. However, the simulated background concentrations (see Section 3.3.5) were in fair agreement with the silt atlas (see Figure C.8-C.9).

Figure 5.2: Locations of output for time series.

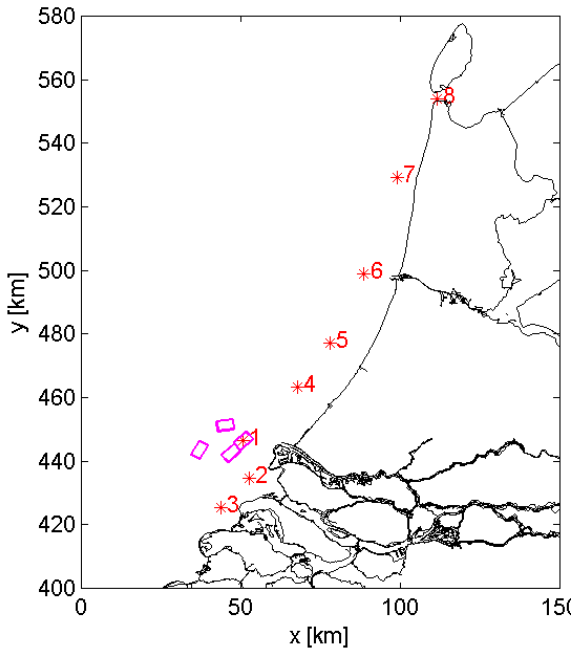

1	Sandpit
2	Voordelta 1
3	Voordelta 2
4	Scheveningen
5	Noordwijk
6	IJmuiden
7	Petten
8	Marsdiep

The results of the other scenarios and sensitivity studies are presented by means of contour maps and time series in such a way that the differences with Scenario 1 become clear. The results of these two scenarios are discussed with less visualisations.

5.2.4 Interpretation

General process, Scenario 1

The release of silt through the overflow of the TSHD-ers working above the sandpits results in an increase in concentration at the pits. Due to the tidal motion the silt is initially transported roughly within the tidal ellipse and settles down in layer 1 and layer 2, with the imposed ratio 86% over 14%. A small percentage travels further from the pit by means of residual currents and diffusion. During mild conditions erosion takes place from layer 1, and hardly from layer 2, as the critical shear stress is high for layer 2. Silt will therefore be buried (buffered) in layer 2 following the leaking process as described in Section 3.2, see Figure F.9 and Figure F.12 in Appendix F.

During storms the top layer erodes and the silt contained in layer 2 is released and comes in suspension. It is transported by the tidal motion and the residual current of that storm. After the storm, the settling and leaking process starts again, i.e. the silt migrates from the water column via layer 1 to layer 2.

In order to get an impression of the area of influence and the corresponding magnitude in relation to the background concentration, the simulated concentration is divided by the simulated background concentration as determined in Chapter 3 (Figure F.2 and F.5). Another way to express the area of influence is the increase of silt in layer 2. The yearly averaged silt percentage of the last construction year is given in Figure F.3. Unfortunately there is no spatial map of a measured silt percentage. A uniform value of 2% is therefore assumed. The contour map of Figure F.3 can then also be interpreted as a relative increase.

An interesting detail is that silt is trapped in the so-called anchor place, close to the sandpits. At this deeper part the shear stresses are smaller, leading to less erosion. The sandpits themselves could therefore act as silt traps as well, although part of this silt may be brought in suspension again during dredging. Depending on the dredging method and the dragheads used, the silt may be dredged several times during the sand extraction process.

Up till now, only the sand extraction period is discussed. After this period the effect of the total amount of silt brought in the water column during the sand extraction will continue for a longer period. In the vicinity of the sandpits, the concentrations drop in a few weeks as the concentration in the near field is highly influenced by the silt release. Further away, the concentration is stronger influenced by the silt in the bottom layers. This silt will be mobilized during storms. After the storms the leakage process starts again. The area of influence will be transported to the north and will expand and diminish gradually. The corresponding time scale is in the order of magnitude of years to decades. Four years after the construction stopped, a large area in the Dutch coast still has a yearly mean concentration in the order of magnitude of 5% of the background concentration. As described above, the sandpits themselves (depth 10 meter relative to the seabed) will also act as silt traps, as the shear stress is smaller and no resuspension by dredging will take place anymore.

Scenario 2, two sandpits

In scenario 2, the total sand extraction is split into two pits. Obviously, the concentration of silt above the pits therefore doubles. The yearly averaged concentration for the last construction year is given in Figure F.13. The differences between 4 and 2 sandpits are mainly local. In the near field higher concentrations are found, but the far field (north of Noordwijk) is hardly influenced.

Based on this simulation it can be concluded that reducing the dredging area results in higher concentrations in the near field, but has almost no effect on concentrations in the far field. Although it has not been analysed by several simulations, it is assumed that a large dredging area, i.e. more or larger sand pits will result in a diminishing of the concentration in the near field.

Scenario 3, double production rate

The yearly averaged concentration field of the last construction year is given in Figure F.15. Obviously, the area of interest is smaller and the magnitudes are higher. The effects at the locations in the vicinity are therefore higher. The effects at the far field locations are smaller. In the longer term and in the far field, the effects of a double production rate vanish, comparable to scenario 2.

It is concluded that a shorter production period leads to a shorter but higher pulse. The long term and far field effects of a shorter construction period are smaller. A longer period will therefore result in lower concentrations in the near field.

Sensitivity 1: Higher waves

The waves play an important role in the mobilisation of the silt from layer 2. In this sensitivity study, the wave load has been increased with 30%. This will result in more erosion during the storms, see Figure F.19 in comparison to Figure F.7. More sediment

is mobilised to the water column (see Figure F.20). The concentration during and after storms therefore increases. During mild conditions the effects vanishes, leading to a similar equilibrium concentration in the water column and percentage in layer 1.
After 6 years the area of influence is enlarged, as shown in Figure F.17-F.18.

Sensitivity 2: Advection by 3D effects
In this sensitivity study the 3D effects are meant to be exaggerated. A depth-averaged advection velocity of 5 mm/s (associated with a cross shore velocity of 12.5 cm/s at the surface and bottom) is used instead of the moderate value of 1 mm/s. This results in pushing the plume towards the coast, as shown in Figure F.21.

On the one hand, this effect can be considered negative, as the concentrations at the coast increase. On the other hand, this is a positive effect as the natural background concentrations are higher close to the coast; thus the relative effect on the entire coastal zone therefore decreases

Sensitivity 3: Smaller thickness layer 2
Decreasing the layer thickness from 30 cm to 10 cm leads to a larger area of influence and higher concentrations. This can be explained by the faster filling of layer 2, resulting in more erosion during storms and therefore higher concentrations during and after storms. Besides the contour plots of the concentration for the last construction year (Figure F.23-F.24), the time series for concentration and layer 2 are given in Figure F.25-F.26.

5.2.5 Summary and conclusions

As the model is linearly scalable, the sand extraction study can be carried out without taking into account the background concentration. The extra concentration due to sand extraction can be superposed on the background concentration of mud.

Six different simulations are carried out to determine the effect of sand mining on the silt concentration in the water. These six simulations exist of three different scenarios about the way of dredging (i.e. production rates per year) and three different sensitivity studies. In all simulations a plume was simulated, with a tendency to migrate to the north. At the vicinity of the sandpits the effects are largest (the extra concentration approximately equals the background concentration) and the farther from the pits the smaller the effects are. At Den Helder the effects are reduced to approximately 1% of the background concentration. After the construction period the concentrations in the vicinity of the sandpits drop in a few weeks. The concentrations in the near field are highly influenced by the silt release. Further away from the sandpits, the concentrations are strongly influenced by the silt in the bottom layers. The effect on the concentration will have a timescale of years to decades after the construction periods stops.

The relative effects are highest at approximately 10-20 km from the coast line. This is partly caused by the high background concentration near the coast. Approximately 50km from the coastline, the effects are reduced to ca 1%. Intensifying the dredging in time or space results in higher concentrations in the near field, but the far field is hardly influenced. A larger dredging area (more or larger sandpits) and dredging during a longer period will result in lower concentrations. More severe storms lead to higher concentrations during storms and to a somewhat larger area of influence. The yearly averaged concentrations are however much less influenced.

5.3 Effects on mud transport with Delft3D

5.3.1 Parameter settings

The sand extraction locations are shown in Figure 1.1. The following scenario (reference alternative) was calculated: a continuous release of fine at a rate of 2 MT/yr for a period of 7 years (1996 – 2002). In the year 2003 no fines are released. This year can be used to assess the relaxation of the system after the end of the sand extraction activities. The initial concentration on 1 January 1996 was set at zero with an empty seabed. Zero boundary concentrations were applied. The applied parameter settings are shown in Table 2.1. For one computation, τ_{crit1} was set at 0.1 Pa and $\alpha = 0.05$. This is mentioned where applicable.

As the sediment mass that can be stored in the buffer layer is uncertain, sensitivity computations were made with an upper limit, best estimate and lower limit of the sea bed buffer capacity. These values were based on a combination of internal and external discussion (expert opinion), model results and literature data:

- Upper limit: 10 kg/m^2, d = 0.6 m, residence time in buffer layer 4 years.
- Best estimate: 5 kg/m^2, d = 0.3 m, residence time in buffer layer 2 years.
- Lower limit: 2.5 kg/m^2, d = 0.15 m, residence time in buffer layer 1 year.

The buffer capacity was varied by a variation of the thickness of the second bed layer. It is equally possible to vary the buffer capacity for a fixed layer thickness through a modification of erosion parameter M_2, as $p_{eq} \sim 1/M_2$, but this approach was not adopted. All other settings remained equal. The buffer capacity B is calculated from the layer thickness d according to:

$$B = p_{eq} (1-n) \rho_s d,$$

where p_{eq} is the mud fraction in the bed at equilibrium with the local time-averaged bed shear stress and suspended sediment concentration. For Noordwijk 10, the parameters where chosen such that $p_{eq} \approx 0.01$ (see Figure 2.11). At locations with a lower time-averaged bed shear stress or a higher time-averaged suspended sediment concentration, p_{eq} will be higher (and vice versa).

The mentioned residence time is the average residence time of mud in the second bed layer. A residence time of 2 years agrees well with an estimate by Laane et al. (1999). A residence time of 2 years with a buffer capacity of 5 kg/m^2 implies an exchange rate between the second bed layer and the water column of 2.5 kg/m^2/yr. Indeed, for Noordwijk 10 $\alpha w_s c \approx 10^{-7}$ kg/m^2/s = 3 kg/m^2/yr.

5.3.2 Sensitivity simulations

Prior to the computations with buffer layer, also sensitivity computations **without** buffer layer are presented in order to assess the effect of the application of ZUNO-GROF instead of ZUNO-DD (with a much higher grid resolution) on the one hand and the effect of the new calibration using CEFAS data on the other hand. The figures starting with reference “WL…” can be found in Appendix G. The other figures are given in the text.

The following results are presented on the sensitivity computations without buffer layer:

1. Spatial dispersal of SPM for 2000/2001 with ZUNO-coarse (Fig.WL01a); Idem for year 1988/89 with ZUNO-DD (high-resolution) (Fig. WL01b). Both computations are based on the parameter settings used in the project MV2 “Passende Beoordeling”, see WL|Delft Hydraulics (2005).
2. Spatial dispersal of SPM for 2000/2001 with ZUNO-coarse, calibration according to CEFAS, original settings (τ_{c1} = 0.3 Pa), no buffer layer (Fig. WL02);
3. Spatial dispersal of SPM for 2000/2001 with ZUNO-coarse, calibration according to CEFAS, new settings (τ_{c1} = 0.1 Pa), no buffer layer (Fig. WL03);

A comparison between Figs. WL01a and WL01b show that a good agreement exists between the impact calculations with ZUNO-coarse and ZUNO-DD. No exact comparison can be made, as the ZUNO-DD computation is only available for the period 1/11/1988 – 1/11/1989 and the ZUNO-coarse computation for the period 1996 – 2003. However, the average effect for 1988/89 lies within the same range as for the year 2000 and 2001. It is therefore concluded that no major inaccuracies are introduced by the application of the coarse ZUNO schematisation instead of the finer domain decomposition grid.

Fig. WL02 shows the plume dispersal based on the new calibration on Noordwijk 10 km (CEFAS). However, the 2nd (buffer) layer has been practically disabled with d_2 = 0.015 m and α = 0.01. Typical SPM surface concentrations due to the release of fines during sand extraction remain much lower compared with the previous calibration according to

the silt atlas. If the critical shear stress for erosion from the near-bed layer is reduced from 0.3 to 0.1 Pa, the agreement with the previous computations is better (see Fig. WL03, compare with Fig. WL01a). Also, the setting of τ_{crit1} = 0.1 significantly improves the background concentration levels (in combination with α = 0.05 for the 2nd layer, see Section 4.4). We conclude that the latter settings yield more realistic results regarding SPM levels than using τ_{crit1} = 0.3 and α = 0.1.

5.3.3 Scenario results

The following results are presented on the scenario computations including the buffer layer. All computations have been made with ZUNO-coarse. Numbers 4, 5 and 6 are based on the new settings τ_{c1} = 0.1 Pa and α = 0.05, all other numbers on the original settings shown in Table 2.1 (with τ_{c1} = 0.3 Pa and α = 0.1). The figures starting with reference "WL…" can be found in Appendix G. The other figures are given in the text.

1. Spatial dispersal of SPM for the years 1996-2003 in the surface layer, average buffer capacity (2 yr, 5 kg/m^2) (Figs. WL04a-d);
2. Spatial dispersal of mud percentage in the bed for the years 1996-2003, average buffer capacity (2 yr, 5 kg/m^2) (Figs. WL06a-d);
3. Spatial dispersal of yearly averaged SPM in the surface layer for 1996-2003 lower limit, best and upper limit for buffer capacity (Fig. WL07a-h);
4. Spatial dispersal of mud percentage in the bed for 1996-2003, lower limit, best and upper limit for buffer capacity (Fig. WL08a-h);
5. Figure with mud percentage near the discharge location (Fig. 5.13);
6. Figure with resuspension potential over the years 1996-2003 (Fig. 5.14);
7. Time series of SPM and mud fraction in seabed at Scheveningen 8 km and Noordwijk 10 km (Figs. 5.15 and 5.16). Daily averages for the year 1996 and 2002.
8. Time series of SPM and mud fraction in seabed at Lichteiland Goeree, Scheveningen 8 km, Noordwijk 10 km, Egmond 20 km, Den Helder and Terschelling Noordzee (Figs. 5.17).

Based on these results, the following analysis is made.

Figs. WL04a-d show the evolution of the dredging plume in time over the years 1996 – 2003. The year-averaged surface concentration is displayed. It is clear that the impact zone grows in time. The width of the impact zone is limited to a 30 km wide band parallel to the Dutch coast, which is caused by the gravitational circulation induced by the freshwater flow from the Rhine River. This circulation pushes the dredging plume towards the coast, where it remains trapped. The isoline of 5 mg/l concentration increase extents from Walcheren to Petten after 6 years of continuous release.

Figures WL06a-d show the increase of the mud percentage in the sea bed caused by sand extraction. The same dispersion pattern is observed as for suspended sediments, which suggests that the mud fraction in the seabed is in dynamic equilibrium with the sediment concentration in the water column. If the length L of the zone with a 0.5% mud fraction increase is plotted as a function of time t, an approximately linear relationship appears to exist. A reasonable fit is obtained using the expression: $L(t) = Ft/(BC)$, where F is the sediment release rate (2 MT/yr), B is the width of the zone (about 30 km) and C is the average buffer capacity of the seabed within the 0.5% contour line (set at 4 kg/m^2). This is illustrated in Figure 5.3. Obviously some variation is observed as the years differ.

Fig. WL07a-h shows the annual averaged SPM concentrations for the lower, best and upper estimate of the buffer capacity. The upper plot shows the results for a buffer capacity of approximately 10 kg/m^2 (residence time in the buffer layer is 4 years) the middle plot for 5 kg/m^2 (2 years) and the lower plot for 2.5 kg/m^2 (1 year).

Figure 5.3. Length-scale of 0.5% mud percentage increase because of sand extraction; dots: based on ZUNO-computation; line: linear relationship *L*(*t*) = *Ft*/(*BC*), see text.

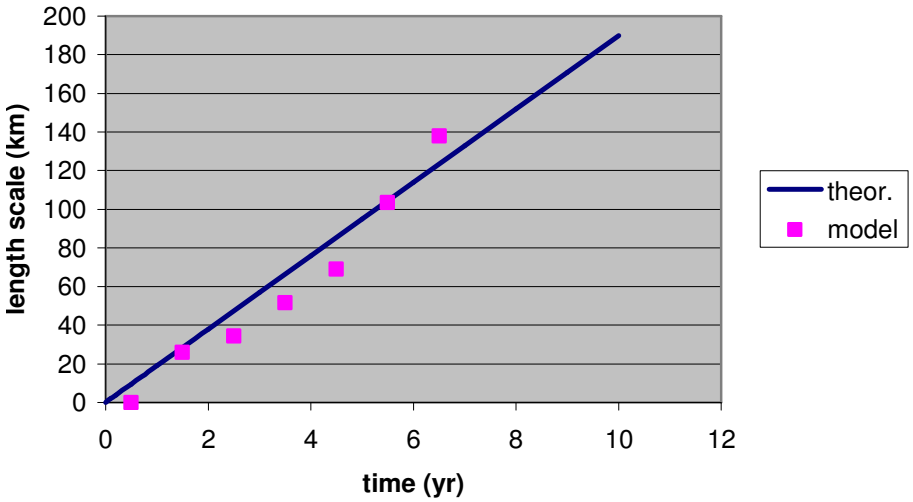

These plots demonstrate that the potential effect of sand extraction is sensitive to the assumed buffer capacity of the seabed. In the Voordelta, for example, the yearly averaged concentration increase due to sand extraction varies between 2 mg/l and 10 mg/l for the lower limit and upper limit, respectively. The same values are observed In front of the Dutch coast. The impact of sand extraction in the Wadden Sea area is small (< 1 mg/l), even for the upper estimate of the buffering capacity.

Fig. WL08a-h shows the bandwidth of the increase in mud percentage in the seabed during 1996-2003. Note that this figure shows the absolute increase in mud percentage and not a relative increase. In the Voordelta the accumulation is much lower than along the Holland coast. This can be attributed to the shallowness of this area, resulting in a significantly higher wave-induced bed shear stress. As a result, the equilibrium mud percentage tends to be lower for a given SPM average concentration. It is remarked that Figs. WL07 and WL08 are based computations using the original settings from the CEFAS calibration (τ_{crit1} = 0.3 Pa; α = 0.1). The rather low absolute SPM concentration levels do not affect the results of the sensitivity analysis of the buffer capacity, however. Mud fraction due to sand extraction in front of the Dutch coast varies between 0.5 and 2% after 6 years.

Figure 5.4 shows the evolution of the mud fraction in time for the period 1996 – 2003 near the discharge location. This figure demonstrates that the residence times in the buffer layer targeted for, i.e. 1, 2 and 4 years, have indeed been achieved with the present parameter settings. The thicker the buffer layer, the longer the residence time and the smaller the amplitude of fluctuations in mud content induced by storms. The drawn lines are theoretical expressions for the mud percentage increase under equilibrium conditions: $p = p_{eq}(1-\exp(-t/\tau))$, with τ the residence time. The green line represents the new settings to improve the concentration levels in the water column. Although the residence time remains unchanged (2 years), the equilibrium percentage is

reduced from 1 to 0.6%. The buffer capacity is therefore only about 3 kg/m^2, close to the assumed lower limit for buffer capacity (2.5 kg/m^2.

Figure 5.4: Mud fraction in the sea bed as a function of time. t_0 = 01/01/1996. Location: close to discharge location. Settings according to Table 2.1 except for 'new' (α = 0.05, τ_{crit1} = 0.1).

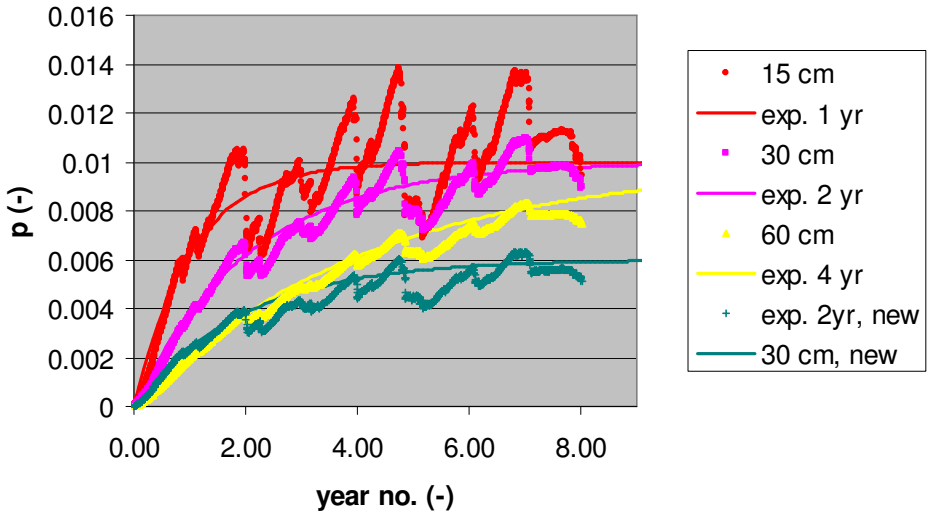

Figure 5.5: Resuspension potential from 2nd layer (in kg/m^2/yr)

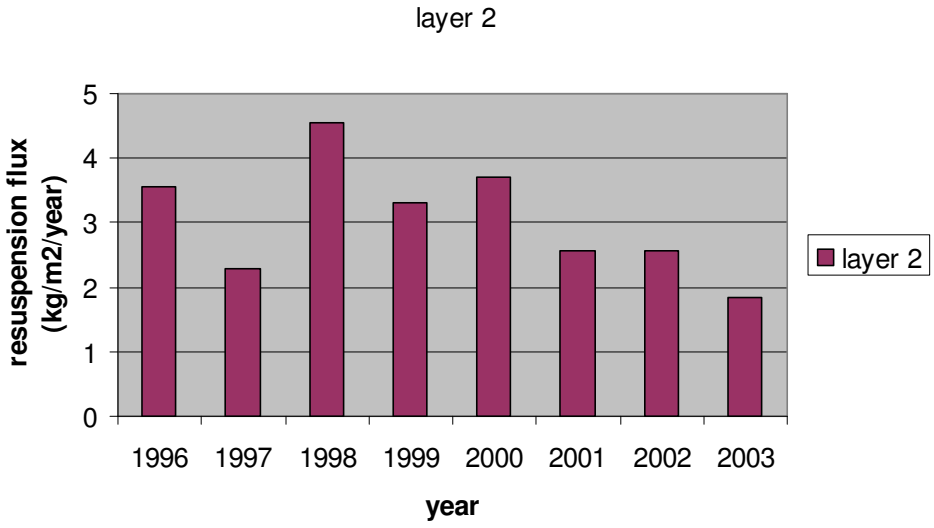

Figure 5.5 shows the resuspension potential for the 2nd layer for the period 1996 – 2006, assuming p = 0.01. It ranges between 1.9 kg/m^2/yr in 2003 to 4.6 kg/m^2/yr in 1998. The number of storms in 1998 was high, 16, which explains the high resuspension potential. The standard deviation is 0.9 kg/m^2/yr. A continuous release of 2 MT/yr therefore adds an amount of fine material to the water column that is equal to the typical inter-annual fluctuation in resuspension in an area with size 75 × 30 km. Within this area, the impact of sand-mining exceeds the impact of natural inter-annual variability. Outside this area, impact of natural inter-annual variability is larger.

Figures 5.6 and 5.7 show the daily-averaged surface concentration and mud content in the seabed at Scheveningen 8 km and Noordwijk 10 for the years 1996 (start of sand extraction) en 2002 (end of sand extraction). In 1996 the effect of sand extraction starts to build up; in 2002 a dynamic equilibrium has been reached at both locations. These figures illustrate that the concentration increase because of sand extraction is highly variable, depending on the meteorological conditions. Assuming that the released fines behave similar to the fine sediment of the natural background, also the time-dependent behaviour will be similar. Although at Scheveningen the surface concentration due to sand extraction ranges between 1 mg/l during calm weather and 15 mg/l during storms, the relative contribution to the natural background will be equal for both conditions.

Figures 5.8a-c show the monthly averaged surface concentration because of sand extraction for the complete simulation period (1996 – 2003) for Lichteiland Goeree, Scheveningen 8 km, Noordwijk 10 km, Egmond 20 km, Den Helder and Terschelling Noordzee. These stations are listed according to their distance from the sand extraction area. Lichteiland Goeree is close to the area of release. The SPM concentration are shown for the minimum, mean and maximum amount of sediment buffering in the seabed. It is clear that the farther from the release area, the longer the spin-up time for the impact. Also, the farther from the release area, the larger the effect of sediment buffering.

The effects of the mud concentration increase caused by sand extraction on the ecology of the Dutch coastal zone will be discussed separately in the next section. The computation with the settings $\alpha = 0.05$ and $\tau_{crit1} = 0.1$ Pa has been used to investigate the ecological effects, as these settings comply well with both CEFAS data at Noordwijk and DONAR data at other locations with regard to the background concentration. The thickness of the buffer layer is 0.3 m, the residence time is 2 years and p_{eq} in the vicinity of the release point is 0.6%, resulting in a buffer capacity of circa 3 kg/m^2.

Figure 5.6a: Daily-averaged surface concentration (mg/l) at Scheveningen 8 km in 1996 (upper panel) and 2002 (lower panel).

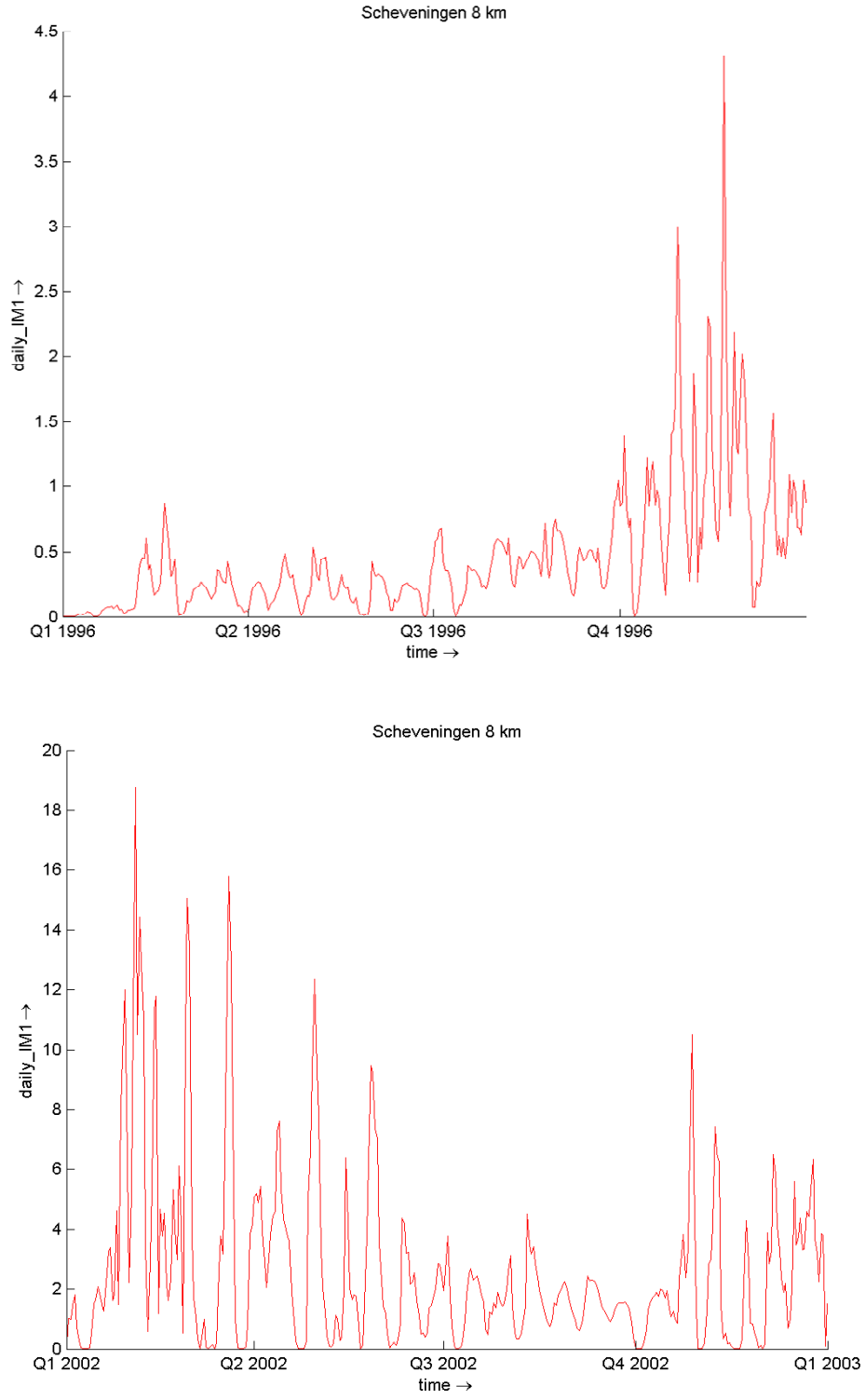

Figure 5.6b: Mud fraction (-) in sea bed in 1996 (lower panel) and 2002 (lower panel). Note different scales on *y*-axis. New settings: $\alpha = 0.05$; $\tau_{crit1} = 0.1$ Pa.

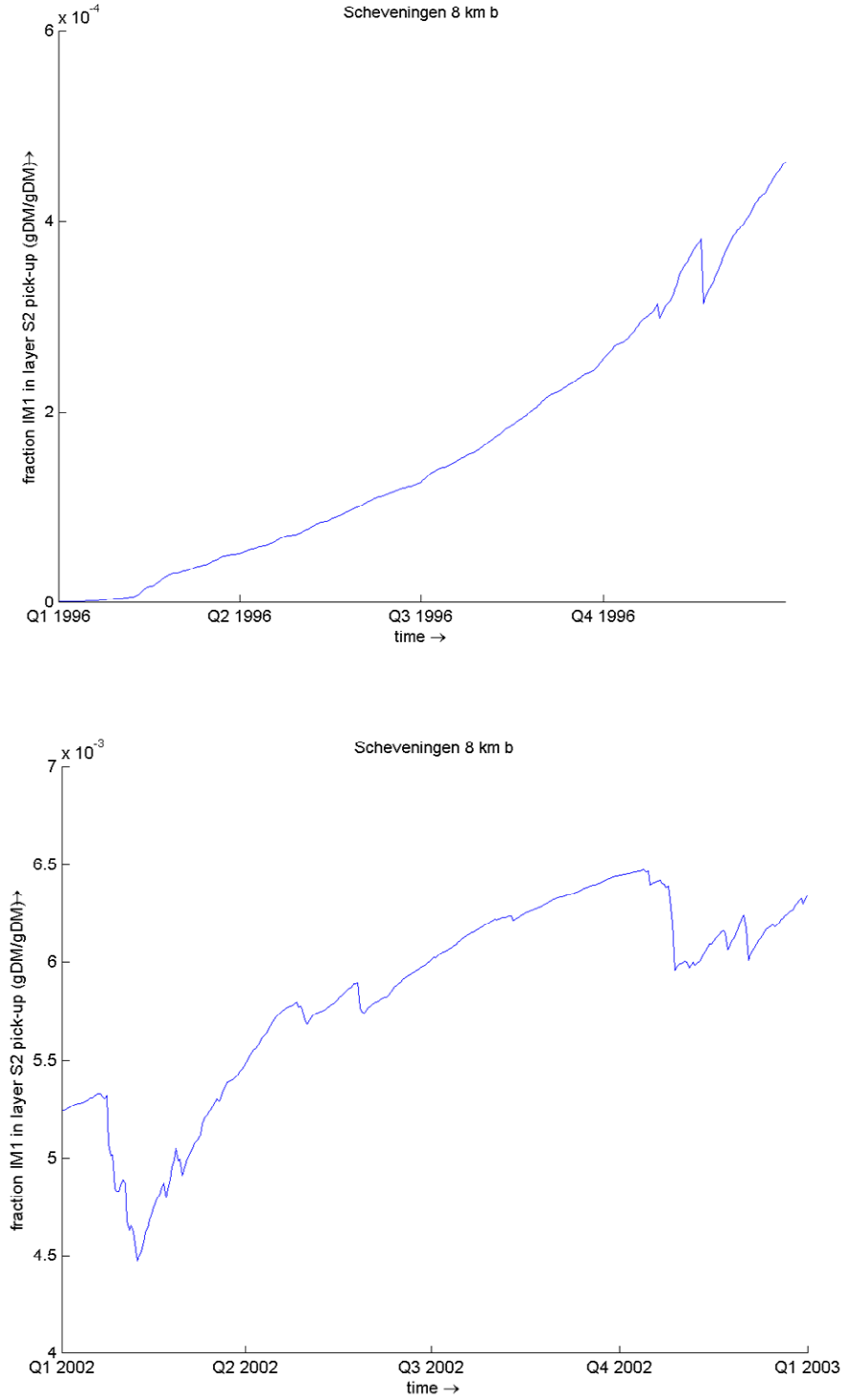

Figure 5.7a: Daily-averaged surface concentration (mg/l) at Noordwijk 10 km in 1996 (upper panel) and 2002 (lower panel). New settings: $\alpha = 0.05$; $\tau_{crit1} = 0.1$ Pa.

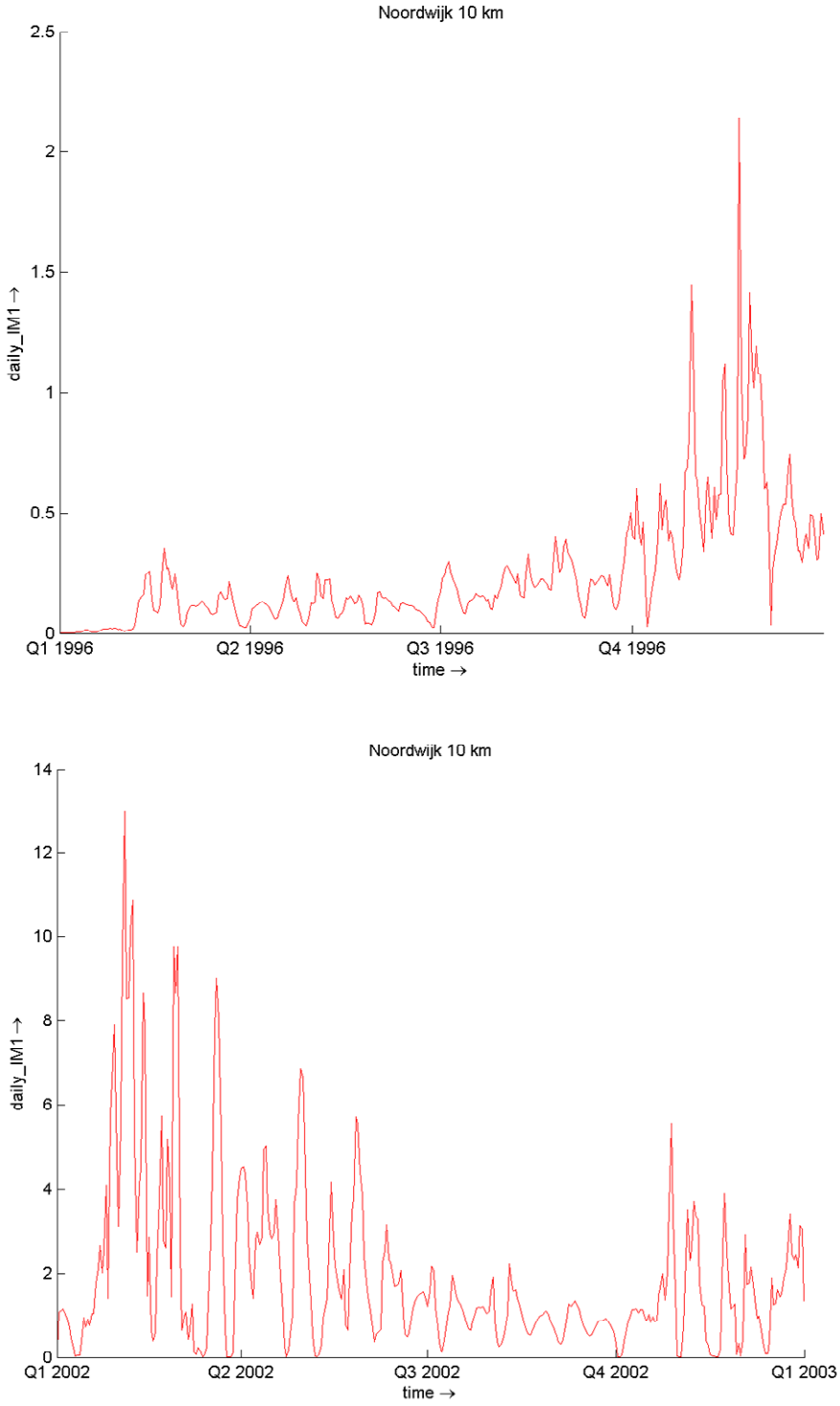

Figure 5.7b: Mud fraction (-) in sea bed in 1996 (upper panel) and 2002 (lower panel). Note different scales on *y*-axis. New settings: $\alpha = 0.05$; $\tau_{crit1} = 0.1$ Pa.

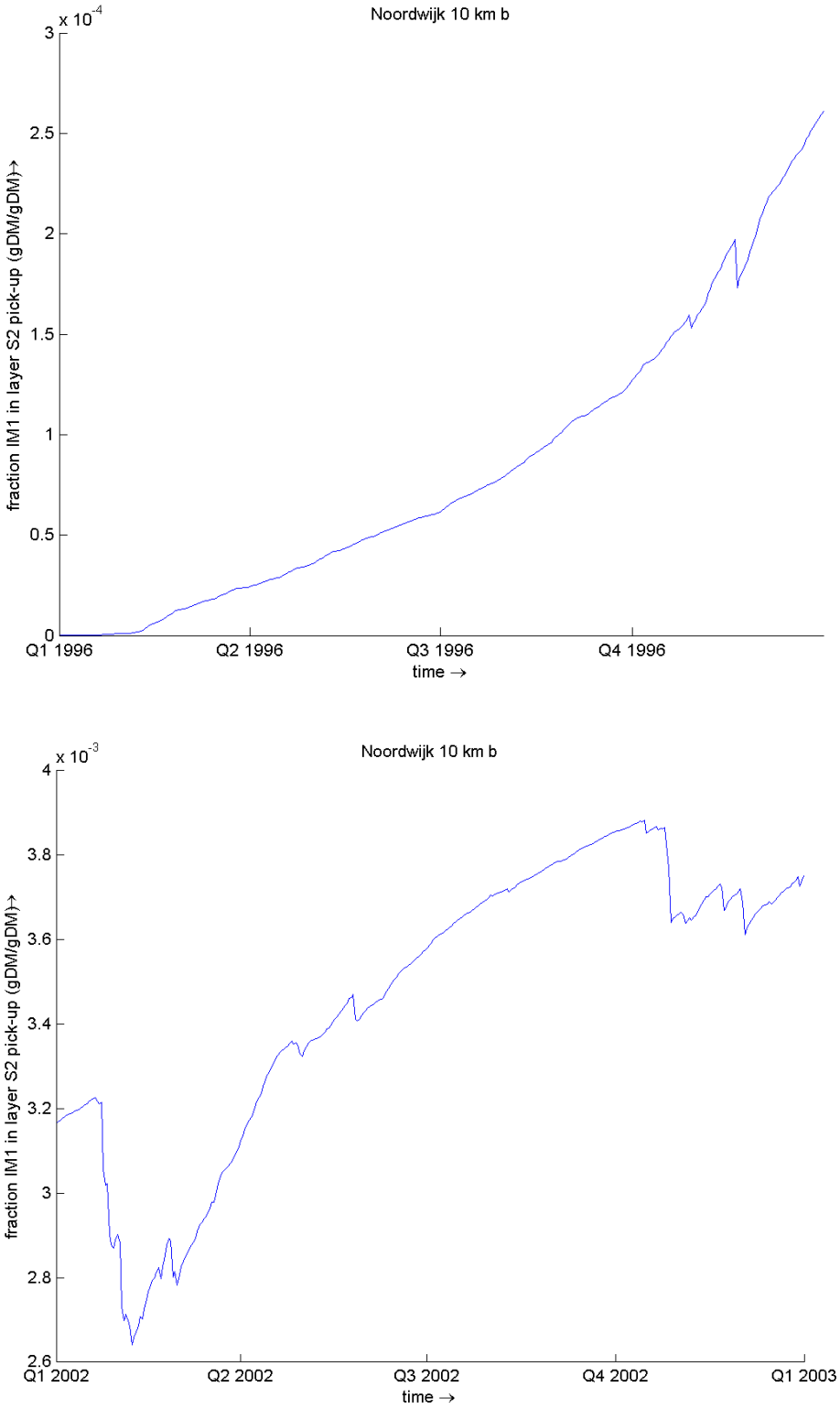

Figure 5.8a: Monthly-averaged surface concentration (mg/l) caused by 2 MT/y sand extraction at locations indicated above the plots. Note different scales on *y*-axis. Settings: $\alpha = 0.1$; $\tau_{crit1} = 0.3$ Pa. Buffer layer: min = 10 kg/m2; mean = 5 kg/m^2; max = 2.5 kg/m^2.

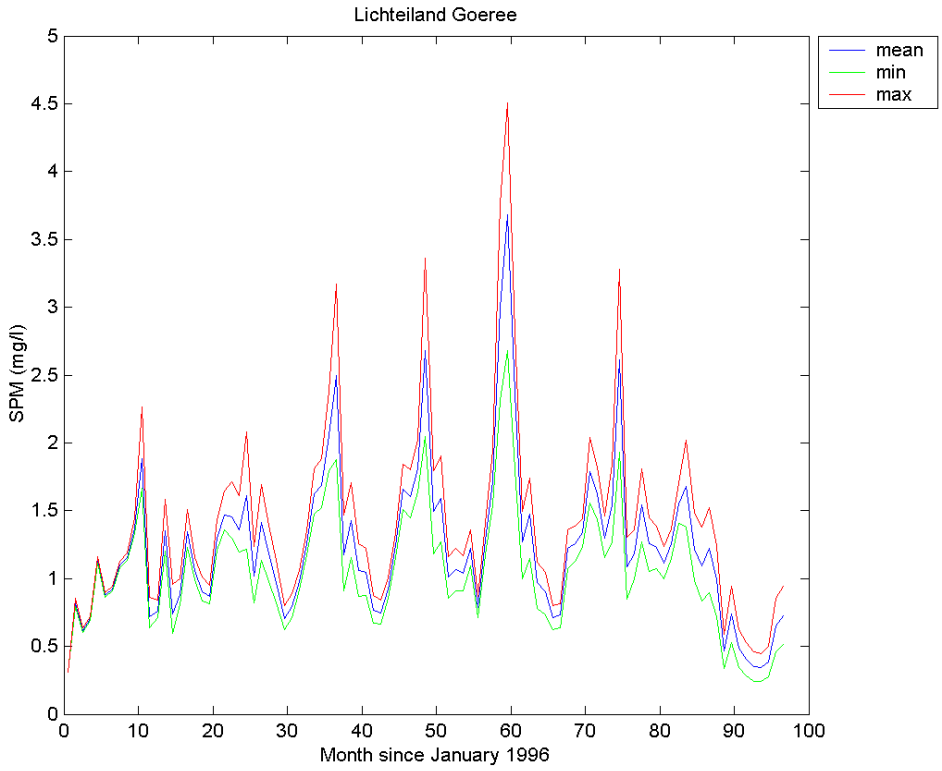

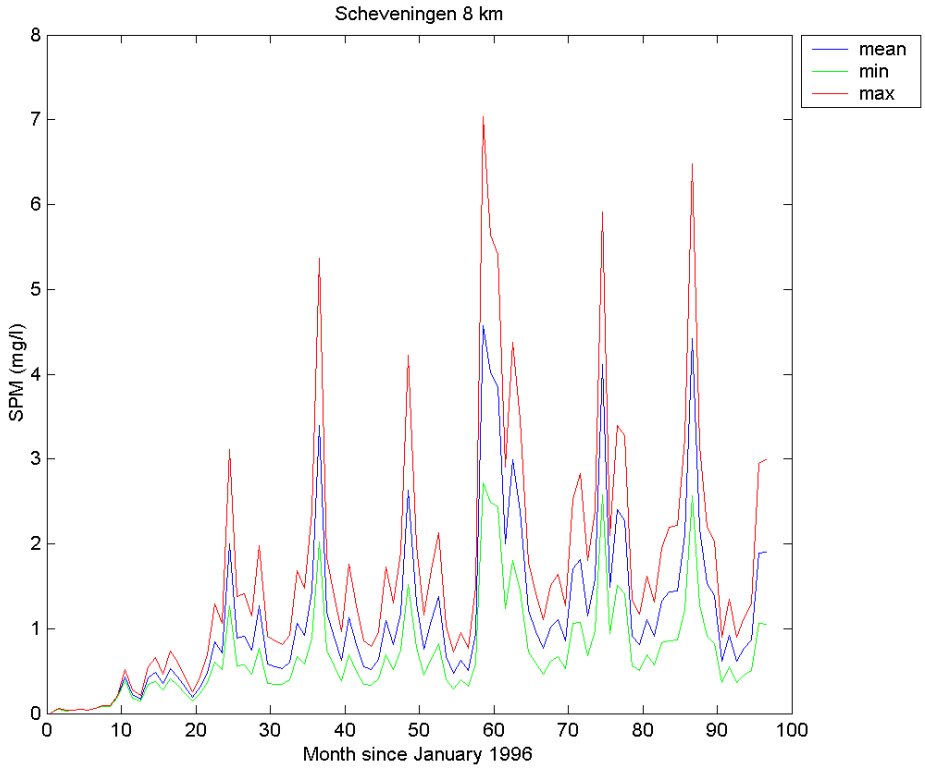

Figure 5.8b: Monthly-averaged surface concentration (mg/l) caused by 2 MT/y sand extraction at locations indicated above the plots. Note different scales on *y*-axis. Settings: $\alpha = 0.1$; $\tau_{crit1} = 0.3$ Pa. Buffer layer: min = 10 kg/m2; mean = 5 kg/m^2; max = 2.5 kg/m^2.

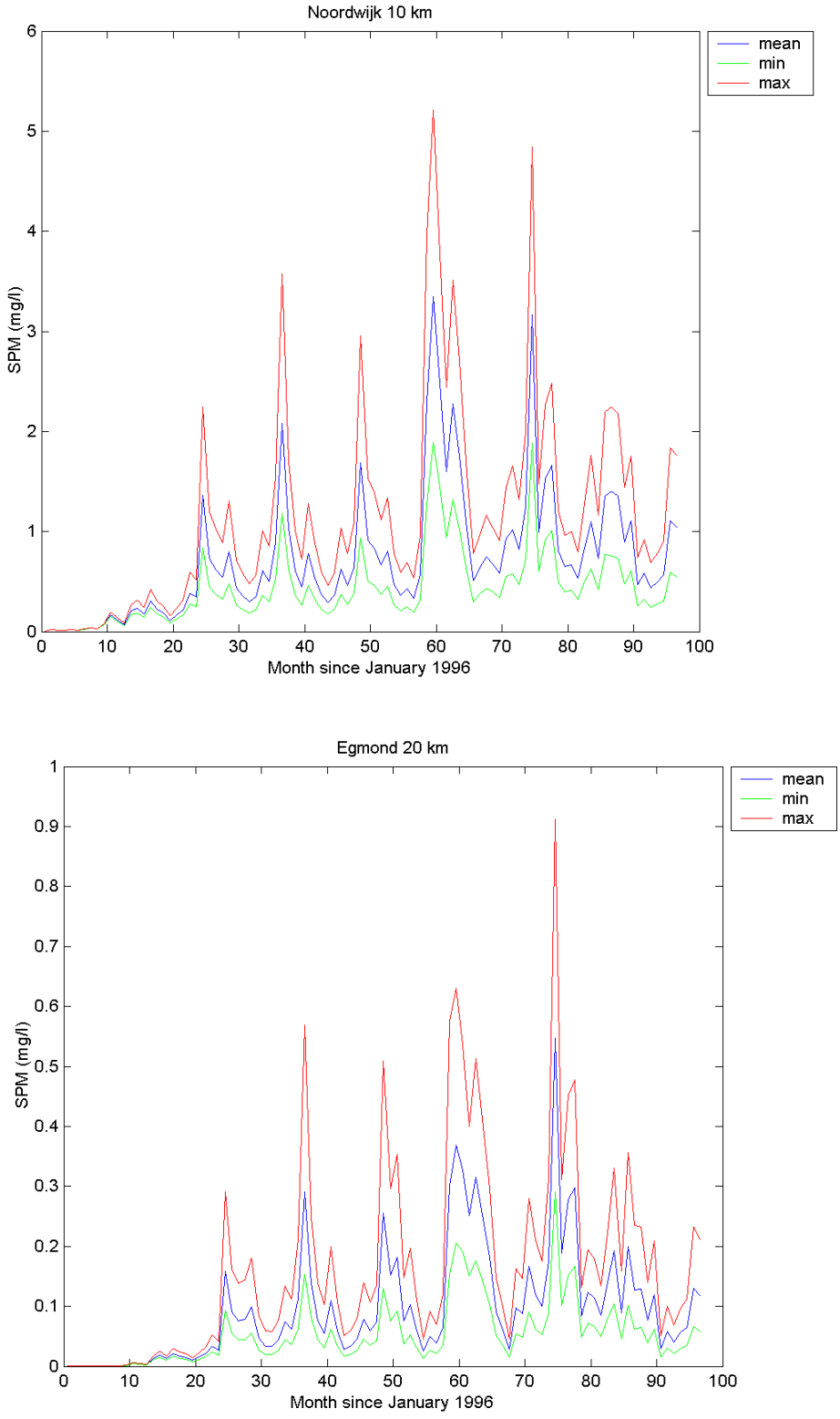

Figure 5.8c: Monthly-averaged surface concentration (mg/l) caused by 2 MT/y sand extraction at locations indicated above the plots. Note different scales on *y*-axis. Settings: $\alpha = 0.1$; $\tau_{crit1} = 0.3$ Pa. Buffer layer: min = 10 kg/m2; mean = 5 kg/m^2; max = 2.5 kg/m^2.

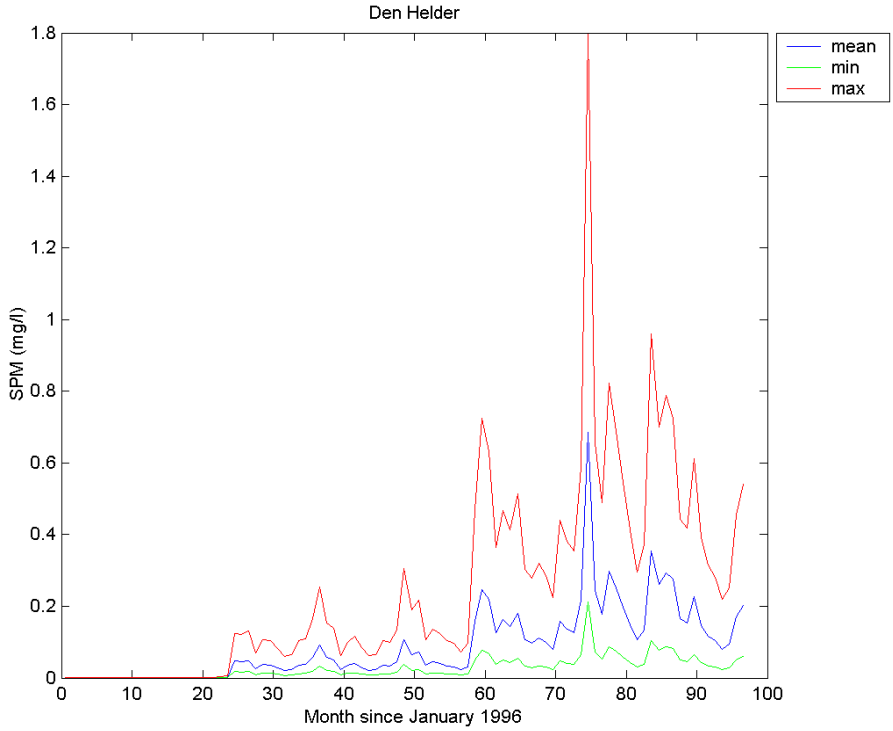

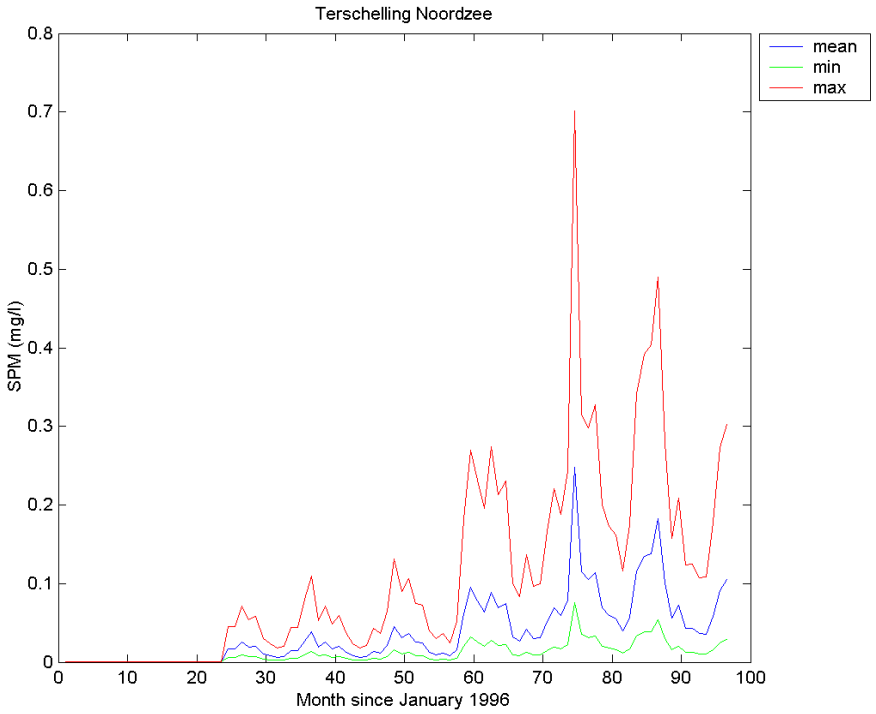

5.4 Comparison of 2D and 3D approach

5.4.1 Introduction

In Section 5.2 and 5.3 two models have been applied to determine the effect of the sand extraction on the silt concentration in the water column, viz. FINEL2D and DELFT3D. These approaches differ in the following ways:

- A *two-dimensional* model with *high* resolution (FINEL2D) and a *three-dimensional* model with *a coarser* resolution (DELFT3D).
- The parameter settings for the water-bed exchange formulations.

Obviously, these differences result in a different impact due to the sand extraction. Because the silt effects are crucial for the impact on nutrients and primary production, this section contains a detailed discussion about the differences.

5.4.2 The effect of a three-dimensional water motion

First, the effect of a different resolution and water motion in FINEL2D and DELFT3D is considered. For this purpose, a run has been made with Delft3D in the “two-dimensional” mode to exclude the three-dimensional effects. Furthermore, (almost) identical settings have been used for the various parameters in the silt model. Figure 5.9 demonstrates that the large-scale mud dispersion patterns of both models are almost identical. This is not obvious because the underlying grid has a different spatial different resolution. FINEL has a much higher resolution in the coastal zone and around the sand extraction pits. Furthermore, the 2D water motion in both models is also not identical. Obviously, the high resolution simulations give more detail, like the burying of silt in layer 2 at the anchor place at the end of the entrance channel. Despite these small differences, it can be concluded that the differences in resolution and 2D water motion of FINEL2D and DELFT3D (2DH mode) have a small effects on the results at a large scale.

Figure 5.9 Effect of sand extraction on the yearly-averaged mud concentration (mg/l) after 6 years with the two-dimensional model FINEL (lower panel) and Delft2D (upper panel). Note that the colorbar is identical.

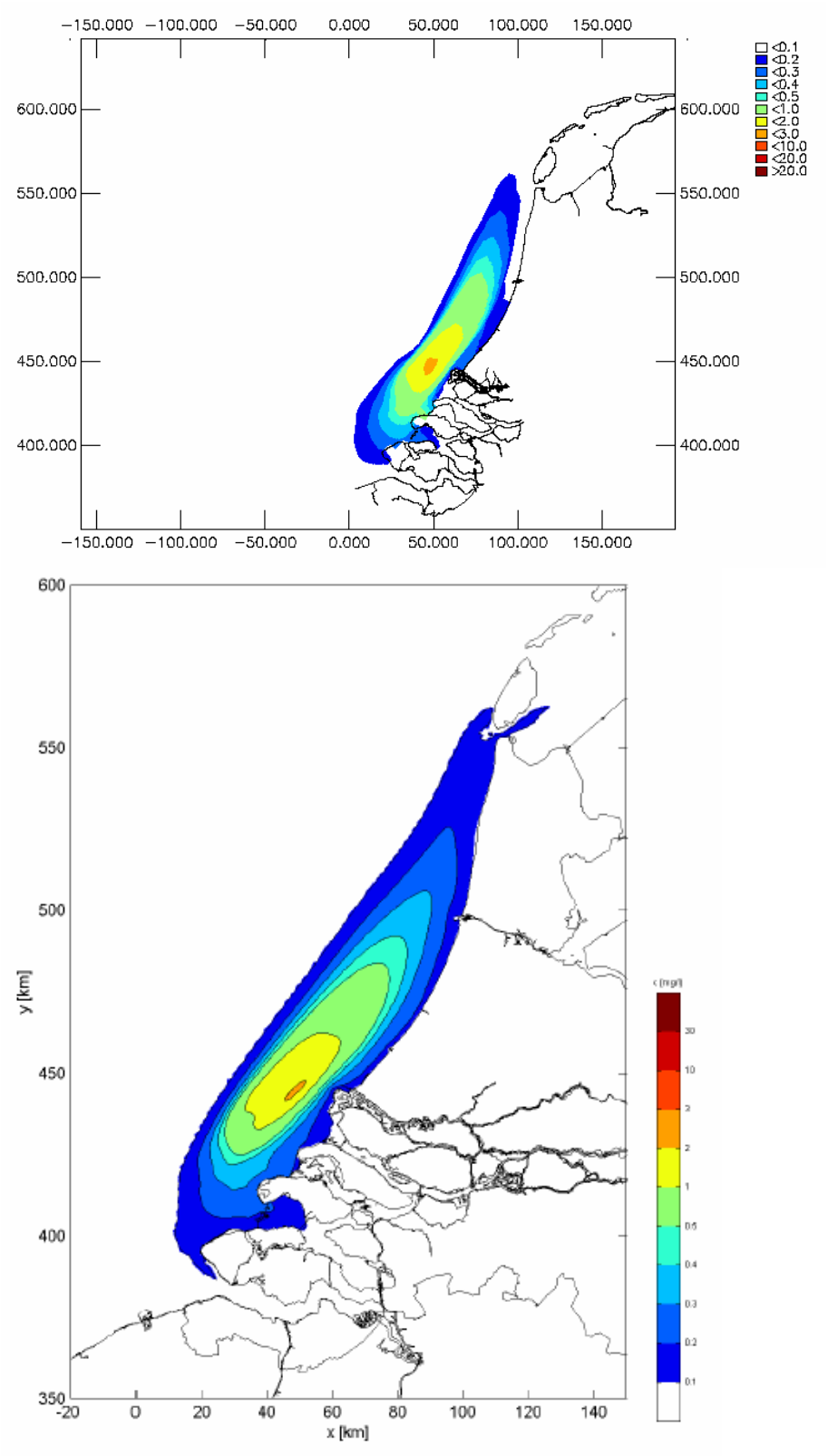

Next, the difference between a two-dimensional and three-dimensional water motion is considered. Figure 5.10 illustrates the results for two situations: a three-dimensional approach with Delft3D and a two-dimensional approach with Delft2D with similar settings for the silt model. As already said before, the results of FINEL2D are comparable with the result of Delft2D. Figure 5.10 demonstrates that the three-dimensional approach has a relatively large effect on the impact computations. Due to the three-dimensional effects, the plume bends towards the coastline. Furthermore, the effect on the mud concentration appears to be higher in the 3D approach. The suspended silt particles are swept towards the coast, resulting in smaller zone with higher concentrations.

Figure 5.10 Effect of sand extraction on the yearly-averaged mud concentration (mg/l) after 6 years. The upper panel shows the results for the three-dimensional approach (Delft2D) and the lower panel shows the results for a two-dimensional approach (Delft2D).

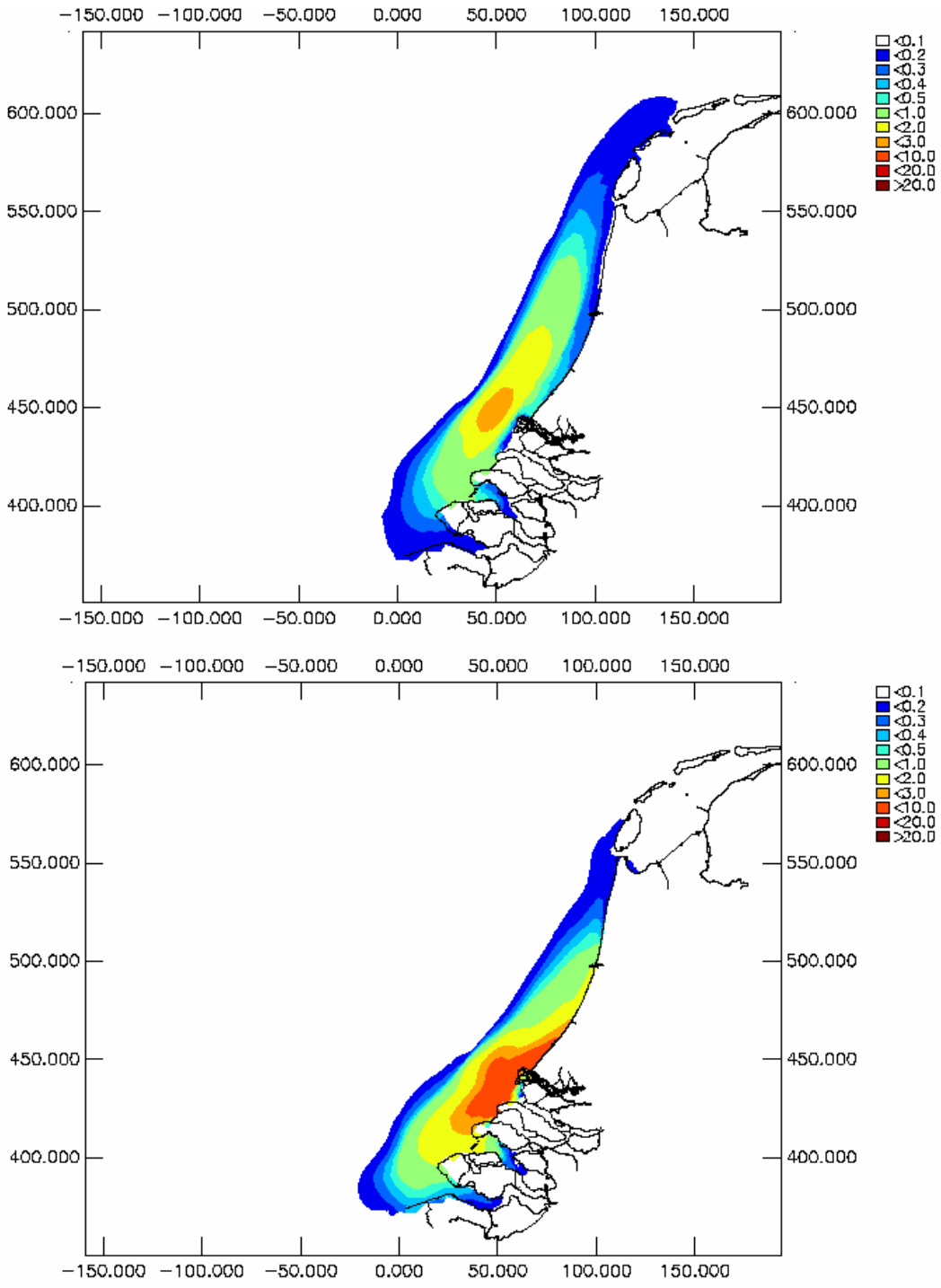

Qualitatively, the three-dimensional “sweeping effect” of the silt particles can be explained as follows. The fresh water discharges of the Nieuwe Waterweg and Haringvliet result in horizontal and vertical density gradients in front of the Dutch coast. Due to settling of particles, vertical gradients in the sediment concentration are created. Horizontal density differences result in a vertical circulation such that the fresh water flows in the upper part of the water column whereas the salt water flows near the seabed towards the coast. This causes a net advection of silt towards the shore because in general the sediment concentrations are higher near the bed than at the water surface.

In FINEL2D, the three-dimensional effects as described above were parameterized by assuming an extra advection velocity towards the coast, based on the long term residual flow profile with an amplitude of 2.5 cm/s. Moreover, a sensitivity computation has been carried out with an advection amplitude of 12.5 cm/s (see Section 5.2, sensitivity study 2). This extra advection term resulted in a bending of the plume to the coast and in an increase in concentration. But even with this exaggeration the pushing of the plume towards the coast is not comparable with the DELFT3D results. The main differences are found at the coast until IJmuiden. Comparing the results of FINEL with DELFT3D shows that the three-dimensional effects near the Nieuwe Waterweg and the Haringvliet are stronger in the three-dimensional model.

There are two possible explanations for the differences between FINEL2D and DELFT3D. The first one is based on the long term residual cross shore current. The second one is based on the tidal fluctuations in the cross shore direction, leading to the so-called tidal straining. Both explanations are discussed below:

Tidal straining
A possible reason for extra advection of silt towards the coast could be the so-called tidal straining as described by Souza&Simpson (1996). Due to stratification and a tidal flow, cross shore fluctuations are present. The amplitude of these fluctuations can be in the order of magnitude of several decimetres per second. In principle this tidal straining is implicitly simulated in the three-dimensional simulations with DELFT3D for mild conditions, although validation would be required. During storms wave induced currents might result in a reduction of the stratification and furthermore in a diminishing of the tidal straining, see Souza&Simpson (1996). This extra mixing by wave induced currents is presently not taken into account in DELFT3D. The effect of tidal straining in DELFT3D might therefore be exaggerated during storms. Although vertical stratification may be exaggerated under some conditions, the computed sediment accumulation along the Dutch coast does also occur for well-mixed conditions. A thorough analysis of the tidal straining, including the implementation of mixing due to waves, is required, but falls out the scope of this project.

Residual flow
Besides the residual flow towards the coast itself, differences between the 2D and 3D can be explained by the difference in residual flow between surface layer and bottom layer. This results in a concentration of sediment near the coast, as water with a higher sediment concentration is transported along the bottom towards the coast, and water with a slightly lower sediment concentration is transported towards the sea. The crux is that sediment from the upper layer is gradually lost to the lower layer and thus returns towards the coast. Of course, an equilibrium will be reached after some time because of

horizontal and vertical dispersion, but strong spatial concentration gradients may nevertheless be generated.

Although it is possible to bend the sediment plume towards the coast in a 2D model by introducing an additional residual current towards the coast, the complicated three-dimensional structure of the water motion and the silt concentration that varies in time and space is not resolved. These differences are likely to cause differences between the 2D and 3D results in the Dutch coastal zone in general and around the outflow of the Nieuwe Waterweg and the Haringvliet in particular. Notice that the three-dimensional model has a relative low resolution in this area. It is recommended to study this behaviour with a more detailed model as well (e.g. ZUNO-DD).

Summarizing, the results of a 3D model significantly differ from the 2D approach due to the density-induced mechanisms initiated by the fresh water discharges in front of the Dutch coast. Although the 2D approach accounts for the residual advective effect of the density current, the complicated interaction between the three-dimensional water motion and the silt concentration around the outflow of the Rhine and Meuse is not resolved. As no detailed calibration of the 3D hydrodynamic and silt model has been performed, it is hard to determine if all complex three-dimensional processes are captured well with the model DELFT3D in combination with the grid ZUNO-coarse. Nevertheless, previous studies have shown that the long-term mean salt and silt patterns are reproduced in a realistic way (e.g. Flyland). We conclude that the presented 3D approach can be considered as the “best estimate” up till now.

5.4.3 Parameter settings

The impact simulations with FINEL and Delft3D have been carried out with different parameter settings. The values for the different calibrations are given in Table 6.1. Notice that the calibration of the various parameters has been carried out with a schematized one-dimensional model as a first step (see Chapter 2). Next, the optimal settings have been used in FINEL and Delft3D to simulate the silt transport in front of the Dutch coast in a two-dimensional and three-dimensional way, respectively (see Chapter 3 and 4). During this calibration the settings have been changed to find an optimal situation. For instance, the original settings for Delft3D have been adapted because the simulated background concentration appeared to be too low with the “original” settings. Therefore, “new” settings were derived that resulted in a better prediction of the background concentration. The silt computations with these settings have been used for the impact simulations on nutrients and primary production (see section 5.5).

Table 5.1 Parameter settings in FINEL and DELFT3D.

	δ [m]	p [%]	M_2 [kg/m^2]	M [kg/m^2/s]	Ws [mm/s]	α [-]
FINEL	0.3	2-2.5	15.9 -19.9	2.0E-7	0.4	0.14
DELFT3D original	0.3	0.6-1.1	4.8 - 8.7	3.5E-7	0.25	0.1
DELFT3D new	0.3	0.4-0.6	3.2 - 4.8	3.5E-7	0.25	0.05

Although the calibrated concentrations at Noordwijk (CEFAS data) are simulated well by both models, the approaches differ in silt mass per area for layer 2 (m_2). The value for this parameter is, to a large extent, irrelevant for the CEFAS calibration. The mass per area in layer 2 is defined by $m_2=\delta * \rho_{silt} * p_2$.

Although these parameter settings give similar results for the calibration, as the silt percentages do not change significantly during the calibration, a difference is found in the sand pit simulations. For the same silt percentage, the erosion for layer 2 will be 3.5/2=1.75 times higher for the DELFT3D simulations than for the FINEL simulations. Furthermore the leaking from layer 1 to layer 2 is faster (0.14/0.1=1.4 or 0.14/0.05=2.8) and the settling is quicker (0.4/0.25=1.6) for FINEL2D than for DELFT3D. This results in higher concentrations for simulations with DELFT3D than with FINEL2D.

Unfortunately, there are no measurements of the spatial variation of the silt percentage in the bottom, nor of the thickness of the active layer. Based on expert judgement, the silt percentage is in the order of magnitude of 1-4% and the layer thickness 0.1-0.5m. This gives a range for m_2 of 2.65-53 kg/m^2, implying that the FINEL2D calibration has been carried out with a moderate m_2, whereas the DELFT3D calibration is carried out closer to the lower limit of m_2. This implies that the computed far field effects on the silt concentration with Delft3D can be considered as a conservative approach. More measurements are necessary to reduce this bandwidth.

5.5 Effects on nutrients and primary production

5.5.1 General

To simulate the sand extraction plume, two different scenarios have been used, both resulting from the silt modelling described in the previous section. The first one is the sand extraction plume without silt buffering in the seabed. The second sand extraction scenario includes the calibrated silt buffering in the seabed (average two-year residence time and first-order resuspension approach). For each scenario we use two reference conditions for the suspended particulate matter (SPM). Hence, a total of six different simulations are considered (Table 5.2).

Table 5.2: The different combinations of background and sand extraction scenarios

Background	Reference	Sand extraction plume	
ZUNO-DD SPM	no sand extraction	without silt buffering in the seabed	with silt buffering in the seabed
ZUNO-grof SPM	no sand extraction	without silt buffering in the seabed	with silt buffering in the seabed

5.5.2 Impact results

The results of the GEM simulations are presented as eight-year time-series for several locations in front of the Dutch coast and as annual averages for defined monitoring areas.

ZUNO-DD background SPM without silt buffering in the seabed
With sand extraction, SPM concentrations increase resulting in a reduction of chlorophyll. The level of reduction is different depending on the reference case chosen. (Appendix H). Also, sand extraction delays the onset of the algae bloom and the end of the growing season occurs earlier. Especially in summer periods, dissolved nutrient levels increase due to a reduction in the uptake by phytoplankton. Salinity does not change, since sand extraction has no influence on the river outflow into the North Sea or

on the hydrodynamics. It also shown that further off-shore the effect of sand extraction fades out (for example compare locations NZR6NW010 and NZR6NW070, 10 and 70 kilometres offshore, respectively). When comparing a location close to the sand extraction locations with a location further north, a similar effect occurs. The impact due to sand extraction on chlorophyll is smaller for more northern locations (for example compare NZR2WC002 and NZR9TS004).

ZUNO-DD background SPM with silt buffering in the seabed
With buffering in the seabed, sand extraction also results in enhanced SPM levels, but the increase is small relative to the simulation without buffering (Appendix I). Consequently impacts on chlorophyll and nutrients are also small compared to the situation without silt buffering in the seabed. Again, further away from the coast and more to the north, the impact of the sand extraction diminishes.

ZUNO-grof background SPM without silt buffering in the seabed
As in the case of ZUNO-DD, sand extraction without silt buffering affects suspended matter, chlorophyll and nutrients at a number of locations (Appendix J). The suspended matter is much higher while the chlorophyll concentration is less than without the sand extraction. In the vicinity of the sand extraction locations, the start of the chlorophyll spring bloom is delayed while in autumn the decrease in chlorophyll starts earlier during the sand extraction. Further off-shore the impacts of sand extraction on the nutrients and primary production fades out.

ZUNO-grof background SPM with silt buffering in the seabed
As in the case of ZUNO-DD, sand extraction without silt buffering has a much stronger impact than sand extraction without buffering (Appendix K). At the Southern locations there is an effect of sand extraction on the chlorophyll levels, especially near the sand extraction location. At location NZR2WC002, for example, the onset of the algae bloom is delayed.

In Appendix L the changes in chlorophyll due to sand extraction is plotted as annual average per monitoring area. Figure XX presents the selected monitoring areas. The impact of sand extraction is presented as the percentage change in chlorophyll concentration compared to the respective reference scenario (i.e. ZUNO-grof is always compared with ZUNO-grof, and ZUNO-DD with ZUNO-DD). For each monitoring area, the annual averages are plotted for both ZUNO-DD and ZUNO-grof, both with and without silt buffering in the seabed. The areas are positioned such that they follow the coastline of The Netherlands, which gives a good view on where and to what extent the sand extraction has an impact on chlorophyll. As expected, the impact of the sand extraction is the largest in areas close to the sand extraction location, with the area ‘Voordelta’ as example for the overall effect in that region. For both background SPM scenarios, the sand extraction without silt buffering in the seabed has the largest effect showing a 50 to 60% decrease in annual-averaged chlorophyll levels. Although the reduction in chlorophyll is less for the sand extraction scenario including sediment seabed buffering, there is still a 20% decrease simulated in the near-shore region. Both sand extraction scenarios show a reduction of the impact of sand extraction further north and further from the shore. The sand extraction plume has little effect on chlorophyll levels in the Wadden Sea.

Appendix L shows the relative effect of sand extraction on the primary production for all monitoring areas. Similar to the effect on chlorophyll, the sand extraction scenario

without sediment buffering shows a larger effect than the scenario with sediment-water exchange, in area Voordelta up to 80% and 30%, respectively. In general the impacts of sand extraction gets smaller at offshore location. This effect is, however, much stronger when silt buffering is taken into account. The impact on primary production is larger than on chlorophyll. Primary production is a flux, not a concentration hence it depends on the local site-specific conditions. Consequently changes in local forcings i.e. the background turbidity have a direct effect. The chlorophyll concentration on the other hand is also the result of horizontal transport between different areas hence a local decrease will be partly compensated by inflowing algae.

5.5.3 Concept of limiting factors

To understand the results from the sand extraction simulations the concept of limiting factors is briefly discussed. Primary production can only occur given the availability of nutrients and solar energy. If dissolved nutrient levels are consistently low or even zero, this indicates a nutrient limitation. Light gets limiting when the amount that is available for growth is just sufficient to promote a gross growth rate that equals all losses (e.g. respiration, mortality, sedimentation). Unlike the availability of nutrients, the availability of light shows very strong short term variations with depth (mixing) and the time of the day. The light attenuation (extinction) is a function of the water itself, and the amounts of suspended matter, dissolved organic matter (or yellow substance; in GEM approximated as a function of the fraction of fresh water), dead algae particles (detritus) and living algae. In the North Sea, there is a spatial and temporal variation in nutrient and light limitation.

In winter when primary production is low, light is generally limiting because of the low irradiance. In contrast, nutrients are generally not limiting in winter as river loads and mineralization of organic matter replenish the nutrient stock and the requirement by phytoplankton is smaller. With the increase of the irradiance in late winter or early spring, primary production can start. The moment at which this occurs strongly depends on the depth and background turbidity and thus varies regionally. Combining nutrient and light limitation, we can distinguish two possible situations:

1. Primary production is mainly limited by light limitation all year round (via self-shading by algae and newly produced organic matter). In practice this leads to a sinusoidal signal in biomass which follows from the availability of irradiance. Relatively low SPM and yellow substance levels in summer amplify this response curve and may modify its shape.

   Noordwijk 2 km is a typical location for this type of behaviour (Figure 5.11). Primary production is limited by light availability almost all year (except in May and June). During the early spring period when nutrients are not limiting, the chlorophyll-a concentration increases even though there is light limitation because the surface irradiance increases and the self-shading due to phytoplankton is still small. To compensate for the strong light limitation, light limited phytoplankton has a high chlorophyll contents per unit of biomass.

2. Summer levels of primary production are primarily nutrient limited. In this type of water, improved light availability or a sufficiently small increase in turbidity will have no effect on primary production.

Terschelling 4 km is a typical location for this type of behaviour (Figure 5.12). Light limitation occurs in winter, during the development of the spring bloom and in autumn. Starting at the peak of the spring bloom and during summer, the phytoplankton biomass is limited by nutrients. Because light is not limiting, phytoplankton has a low chlorophyll contents per unit of biomass in summer.

Figure 5.11: Chlorophyll-a concentration (in µg/l) and limiting factors at Noordwijk 2 km in 1998 (reference condition with ZUNO-grof SPM). Limiting factors: light (brown); nitrogen (red); phosphorus (yellow); silicon (light blue); growth (blue); mortality (dark blue).

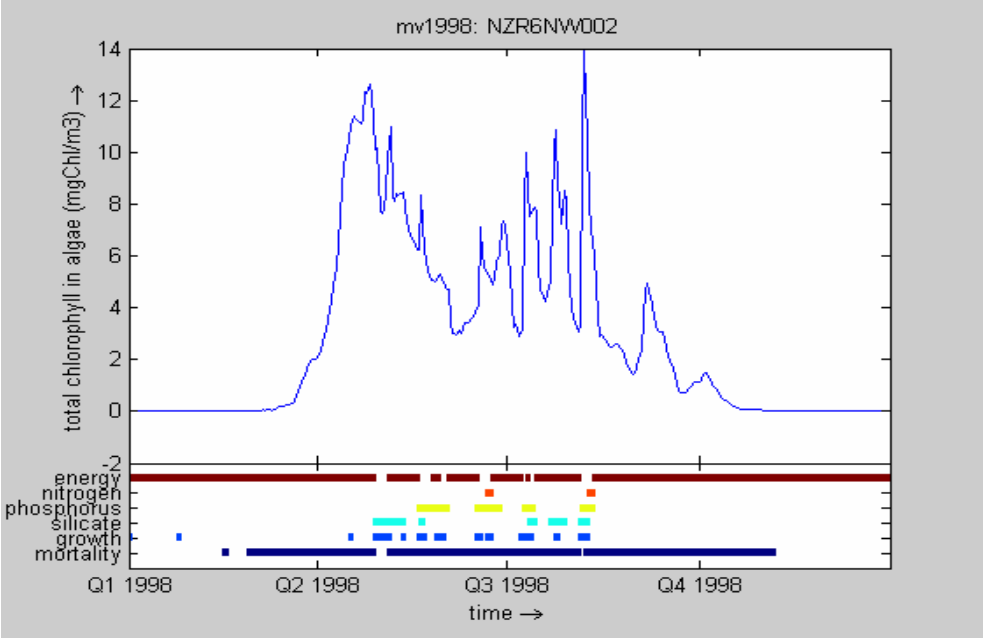

Figure 5.12: Chlorophyll-a concentration (in µg/l) and limiting factors at Terschelling 4 km in 1998 (reference condition with ZUNO-grof SPM). Limiting factors: light (brown); nitrogen (red); phosphorus (yellow); silicon (light blue); growth (blue); mortality (dark blue).

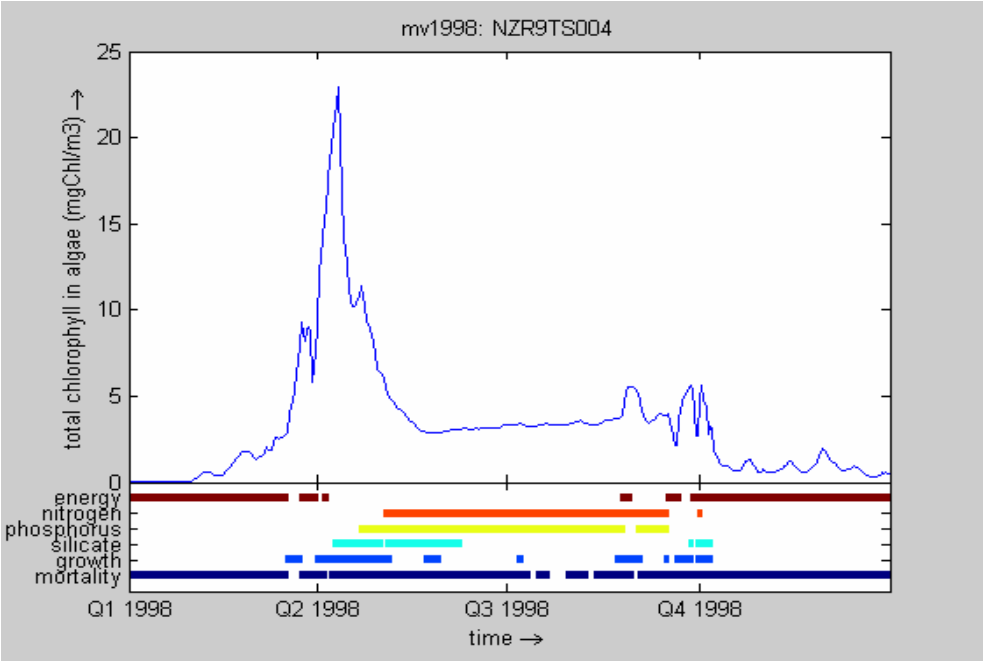

5.5.4 Impacts of sand extraction

Given the concept of limiting factors, the results of the sand extraction simulations can be understood. By increasing the suspended matter concentration in the water column, sand extraction influences the light availability and thus has an effect on primary production. Sand extraction will directly affect the primary production in those areas that are light limited: the Voordelta and the near-shore coastal zone. For areas that are nutrient limited, it depends on the level of increase whether or not an effect will occur at a certain location. If nutrients remain limiting, no direct effects on primary production of increased SPM due to sand extraction are to be expected: the offshore regions and north. However, there may be an indirect effect since a reduction in primary production in one area implies that less nutrients are used over there hence more remain available for other areas. This could even lead to an increase in primary production in the nutrient limited areas. These different types of response are more schematically shown in Figure 5.13 and 5.14.

Figure 5.13: In light limited areas, all available light is used for primary production. Higher SPM values result in lower primary production.

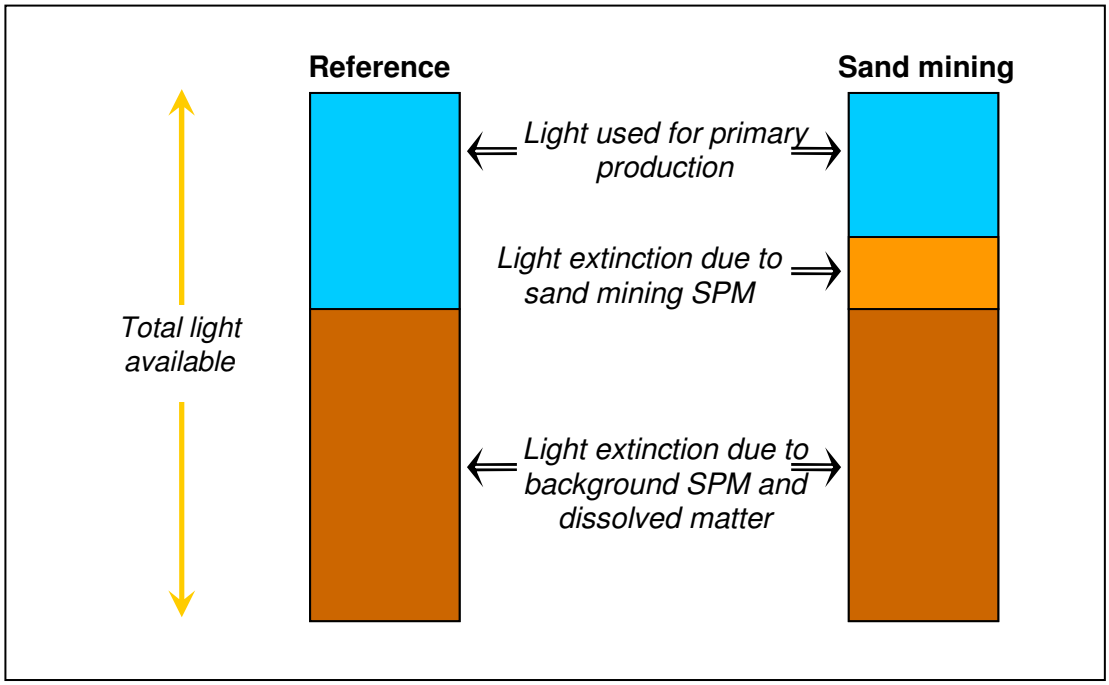

Figure 5.14: In nutrient limited areas, not all available light is used for primary production. Higher SPM values do not result in lower primary production.

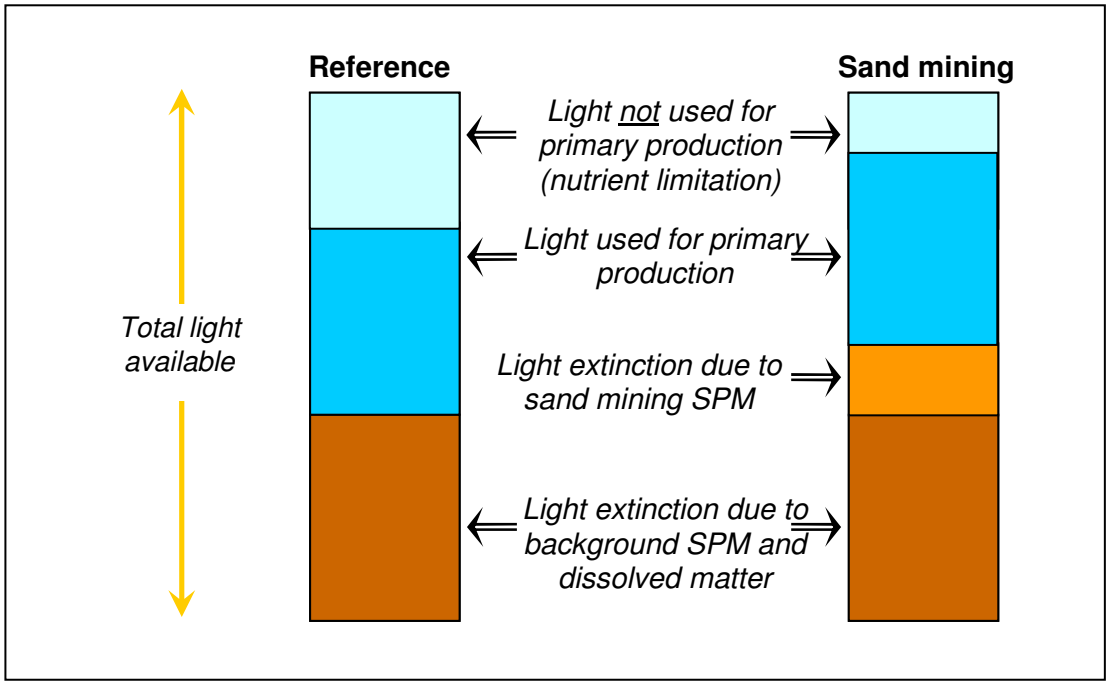

Figure 5.15: Impact of sand extraction on phytoplankton biomass (gC/l) and chlorophyll-a (µg/l) at location Walcheren 2km (WC002) for 2002 given as year average and per month for the ZUNO-grof reference condition, with sand extraction and buffering (1st order exchange) and with sand extraction without buffering.

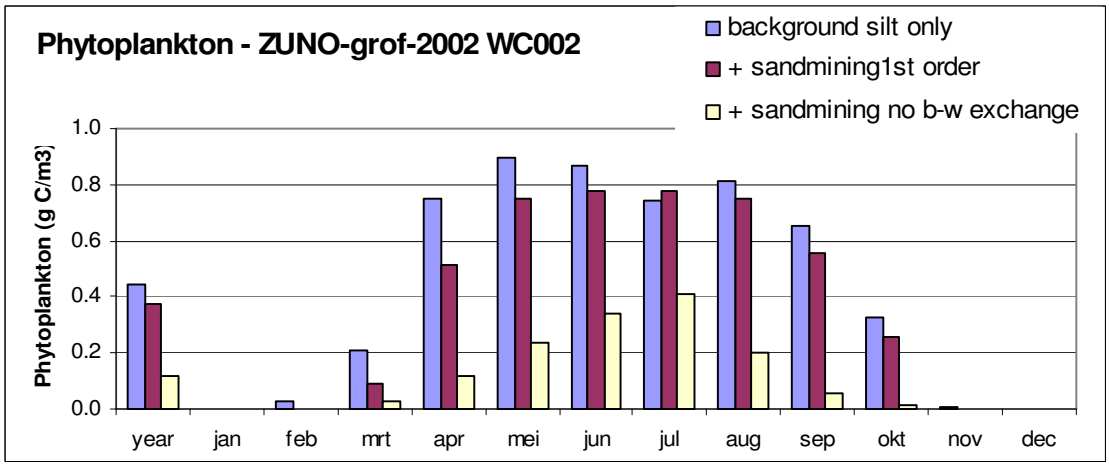

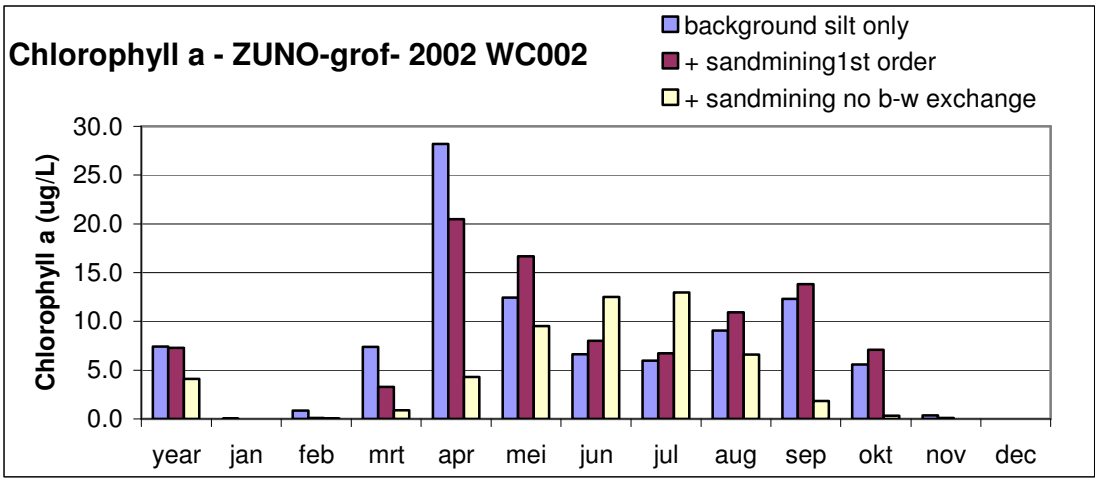

Biomass and chlorophyll do not always respond in a similar way. As an illustration consider Figure 5.15 for location Walcheren 2. With sand extraction, algal biomasses decline all year round at this location. The strongest reduction is simulated during the spring peak when the irradiance is still rather low and SPM concentrations have not yet declined to the lower summer levels. In this example the limiting factors controlling the algal biomass change in response to sand extraction. Due to an enhanced extinction by SPM, the spring bloom starts later. In summer nutrients are no longer limiting, but light remains the main limitation. As a consequence the phytoplankton biomass declines, but due to a shift in biomass to chlorophyll ratio, simulated chlorophyll concentrations in summer even exceed those under reference conditions. Hence, the annual change in chlorophyll is considerably smaller than the change in biomass for both scenario simulations.

In general the scenarios without silt buffering in the sediment lead to higher SPM concentrations than the scenario with silt buffering (Figure 5.15). As a result primary production goes down by as much as 80% in the light limited areas if silt buffering is not taken into account. Silt buffering in the seabed reduces the effect on the average SPM

concentration and the area where the influence of sand extraction is noticeable. However, silt buffering also introduces a delayed response further away from the point of origin. The percentage change in primary production shows an increasing trend in virtually the whole coastal zone, as silt buffering increases the travel time of the released SPM along the Dutch coast.

The SPM behaviour is equivalent to adsorption of chemicals percolating through an extraction column filled with adsorbents: the stronger the chemical binds to the adsorbents, the longer it takes before the chemical leaves the column. For SPM, the more the SPM is buffered in the seabed ('bounded to the seabed'), the longer the travel time from the release point to the Wadden Sea coast. Without silt buffering, the released SPM mostly resided in the water column and is transported quickly to the north. The high concentration has a large effect on chlorophyll and primary production. On the other hand: shortly after the sand extraction is stopped, the seabed and the SPM concentration quickly revert to the previous background values and the effect on primary production and chlorophyll diminishes rapidly. When silt buffering is taken into account, the released SPM stays in the seabed of the coastal zone for a longer time and therefore has a longer lasting effect on primary production and chlorophyll when resuspension occurs. In the simulations primary production and chlorophyll rapidly return to their reference conditions in year 8 after stopping the sand extraction operations. However, this quick restoration to normal values may be attributed to the SPM model concept that simulates background and sand extraction SPM separately. We conclude therefore that when sand extraction is stopped the overall trend will be a recovery of chlorophyll and primary production to the reference conditions, but the present study gives no indication on the time scale of this recovery.

In year 7 (2002), a particularly large decrease occurs in average chlorophyll and primary production levels especially in the near-coastal zone. This is due to the more than average contribution of sand extraction to the total suspended matter. In February 2002, high wind speeds were measured, which resuspend the silt into the water column.

The scenario with silt buffering reflects the most recent scientific insight into the SPM increase resulting from sand extraction. The predicted effect on nutrients and primary production is therefore the most realistic estimate that can currently be provided. In the Voordelta, sand extraction will reduce the primary production by 20% and chlorophyll by 20%. In the coastal zone from Hoek van Holland to Noordwijk, sand extraction will reduce the primary production by 40% and chlorophyll by 20%. In the near-shore coastal zone north of Noordwijk, sand extraction will reduce the primary production by 20% and chlorophyll by 10%. No effects are expected in the coastal zone in front of the Wadden Sea islands and in the Wadden Sea itself due to sand extraction.

5.5.5 Uncertainties

Herein, we review two important uncertainties in the simulations for nutrients and primary production:

- extinction coefficient;
- background silt concentration.

Extinction coefficient
It is assumed that the SPM released during sand extraction has the same extinction characteristics as the background SPM: both fractions have been given the same specific extinction coefficient of 0.025 m^2/g. It is uncertain whether this assumption is valid. It is not unlikely that the sand extraction SPM consists of finer material than the background, as no time for flocculation has occurred. If the silt particles are indeed smaller, a higher specific extinction coefficient should be used and the effect on primary production and chlorophyll would be larger.

Background concentration
In this study we make use of two different background SPM concentration patterns. The background SPM concentration has been based on silt computations with a relatively low (ZUNO-grof) and a relatively high resolution (ZUNO-DD). Another difference is that the background concentration of the ZUNO-DD has been calibrated more intensively than the ZUNO-grof. In Section 4.6 we concluded that the SPM concentration from ZUNO-grof is underestimated in the southern area relative to the measurements. However, the computation with the SPM from ZUNO-grof for nutrients and primary production performs better in comparison with the measurements than that based on the SPM from ZUNO-DD, see for explanation Section 4.6.

Figure 5.16 presents the effect on chlorophyll-a and primary production in the Voordelta using the SPM background concentration of ZUNO-grof (blue) and ZUNO-DD (green). It appears that the SPM background concentration of ZUNO-grof results in a smaller effect than using the SPM background concentration from ZUNO-DD. However, the differences are small between ZUNO-grof and ZUNO-DD. In view of other uncertainties (see e.g. silt transport) this uncertainty is considered to be small.

Given the uncertainties and model assumptions in the simulations for nutrients and primary production, the computed effects should be considered with a 50% uncertainty margin within the model context of this specific model. This band width is based on expert judgement; no systematic analysis of the uncertainties has been carried out. The initial assumptions in this study should be considered as well to define a realistic bandwidth for the overall impact assessment on nutrients and primary production. This is further discussed in Chapter 6.

Figure 5.16: Effect on primary production (left panel) and chlorophyll-a (right panel) in the Voordelta. The lines represent the effect using the background SPM from ZUNO-grof (blue) and ZUNO-DD (green).

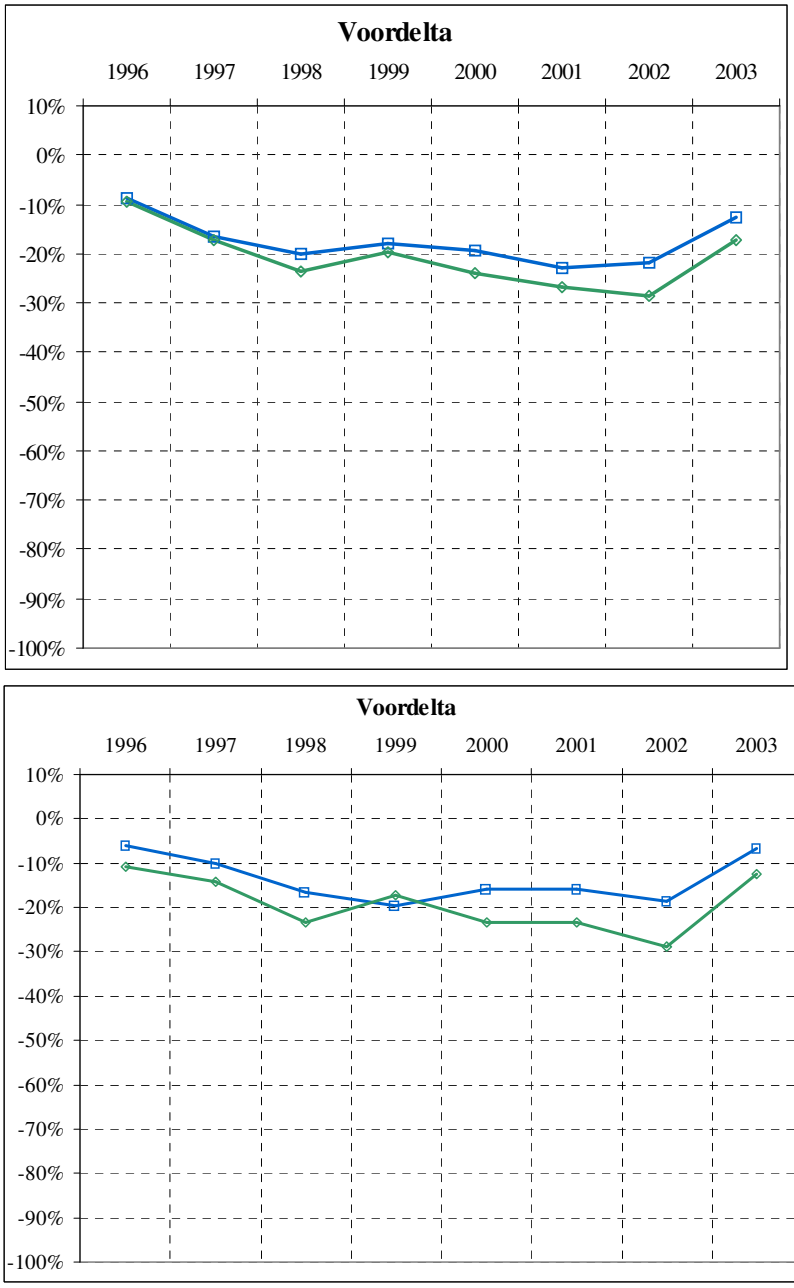

6 DISCUSSION AND CONCLUSIONS

In this study a new approach is adopted to quantify the effects of sand extraction on the North Sea, in particular the release of fines during extraction in combination with buffering of silt in the seabed (water-bed exchange) on nutrients and primary production as a function of time and location. An innovative element in this study is that the buffering and release of mud from the sediment bed at various time scales (tides, spring-neap, seasons) has been modelled as well. This phenomenon was known qualitatively based on observations. However, up till it was not possible now to quantify this effect in the available numerical models due to lack of validated formulations.

New formulations have been proposed for seasonal water-bed exchange (Chapter 2) and these formulations are validated against field data (Chapter 3 and 4). Next, these formulations have been used to investigating the effect on mud dispersion due to sand extraction (Chapter 5). Two different model approaches have been applied to quantify the effects on silt transport (source → near field → far field) : a two-dimensional model approach with FINEL and a three-dimensional model approach with Delft3D. Furthermore, the effects on nutrients and primary production were computed with Delft3D. This chapter highlights the important findings in the previous chapters.

An innovative model including seasonal water-bed exchange
An innovative model has been developed that accounts for seasonal exchange of silt between the sediment bed and the water column. The calibration against the CEFAS data at Noordwijk shows that the observed concentration variations are well reproduced at various time scales (tides, spring-neap cycle, storms, and seasons). However, the calibration of the presented model is limited to this single point at Noordwijk only. Therefore, the calibrated parameter settings are uncertain and the impact results still have a relatively large bandwidth. Especially the buffer capacity in the sediment bed is an important parameter for the far field effects of sand extraction. The setting of this parameter could not be calibrated with the CEFAS measurements. Despite this drawback, this model development is an important step forward and the model can be used for estimating the impacts of sand extraction in a realistic way.

Role of water bed exchange
This study clearly shows that seasonal water-bed exchange decreases the magnitude and the spatial extent of the mud dispersion pattern due to sand extraction. Figure 6.1 shows the impact on the (yearly-averaged) mud concentration at the water surface due to sand extraction for a situation with and without seasonal buffering after six years of sand extraction. Due to temporal buffering in the sediment bed, the mud plume becomes significantly smaller, and the effect on the mud concentration in the water column becomes significantly lower. Although the sediment bed buffers a significant part of the mud load due to sand extraction, the mud content in the sediment bed below the plume increases only slightly with say 0,5 to 1% at maximum (due to the large available surface area for buffering).

Figure 6.1: Effect of sand extraction on the yearly-averaged mud concentration after 6 years without buffering (upper panel) and with buffering (lower panel) in the sediment bed. Note that the scale is not linear and that the values are for the extraction only. The background (autonomic development) has not been incorporated.

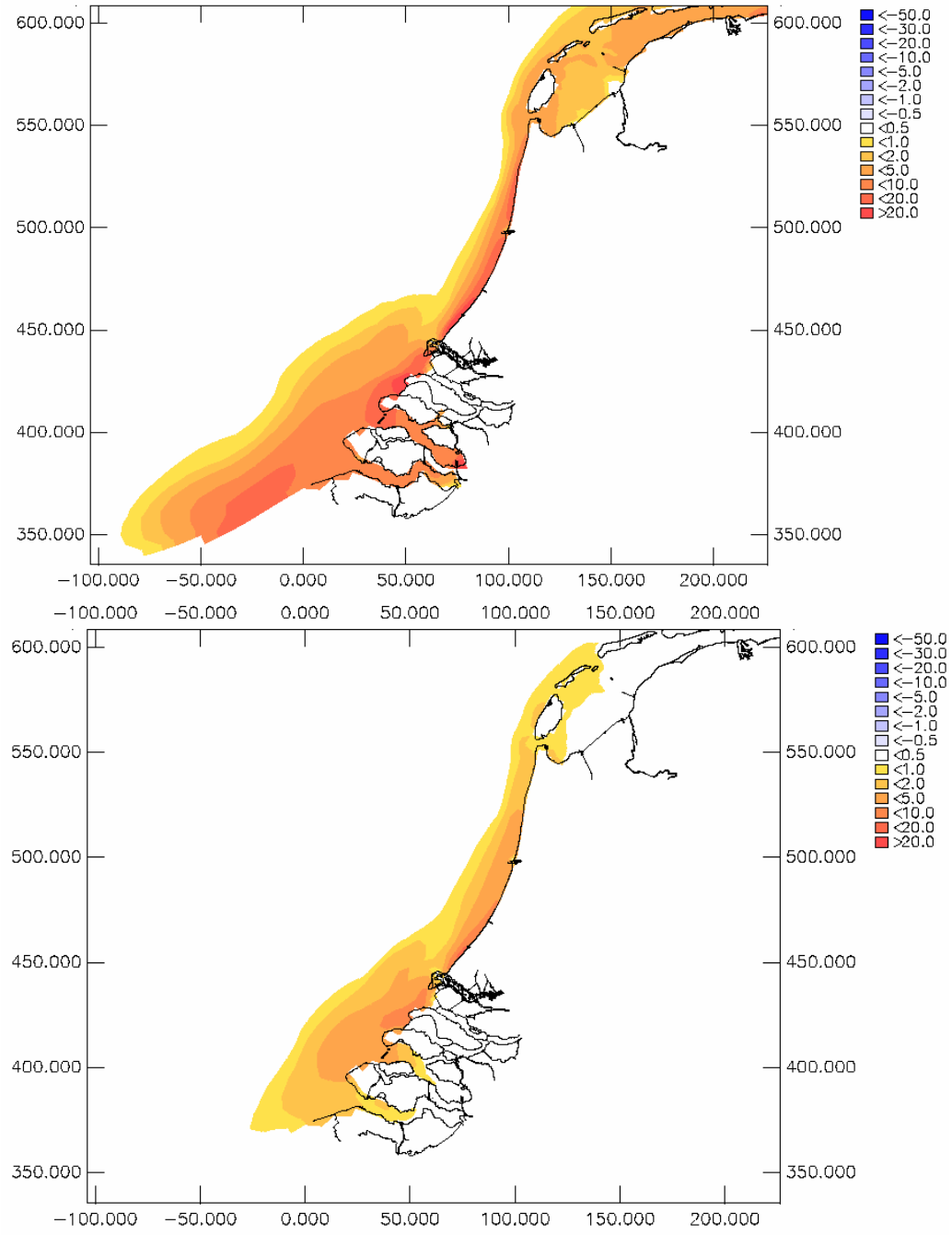

The results in this study also indicate that the effect of sand extraction last longer than the extraction period due to seasonal water-bed exchange. Gradually, the amount of mud that has been stored in the sediment bed will be dispersed over a larger area. Thus, the effect of the extra buffered silt release will be ongoing for several years during mild and storm conditions, i.e. after stopping the sand extraction activities. Notice that this holds for the far field effects of the sand extraction. The near-field effect of the sand

extraction with high mud concentrations near the sand pits directly stops after ending the sand extraction activities. The presented effects with seasonal water-bed exchange are considered to be more realistic than the approach without this effect as from a physical point of view it is a better representation of reality. The calibration of the model formulations in Chapter 2 has shown that the model is able to reproduce the measured characteristics of the mud concentrations in time due to the tide and due to storms. Although the formulations are still largely empirical, and the calibration is limited due to lack of data, it is concluded that seasonal water-bed exchange should be included to assess the impacts of sand extraction.

Differences between a 2D and 3D approach
The impacts simulations show that the 3D silt model predicts a much larger effect on the silt concentration due to sand extraction than the 2D model. This holds in particular for the zone near the outflow of the Maas, Haringvliet and near the Dutch coastal zone and in the Voordelta. In these areas, the interaction between fresh and salt water is very important. Notice that the 2D approach takes into account the effects of density-driven flow in a simplified way. Although the differences between the 2D and 3D model results can be explained qualitatively, a more thorough calibration and validation is required to understand the complex transport and mixing behaviour and to reduce the uncertainty regarding the reproduction of the natural 3D behaviour in a quantitative sense.

Parameter settings water-bed exchange
The parameter settings for the water-bed exchange formulations have an important influence on the predicted impact of sand extraction on silt (and thus on primary production etc.). The calibrated settings based on the CEFAS data set determine the near field effects, whereas the settings for the buffer capacity are crucial for the impact in the far field zone. As already stated, the settings for the buffer capacity are uncertain and difficult to calibrate at this moment due to lack of data. The silt computations that have been used for predicting the effects on nutrients and primary production are carried out with a relatively low buffer capacity.

Due to this parameter setting it is expected that the calculated effects on the silt concentration in the water column are *a conservative estimate at larger distances from the sand extraction pit (> 10 km)*. More field data of the buffer capacity (silt percentage, active layer) would reduce this bandwidth.

Impact sand extraction on silt transport
The results of the impact computations show that the silt concentration increases with more than 10% in a zone of say 30 km width between Walcheren and IJmuiden. The increase is about 100% near the sand extraction pit. The increase of the silt concentration occurs during storms but also during mild conditions. Moreover, silt is trapped in the sediment bed and the silt percentage in the sea bed increases (+/- 1%). After the sand extraction period the silt concentration near the sand extraction pit quickly drops towards the far-field impact level. At a larger distance the effects of sand extraction are visible during a relatively long period. It is expected that the silt behaviour gradually returns to its original situation within a period of several years.

Impacts sand extraction on nutrients and primary production
The simulations with nutrients and primary production for the reference situation show that the model results agree well with the measurements. The impact simulations show

that primary production and chlorophyll-a levels decrease in the Dutch coastal zone and the Voordelta. No effects occur in the Wadden Sea. The results of these simulations can be explained as follows: an increasing silt concentration in the water column reduces the light availability, and consequently the primary production. This holds in particular for areas that are “light-limited” in the present situation (e.g. near the coast).

A systematic investigation of the uncertainties was beyond the scope of this research. However, the conservative approach in the silt computations implies that the effects on nutrients and primary production are also expected to be conservative for the short term. At longer time scales the impact of sand extraction with the present silt results might be under estimated in the Dutch coastal zone due to the longer residence time in the sediment bed.

Initial assumptions

At the beginning of this project several assumptions have been made regarding the impact assessment (see also Chapter 1). It is assumed that the total volume of silt during the overflow process behaves as a passive plume in the water column. This assumption can be considered as an “upper limit” approach because it is expected that part of the silt overflow will deposit due to the density-driven current towards the sediment bed (the so-called dynamic plume). The magnitude, however, is uncertain. Moreover, the silt percentage in the sediment bed is estimated at 2,5%. This value is also uncertain, and possibly too high. Finally, it is known from observations that small (consolidated) silt layers are present at the beach after nourishments. This indicates that part of the silt that is extracted from the sea bed will not contribute to the overflow all at the borrow pit locations at sea.

Conclusions

This project has resulted in an innovative modeling concept that accounts for the temporal fluctuations of the silt concentration in the water column and in the sediment bed. Comparison with field data indicates that the models can be applied for impact assessment of sand extraction. The impact assessment shows at the end of the sand extraction period the +10%-contour of the silt concentration in the water column lies between Schouwen and IJmuiden and covers a width of approximately 30 km. The increase of silt in the water column results in a decrease of the primary production, in particular in the Dutch coastal zone and the Voordelta. After stopping the sand extraction, it may take several years for the silt concentrations to return to the original background concentration (assuming that the original concentration is static). Only the effect of the offshore sand extraction has been modeled and presented. The variability of the silt concentrations in the seabed of the so-called background concentrations has not been investigated. The effects of the sand extraction shall be weighted against the background variability.

Given the initial assumptions (see paragraph 1.4) and the assumptions in the modeling study, it is expected that the presented effects on silt, nutrients and primary production are an upper limit estimate of the effects of sand extraction for the construction of Maasvlakte 2. More field measurements with respect to the silt concentration in the water column and in the sediment bed are needed to reduce the bandwidth of the effects.

7 CONCLUSIONS

The objective of this study is to quantify and explain the effects of sand extraction including the band width on mud transport, nutrients and primary production in the North Sea coastal zone in the framework of the construction of the Maasvlakte 2 Port extension.

An innovative element in this study is that the effect of exchange of mud to and from the sediment bed at various time scales (tide, spring-neap, seasons) has been introduced. The present study focuses on the simultaneous extraction of sand from four borrow area, i.e. pits P2, P4, P5 and P6 near Maasvlakte 2 (see Figure 1.1).

For this study it is assumed that the sand extraction production equals 50 Mm^3/year during a period of 6 years. Assuming a silt percentage (particles < 63 µm) of 2,5% in the sediment bed, this results in a silt load of 2 Mton/year. Furthermore, it is assumed that the silt fraction behaves “passive”, i.e. no sediment directly deposits in the sand extraction pit due to a density-driven current (so-called dynamic plume), but disperses into the surrounding water body. The assumptions made in this study imply that the conclusions below should be considered as a worst-case scenario for this specific sand mining scenario.

The following conclusions can be drawn:

- Seasonal water-bed exchange has a clear effect on the mud dispersion pattern in time and space due to sand extraction. After six years of sand extraction the plume extends from Walcheren to IJmuiden and has a width of approximately 20 – 30 km. Apart from the area in the vicinity of the sand extraction pits the suspended sediment concentration in this area increases with 10 - 20% compared to the background values.
- The effect of sand extraction in the far field will last for a longer period than the actual extraction period, due to seasonal water-bed exchange. Gradually, the amount of mud that has been stored in the sediment bed will be dispersed over a larger area. Thus, the effect of sand extraction only (as computed in the numerical model) will be visible for several years after stopping the sand extraction activities.
- The difference between a two-dimensional (FINEL) and a three-dimensional approach (DELFT3D) for simulating the silt transport appears to be quite large and are contributed by the complex density differences of mixing of fresh and salt water along the Dutch coast. The three-dimensional model predicts a higher effect on the suspended sediment concentration in the water column and the plume is shifted more to the coast. These differences can be understood qualitatively. A more thorough calibration/validation is however required to understand and validate the complex three-dimensional processes quantitatively.
- Because of the low estimate of the buffer capacity applied in the 3D silt transport simulation that has been used as input for the nutrient and primary production simulations, it is concluded that using the 3D results for the impact on nutrients and primary production is a conservative approach on the short time scales. At longer time scales (several years) the impact of sand extraction with the present silt results might be under estimated in the Dutch coastal zone due to the longer residence time in the sediment bed.
- The computations with silt buffering reflect the most recent scientific insight into the SPM increase resulting from sand extraction. The predicted effect on nutrients and primary production is therefore the most realistic estimate that can currently be

provided. In the Voordelta sand extraction will reduce the primary production by 20% and chlorophyll by 20% on annual average. In the coastal zone from Hoek van Holland to Noordwijk, sand extraction will reduce the primary production by 40% and chlorophyll by 20%. In the near-shore coastal zone north of Noordwijk, sand extraction will reduce the primary production by 20% and chlorophyll by 10%. It should be noted that inter-annual variations between the months could be larger than the annual averaged. No effects are simulated in the Wadden Sea due to sand extraction.

- The sensitivity of the results for various settings (waves, silt parameters) has been investigated. It is concluded that the uncertainties in the silt parameters (e.g. buffer layer thickness) have a large effect on the effect assessment. In view of the applied lower estimate for buffer capacity, the silt computations that have been used for the nutrients and primary production computations can be considered as an upper limit for the period during sand extraction. However, applying higher buffer capacity will probably lead to a longer lasting impact on the primary production in the Dutch coastal zone. More field measurements with respect to the silt concentration in the water column and in the sediment bed are needed to reduce the bandwidth of the effects.

REFERENCES

Boudreau, B.P. and Jorgensen, B.B., 2001, The Benthic Boundary Layer", Oxford University Press.

Boutmy, A.E.G. (1998) Morphological impact of IJmuiden harbour. Validation of Delft3D 1968-1996.

Dam, G., 2004. Bandbreedte morfologische voorspellingen Haringvlietmond. Svašek Hydraulics report gd/04459/1306.

Dankers, P.J.T., 2005. The intrusion of fine suspended sediment into a sandy sediment bed, a literature review, report no. 01-05

Ferry observation on temperature, salinity and currents in the Marsdiep inlet between the North Sea and Wadden Sea. Proc. 2nd Int. Conf. on EuroGoos, Elsevier oceanographic series.

Giessen, A. van der, W.P.M. de Ruijter and J.C. Borst, 1990. Three-dimensional current structure in the Dutch coastal zone. Netherlands Journal of Sea Research, 25 (1/2), p. 45-55.

Goede, E.D. de, & D.S. van Maren, 2005. Impact of Maasvlakte 2 on the Wadden Sea and North Sea coastal zone. Track 1: Detailed modelling research. Part I: Hydrodynamics. WL|Delft Hydraulics report z3945.20. Royal Haskoning 9R2847.A0.

Jeuken, M.C.J.L., S.G.J. Aarninkhof, R. Bruinsma, G. van Holland and J.A. Roelvink (2000) Modellering van de grootschalige bodemveranderingen in de voordelta van Oosterschelde en Grevelingen. WL-rapport Z2422, mei 2000.

Langeveld, C., 2005, "Verdiepte Loswal – fysisch onderzoek naar het gedrag van baggerspecie", Port of Rotterdam & Delft University of Technology, MSc thesis.

MARE consortium, 2001. Description and modelrepresentation T0 situation, Part 2: Transport, nutrients and primary production Perceel 3, Deelproduct 2, project Z3030.10, Hans Los and Sharon Tatman, Prepared for Flyland project by WL | Delft Hydraulics.

MARE, 2001, "Reference scenarios and design alternatives; Phase 1", Parcel 3, Subproduct 3, Report Z3029.20.

Prandle, D., G. Ballard, D. Flatt, A.J. Harrison, S.E. Jones, P.J. Knight, S. Loch, J. McManus, R. Player & A. Tappin, 1996. Combining modelling and monitoring to determine fluxes of water, dissolved and particulate metals through the Dover Strait. Cont. Shelf Res., 16, p.237-257.

Ridderinkhof, H., H. van Haren, F. Eijgenraam & T. Hillebrand, 2000.

Roelvink, J.A., G. van Holland and R.C. Steijn (1998b). Gevoeligheidsberekeningen Eijerland en ZW-Texel - fase 1: Eijerland. Rapport van het Samenwerkingsverband Alkyon / WL|Delft Hydraulics. (A266 / Z2430). May 1998. (Sensitivity computations Eijerland and Southwest Texel - phase 1: Eijerland).

Roelvink, J.A., G. van Holland en J. Bosboom (1998a). Kleinschalig Morfologisch Onderzoek MV2. Fase 1. Validatie morfologische modellering Haringvlietmonding. WL rapport Z2428, december 1998. (Small-scale morphological research Maasvlakte-2. Validation morphological modelling Haringvliet mouth)

Salden, R.M., 1998, “A model for the transport of fine-grained sediment in the Dutch coastal zone”, RWS/RIKZ, Report RIKZ/OS/98.119X.

Sandeh Stutterheim, 2002, “Van Noord tot Noordwest – Een studie naar de berging van baggerspecie op loswallen”, Directoraat-Generaal Rijkswaterstaat, Rijksinstituut voor Kust en Zee/RIKZ, rapport RIKZ/2002.047.

Steijn, R.C., G.K.F.M. van Banning and J.A. Roelvink (1998). Gevoeligheidsberekeningen Eijerland en ZW-Texel - fase 2: ZW Texel. Rapport van het Samenwerkingsverband Alkyon / WL|Delft Hydraulics. (A266 / Z2430). June 1998. (Sensitivity computations Eijerland and Southwest Texel - phase 2: Southwest Texel).

Stelling, G.S., 1983. On the construction of computational methods for shallow water flow problems. PhD thesis, Delft University of Technology.

Suijlen, J.M. and Duin, R.N.M., 2001, “Variability of near-surface total suspended matter concentrations in the Dutch coastal zone of the North Sea”, RWS/RIKZ, Report RIKZ/OS/2001/150X.

Thibodeaux, L.J. and Boyle, J.D., 1987, Bedform-generated convective transport in bottom sediment”, Nature, Vol 325, No 22, pp 341-343.

Torenga, E.K., 2002, “Wave-driven transport of fine sediments in the surf zone”, Delft University of Technology, Faculty of Civil Engineering and Geosciences, Section of Environmental Fluid Mechanics, Report 02-01.

Van Rijn (1990). Principles of fluid flow and surface waves in rivers, estuaries, seas and oceans. Aqua publications, The Netherlands, p. 268.

Van Rijn, L.C., 1993, “Principles of sediment transport in rivers, estuaries and coastal seas”, Aqua Publications, ISBN 90-800356-2-9, 700 p.

WL|Delft Hydraulics, 1998. Calibration of the ZNZ model. PGJ Brummelhuis, H. Gerritsen, D. Verploegh, Z2544.

WL|Delft Hydraulics, 2005. Effect assessment Maasvlakte 2 in the framework of the Appropriate Assessment Wadden Sea, Part 3: Nutrients and Primary production, Report 9R2847.A0/Z3945, Arno Nolte, Jan van Beek, Pascal Boderie, and Hans Los, Prepared for Port of Rotterdam and RIKZ, November 2005.